

**MULTIPLE FUNCTIONAL ROLES OF THE BACTERIOPHAGE HK97 DELTA
DOMAIN IN CAPSID ASSEMBLY**

by

Bonnie Oh

B.S. Biology, University of Virginia, 2009

Submitted to the Graduate Faculty of
the Kenneth P. Dietrich School of Arts and Sciences in partial fulfillment
of the requirements for the degree of
Doctor of Philosophy

University of Pittsburgh

2015

UNIVERSITY OF PITTSBURGH
KENNETH P. DIETRICH SCHOOL OF ARTS AND SCIENCES

This dissertation was presented

by

Bonnie Oh

It was defended on

June 29, 2015

and approved by

James Conway, Ph.D., Associate Professor, Department of Structural Biology

James M. Pipas, Ph.D., Professor, Department of Biological Sciences

Anthony Schwacha, Ph.D., Associate Professor, Department of Biological Sciences

Thomas Smithgall, Ph.D., William S. McEllroy Professor of Biochemistry

Dissertation Advisor: Roger Hendrix, Ph.D., Distinguished Professor, Department of

Biological Sciences

Copyright © by Bonnie Oh

2015

**MULTIPLE FUNCTIONAL ROLES OF THE BACTERIOPHAGE HK97 DELTA
DOMAIN IN CAPSID ASSEMBLY**

Bonnie Oh, PhD

University of Pittsburgh, 2015

The bacteriophage HK97 capsid assembly and maturation pathway has been well studied. Despite this, little is known about the initial steps of assembly. How do 415 capsid proteins, ~120 copies of protease protein, and 12 copies of portal protein interact to form a correctly sized and shaped capsid? Most dsDNA phages and herpesviruses require the use of separate scaffolding proteins in order to assemble properly. HK97 does not have a separate scaffolding protein; instead it has a 102 amino acid N-terminal extension of its major capsid protein, called the delta domain. Like other well-known viral scaffolding proteins, the delta domain is present during initial assembly but is absent in the mature structure, is mostly α -helical in nature, has a high propensity of forming coiled coil interactions, and is flexible. We hypothesize that the delta domain is playing a scaffolding-like role in capsid assembly. Because the scaffolding-like region is actually part of the capsid protein, studying how a scaffolding protein contributes to capsid assembly is easily achievable using HK97. Using mutational analyses in a plasmid based system, I have tested the effects of delta domain point mutations, small insertions, and deletions on capsid assembly. Even single point mutations can cause assembly defects, rendering the capsid protein nonfunctional. Using biochemical and genetic assays, I have shown that different regions of the delta domain play different roles in capsid assembly. The HK97 delta domain is a multifunctional protein that is important for capsid protein solubility and expression, capsid shape, capsid size, protease incorporation, and portal incorporation. The flexibility and structure

of the delta domain plays an important role in its ability to regulate the assembly process. Learning about how the delta domain interacts with different proteins during assembly provides a greater understanding of how a single protein functions in order to build macromolecular complexes. Important roles and regions identified in the HK97 delta domain are applicable to other related phage and herpesvirus scaffolding proteins, providing insight on the biological processes and requirements of viral capsid formation.

TABLE OF CONTENTS

Preface.....	ix
1.0 Introduction.....	1
1.1 Bacteriophages and their Lifecycle	1
1.2 Capsid Assembly and the use of Scaffolding Proteins.....	2
1.3 HK97 Capsid Assembly and the Delta Domain	6
1.4 HK97 Model System	10
2.0 The delta domain is required for capsid protein solubility, assembly, and size....	16
2.1 Introduction.....	16
2.2 Results.....	19
2.2.1 Full length delta domain is required for capsid protein expression and solubility	19
2.2.2 Different sized deletions prevent capsid protein expression and functionality.....	21
2.2.3 Mutations in the delta domain C-terminal region affect capsid assembly and geometry	25
2.2.4 The search for 2nd site suppressors of W89A	39
2.2.5 Linker Insertion Mutations (LIMs) affect capsid assembly	43
2.2.6 ‘Hinge’ Deletions affect capsid assembly and size	48

2.3	Discussion	72
3.0	The delta domain is important for portal and protease incorporation.....	83
3.1	Introduction.....	83
3.2	Results.....	84
3.2.1	The 2 nd predicted helical region plays a role in portal incorporation....	84
3.2.2	The portal can enhance capsid assembly	106
3.2.3	Identifying a 2 nd site suppressor in the portal.....	113
3.2.4	Discussion.....	120
3.2.5	The N-terminal region plays a role in protease incorporation	125
3.2.6	Discussion.....	134
3.3	Different regions play different roles in assembly.....	136
4.0	Materials and Methods	140
	Appendix A: Interesting and unexplainable mutant K92A	155
	Appendix B: Stabilizing the delta domain with mutant S88C	167
	Bibliography	174

LIST OF TABLES

Table 1. Complementation Spot Test Results.....	149
Table 2. Complementation test results of A65E (gp5) and D135G (gp3).....	150
Table 3. Delta Domain Mutant Summary Table.....	151
Table 4. Relative and net band quantification for pVP0 g4 (H65A) K92A protein.....	162
Table 5. Ratio of portal:mcp and protease:mcp for WT and K92A.....	162

LIST OF FIGURES

Figure 1. Bacteriophage HK97 electron micrograph.....	8
Figure 2. Schematic of HK97 capsid assembly pathway.....	8
Figure 3. HK97 WT pV0 expression plasmid.....	11
Figure 4. Representative native agarose gel of HK97 protein.....	13
Figure 5. Proposed Model of the HK97 delta domain.....	14
Figure 6. Radiolabelling data from pNoDelta1 and pNoDelta2 full deletion mutants.....	18
Figure 7. Miniprohead prep results from pNoDelta2 full deletion mutant.....	20
Figure 8. Different sized deletions have deleterious effects on assembly.....	23
Figure 9. Internal spoke densities of WT Prohead I.....	26
Figure 10. Miniprohead prep results of W89A and D90A.....	28
Figure 11. Representative EM images of W89A and D90A.....	30
Figure 12. Miniprohead prep results of C-terminal point mutations.....	32
Figure 13. Representative EM images of C-terminal point mutations.....	33
Figure 14. Miniprohead prep results of C-terminal mutants that 'mimic' the WT residue.....	35
Figure 15. Representative EM images of C-terminal 'mimic' mutants.....	37
Figure 16. C-terminal mutant protein assemblies may be cross-linked and do not dissociate.....	38
Figure 17. Schematic of galK recombineering and search for 2 nd site suppressors.....	41

Figure 18. Miniprohead prep results of Linker Insertion Mutants (LIMs).....	45
Figure 19. Representative EM images of LIMs.....	47
Figure 20. Del 1 st and 2 nd Hinge mutants affect capsid assembly.....	49
Figure 21. pVP0 g4 H65A plasmid used to test for portal and protease incorporation.....	53
Figure 22. Del 2 nd Hinge is defective in portal and protease incorporation.....	56
Figure 23. Purification of Del 2 nd Hinge isolates different sized particles.....	58
Figure 24. Representative Cryo-EM image of Del 2 nd Hinge mutant capsids.....	60
Figure 25. Density map of Del 2 nd Hinge T=4 sized capsid compared to WT.....	63
Figure 26. Slice of Del 2 nd Hinge T=4 map shows more of the delta domain.....	65
Figure 27. Secondary Structure prediction of Del 2 nd Hinge delta domain.....	67
Figure 28. Density map of Del 2 nd Hinge T=7 capsids compared to WT.....	68
Figure 29. Delta domains in Del 2 nd Hinge T=7 capsids are similar to mutant T=4.....	69
Figure 30. Spoke densities of WT and Del 2 nd Hinge mutant capsids.....	71
Figure 31. Portion of HK97 delta domain protein sequence alignment.....	85
Figure 32. Miniprohead preps of E61A and Q62A.....	87
Figure 33. Representative EM images of E61A and Q62A.....	88
Figure 34. E61A and Q62A expressed with the portal and inactivated protease.....	90
Figure 35. Projection wheel of 2 nd predicted helical region showing mutant candidates.....	92
Figure 36. Agarose gel of 2 nd helix mutants with WT phenotypes.....	94
Figure 37. SDS gel of 2 nd helix mutants with WT phenotypes.....	95
Figure 38. Agarose gel of defective mutants in predicted 2 nd helix.....	96
Figure 39. SDS gel of defective mutants in predicted 2 nd helix.....	97
Figure 40. Representative EMs of 2 nd helix mutants.....	98

Figure 41. SDS gel of 2 nd helix mutants with portal and inactivated protease.....	100
Figure 42. Agarose gel of 2 nd helix mutants with portal and inactivated protease.....	101
Figure 43. Helical model of 2 nd predicted helix of the delta domain.....	103
Figure 44. LIM 49 shows a portal and protease incorporation defect.....	105
Figure 45. E363A produces cleaved mcp in the presence of the portal.....	107
Figure 46. Miniprohead prep of K63A shows a cleavage defect.....	108
Figure 47. Representative EM image of K63A.....	109
Figure 48. K63A expressed with the portal and inactivated protease.....	110
Figure 49. K63A only produces cleaved mcp when the portal is present.....	112
Figure 50. Double mutant D135G (gp3)/A65E (gp5) rescues functionality.....	116
Figure 51. Sequence alignment of <i>C. diphtheria</i> phage and HK97 portal.....	118
Figure 52. HK97 portal homology model.....	119
Figure 53. Del1 is defective in protease incorporation.....	126
Figure 54. Miniprohead prep of 1 st predicted helix mutants.....	128
Figure 55. Representative EM images of 1 st helix mutants.....	129
Figure 56. N-terminal mutants expressed with the portal and inactivated protease.....	131
Figure 57. LIM20 causes a protease incorporation defect.....	133
Figure 58. Proposed model showing the multifunctional roles of the delta domain.....	138
Figure A-1. K92A causes a cleavage defect.....	157
Figure A-2. K92A can incorporate the portal and protease.....	159
Figure A-3. Dilutions of K92A with portal and inactivated protease.....	160
Figure A-4. Representative EM image of K92A with portal and inactivated protease.....	163
Figure A-5. Higher magnification EM image of pVP0 g4 (H65A) K92A.....	164

Figure A-6. K92A expressed with portal and active protease.....	166
Figure B-1. Miniprohead prep results of S88C.....	169
Figure B-2. S88C shows increased capsid stability.....	171
Figure B-3. Native gel shows S88C only dissociates with 1 M DTT.....	172
Figure B-4. Non-denaturing acrylamide gel shows S88C can form gp5 dimers.....	173

PREFACE

Thank you Roger, for giving me the great opportunity to work, learn, and grow in your lab. You have been a very kind and supportive mentor, helping to encourage and guide me throughout my graduate career. Your knowledge and love for all things phage and non-phage are inspiring. Thank you for giving me the opportunity to travel, present my work, learn from, and meet other scientists. Thank you to my committee members, James, Jim, Tony, and Tom for all of your support, insight, and great ideas during our meetings. You have really helped my project and I grow. Thank you Bob, for all of your guidance and ideas about experiments and modeling. I really appreciate our discussions, whether it be about food, or weird gel results. Thank you Susan and Craig, for all of your advice and insights during lab meetings.

Thank you Megan, Rob, Julia, Paul, Annemarie, Moulika, Jenn, Linda, Gaibo, and Jonathan, for making the lab silly and fun. It has been great working with and/or teaching you all. Thank you to Brian, Rob, Welkin, Dan, Jianfei, Alexis, Josh, Patricia, Jacob, Suvrajit, and Aletheia for making my time in the lab and Pittsburgh so memorable. Your helping hands, support, and friendship mean so much to me. Thank you Rob, Brian, Nicole, Ching, and Patricia, for always being there when I needed life advice, science advice, or good food and company.

I would also like to thank my wonderful family, and especially my husband Cecil, for all of their love, non-stop support, and encouragement through the hard times and the good times.

1.0 INTRODUCTION

1.1 BACTERIOPHAGES AND THEIR LIFECYCLES

Bacteriophages are the most abundant organism on our planet with their total numbers estimated to be about 10^{31} particles (Roger W. Hendrix and Casjens 2006). They have been discovered in almost every type of habitat, possess a wide range of structural differences, and play important roles in controlling bacterial populations and evolution (Wommack and Colwell 2000; Suttle 2007). dsDNA tailed phages belong to the order *Caudovirales* and are grouped by taxonomists into three families, *Podoviridae*, *Myoviridae*, and *Siphoviridae*. Podoviruses have short stubby tails, Myoviruses have long contractile tails, and Siphoviruses have long flexible tails. The general structure of these bacteriophages consists of a capsid (icosahedrally symmetric, prolate, or filamentous) protein shell where the genetic material is stored, a tail for contacting the host, and a connector or portal protein which connects the head to the tail and through which the genetic material is packaged and later injected (Ackermann 2006). During bacterial infection, the phage uses its tail fibers to contact and attach to host protein receptors. After injecting its genome, it usurps the host cell machinery for replication (Mosig and Eiserling 2006). There are two types of phage lifecycles, some phages are temperate and can cycle between lytic and lysogenic phases, while others are purely lytic. During a lysogenic phase, the phage remains dormant after its genome has integrated into the host genome and replicates along with the host.

Upon cellular stress responses, the phage can activate its lytic cycle by excising itself from the host chromosome, replicate its genome, assemble new phage particles, and lyse the host for release into the environment. On the other hand, lytic phages never integrate, and lyse the host after phage assembly is complete (Little 2006).

1.2 CAPSID ASSEMBLY AND THE USE OF SCAFFOLDING PROTEINS

Bacteriophage capsid assembly is a complex and highly coordinated process involving the interaction of many different structural components and chaperone proteins. Capsids are icosahedral and isometric in most cases, or prolate in shape, though still based largely on icosahedral symmetry. They may include ‘decoration’ proteins as well, which are proteins that help to stabilize the capsid during genome packaging (Dokland and Murialdo 1993). The icosahedron is made of 20 equilateral triangular faces and 12 vertices, with 2-, 3-, and 5-fold rotational symmetries. The simplest capsid would be composed of 12 pentamers, and have a total of 60 subunits. In this case, all 60 subunits could be placed in strictly equivalent positions. The introduction of hexamers into the capsid means that some subunits can no longer be placed in equivalent positions; their relations to each other are now described as quasi-equivalent. The theory of quasi-equivalence uses the triangulation number (T number) to characterize viral capsid size. The smallest capsid would have a triangulation number of $T=1$. The formula for the T number is $h^2 + hk + k^2 = T$ (Caspar and Klug 1962). h and k are integers which indicate the number of steps, in two directions, on the icosahedral capsid to get from one pentamer to another. “Steps” are defined as a jump between two adjacent vertices by stopping on hexavalent capsomers. In an icosahedral capsid, the triangulation number represents the number of subunits

in an “asymmetric unit”. The capsid can be described as 60 such asymmetric units, arranged in icosahedral symmetry. Based on this theory and equation, not all numbers are possible triangulation numbers. For larger capsids with bigger T numbers, it would be more advantageous for the phage to have more subunits rather than bigger subunits, possibly to increase protein folding efficiency and efficacy. The most abundant T number discovered to date is T=7 (Jianfei Hua, Bob Duda, personal communication), and this includes the capsid of phage HK97, the subject of this thesis.

Capsid assembly is very similar among dsDNA bacteriophages and herpesviruses (Casjens and Hendrix 1988; Homa and Brown 1997). In general, bacteriophage capsid assembly requires the coordination of a number of structural and chaperone proteins (Dokland 1999; Peter E. Prevelige and Fane 2012). Most dsDNA phage capsids are composed of one type of capsid protein subunit that forms pentamers and hexamers. Phage T4 has two different types of capsid proteins, one that produces the hexamers, and a different though similar protein that produces the pentamers (van Driel, Traub, and Showe 1980). With the aid of phage scaffolding proteins, the capsid proteins assemble into hexamers and pentamers, which then assemble along with portal protein into a procapsid, the immature form of the capsid. After assembly, the scaffolding protein leaves the procapsid, either intact or more commonly following proteolysis by a phage-encoded protease, resulting in an empty capsid. DNA is then packaged through the portal, which causes expansion of the shell through conformational changes of the subunits, to form the mature capsid, commonly referred to as the head. This genome-filled capsid can then attach to the separately assembled tail to create a phage (Casjens and Hendrix 1988; Hendrix and Garcea 1994; Casjens 1997).

Scaffolding proteins aid assembly by ensuring the proper size and shape capsid. There are two classes of scaffolding proteins, external, and internal, and some viruses utilize both (Dokland 1999). They are present during the initial stages of assembly but are absent in the mature virion (Dokland 1999; Jonathan King and Casjens 1974; Casjens and Hendrix 1988). The scaffolding proteins take up space inside the capsid, suggesting that another role scaffolding proteins play is to occupy space and exclude cellular components from being incorporated into the assembling capsids (Casjens 1997; Earnshaw and Casjens 1980). Internal scaffolding proteins are predicted to be elongated in structure with their C-terminal ends interacting with the internal surface of the capsid shell and the N-terminal ends facing towards the interior of the capsid (Dokland 1999; Zhou et al. 1998). They are mostly α -helical in secondary structure (Morais et al. 2003; Tuma et al. 1996; Dokland 1999; Prevelige and Fane 2012) but are also quite flexible, which makes structure determination difficult, whether by crystallography or electron microscopy. The N-terminal region of the phi29 scaffolding protein has been crystalized and the structure solved. This shows a mostly α -helical and coiled coil structure (Morais et al. 2003). The C-terminal ends of the scaffolding protein, which are closer to the interior surface of the shell, are more ordered than the regions of the scaffolding protein at the center of the capsid (Thuman-Commike et al. 1996). In P22, the C-terminal capsid binding domain of its scaffolding protein was solved by NMR and showed a helix turn helix motif (Sun et al. 2000).

In phages with known scaffolding proteins, one scaffolding protein can interact with several capsid proteins during assembly. For P22, there are about 250 scaffolding molecules that interact with the 415 capsid proteins (King and Casjens 1974). However, 120 molecules of scaffold are required for assembly (Prevelige, Thomas, and King 1988), which exist mostly as dimers (Parker et al. 1997), though monomeric forms are required for complete capsid assembly

in vitro (Tuma et al. 1998). In T7, about 110-140 copies of the scaffolding protein interact with the 415 copies of capsid proteins. They are visible in cryoEM reconstructions as small protrusions (“nubbins”) underneath the hexamers (Cerritelli et al. 2003). During P22 assembly, the capsid and scaffolding proteins assemble together in the growing shell (Prevelige et al. 1993), their interactions allowing for proper assembly (Thuman-Commike et al. 1996). After exit from the capsid, the intact scaffolding proteins are recycled for further rounds of assembly (King et al. 1973). There are regions of the hexameric subunits with projections that extend towards the interior of the capsid. These extensions are possible connection points between the capsid proteins and the scaffolding proteins. In this case, scaffolding proteins are believed to be arranged as dimers underneath the hexons and five copies underneath the pentons (Thuman-Commike et al. 1996). Herpes simplex virus assembly is very similar to those of dsDNA phages (Casjens and Hendrix 1988) but has a scaffolding like core, which the capsid proteins assemble around (O’Callaghan, Kemp, and Randall 1977; Newcomb and Brown 1991; Rixon 1993).

In a number of dsDNA phage and herpesvirus, when the scaffolding protein is not present, or is mutated, capsid assembly fails to occur or abnormal tubes and irregular shaped structures, referred to as “monsters”, are made (Cerritelli and Studier 1996; Earnshaw and King 1978; Hagen et al. 1976; Lee and Guo 1995; Roeder and Sadowski 1977). In some cases, polyheads (Howatson and Kemp 1975; Kellenberger 1980) or smaller than normal sized capsids are made (Earnshaw and King 1978; Thuman-Commike et al. 1998; Choi et al. 2006). Not only can the lack of scaffolding protein or mutant scaffolding protein affect the capsid shape and size, but it can also affect the inclusion of other important proteins in the capsid. Previous P22 studies show that mutants in the scaffolding protein affect incorporation of pilot and portal proteins in the capsid and the release of pilot proteins later (Bazinet and King 1988; Greene and King 1996).

Mutants in the scaffolding protein can also block later release of the scaffold after assembly is complete, which prevents the DNA packaging step (Thuman-Commike et al. 1996). The incorporation of core proteins in T4 is also dependent on the scaffolding protein (Paulson, Lazaroff, and Laemmli 1976). Mutations in the herpesvirus scaffolding protein have been shown to affect portal incorporation (Newcomb, Homa, and Brown 2005).

1.3 HK97 CAPSID ASSEMBLY AND THE DELTA DOMAIN

HK97 is a dsDNA temperate phage that infects *Escherichia coli*. It was discovered in Hong Kong in 1980 (Dhillon et al. 1980) and is very similar to the well-studied phage Lambda. HK97 is made of an icosahedral capsid with a triangulation number of 7 and a long flexible tail (Dhillon et al. 1980) (Figure 1). A schematic of HK97 capsid assembly is shown in Figure 2. HK97 capsids are composed of three genes: gene product 3 (gp3) which encodes the 47 kDa portal, gene product 4 (gp4), which encodes the 25 kDa protease, and gene product 5 (gp5), which encodes the 42 kDa major capsid gene (mcp) (Duda, Martincic, and Hendrix 1995).

With the aid of chaperonin proteins GroEL and GroES, the mcp folds and assembles into hexamers and pentamers, collectively called capsomers (Popa, M 1988; Ding et al. 1995; Duda, Martincic, and Hendrix 1995). 415 capsomers, along with the 12 subunit dodecameric portal protein interact with approximately 120 copies of the phage encoded protease to build the immature procapsid, Prohead I. Prohead I is about 470 Å in diameter, has a fairly bumpy surface, and the hexamers have a skewed symmetry (Conway et al. 1995). Once assembly is complete, the protease becomes activated and the 42 kDa mcp is processed to 31 kDa. 102 amino acids have been removed to produce this truncated mcp product (Duda, Hempel, et al. 1995). Regions

of the major capsid protein that are not present in the mature structure were termed delta domains, a term originally used to describe the corresponding part of the Phage T4 mcp (Tsugita, Black, and Showe 1975). HK97 possess a delta domain instead of a separate scaffolding protein. Proteolysis produces Prohead II, which is similar in structure to Prohead I, but the interior has been remodeled (Conway et al. 1995) by the removal of the delta domain and the protease (Duda, Martincic, and Hendrix 1995). Like most dsDNA phages, the HK97 genome is packaged through the portal and fills the capsid (Bazinet and King 1985). During packaging, the capsid undergoes a series of structural changes and expands. The capsid shell becomes thinner and more angular, and the hexamers become symmetrical (Lata et al. 2000). The capsid subunits autocatalytically crosslink, to create a catenated, chainmail like pattern throughout the mature capsid, known as Head II (Popa et al. 1991; R L Duda, Martincic, et al. 1995; Robert L. Duda 1998; William R. Wikoff et al. 1999; W R Wikoff et al. 2000; Helgstrand et al. 2003; Gan et al. 2004). The enclosed volume has increased by about 100% (Conway et al. 1995). In phage λ , expansion follows directly after DNA packaging begins (Hohn 1983) and this is predicted to be true for HK97 also. In dsDNA phages, the expansion step is believed to stabilize the capsid (Steven et al. 1976; Ross et al. 1985; Steven et al. 1992; Conway et al. 2001; Teschke et al. 2003; Ross et al. 2005; Duda et al. 2009). The mature capsid is now ready to attach to the tail, which is assembled simultaneously in a separate pathway.

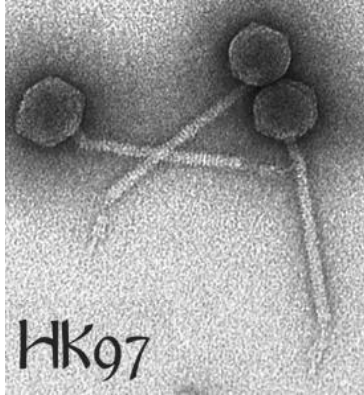


Figure 1. Bacteriophage HK97

Transmission electron micrograph of HK97 stained with 1% Uranyl Acetate. HK97 consists of an icosahedral T=7 capsid, long tail, and tail fibers. Image taken by Bob Duda.

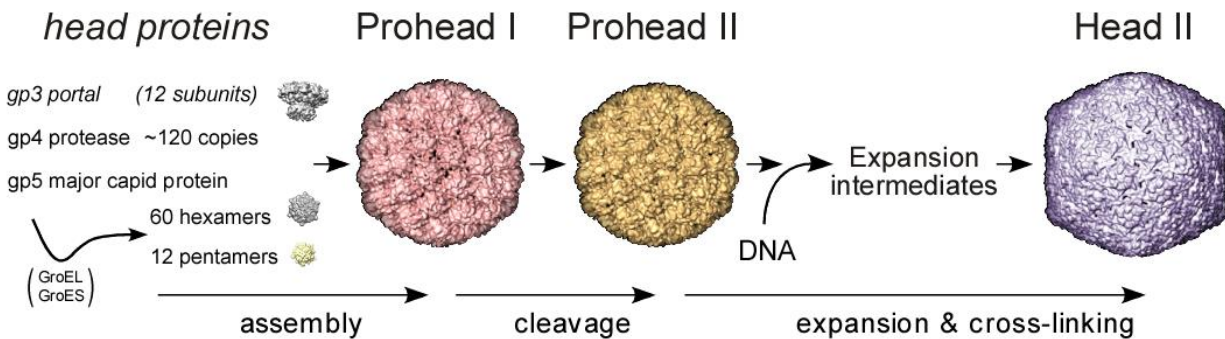


Figure 2. Schematic of the HK97 capsid assembly pathway.

Capsid assembly involves the interaction of three gene products: gp3 (portal), gp4 (protease), and gp5 (major capsid protein, mcp). With the aid of chaperone proteins, the capsid proteins assemble into hexamers and pentamers, which are collectively called capsomers. The capsomers, along with the portal and protease form the icosahedral immature capsid, Prohead I. Internal cleavage by the protease creates the empty Prohead II shell. DNA is packaged through the portal, causing a series of expansion and cross-linking steps to produce the mature capsid, Head II. This figure was made by Bob Duda

HK97 capsid assembly and maturation has been studied in great detail, however, not much is known about the initial steps of assembly, in particular, about the role that the delta domain plays in assembly. Phages T5, D3, and phi1026b also possess delta domains instead of separate scaffolding proteins (Effantin et al. 2006, Duda and Conway, unpublished data). Raman spectroscopy shows that this domain in HK97 is mostly α -helical (Benevides et al. 2004). The delta domain secondary structure is composed of three predicted α -helical regions and a β -sheet region near the C-terminal end. However, like other known scaffolding proteins, this domain is flexible and has so far resisted all attempts to determine its structure at high resolution. The 1st and 2nd predicted helices have a high propensity for coil coiled interactions (Conway et al. 1995). The published X-ray structure of Prohead I revealed little about the delta domain, which was found to be disordered compared to the rest of the major capsid protein. Samples of soluble purified delta domain were studied using NMR spectroscopy. However, the delta domain seemed to aggregate, possibly due to the highly α -helical nature of this protein. Upon cryo-Electron Microscopy of Prohead I, low resolution images of the delta domains show them to be shaped as blob-like densities protruding from the internal surface of the capsid. The delta domains are grouped as one 'blob' underneath the pentamers, and 'two' blobs underneath the hexamers (Conway et al. 2007). The delta domain holds the same position in the genome as most scaffolding protein genes, directly upstream of the capsid gene. While some scaffolding proteins have a C-terminal capsid binding domain (Dokland 1999), the C-terminal end of the delta domain is connected to the rest of the capsid protein. The lack of structural information about the delta domain led us to study the functional roles of this domain using biochemical and genetic methods in plasmid and phage systems.

1.4 HK97 MODEL SYSTEM

The HK97 capsid protein fold seems to be important in an evolutionary sense because it is found in prokaryotic, eukaryotic, and archaeal viruses and also in capsid like particles called encapsulins (Akita et al. 2007; Sutter et al. 2008; Duda, Oh, and Hendrix 2013; Suhanovsky and Teschke 2015). HK97 has been used as a model system to study capsid assembly due to its ease of expression requiring only a small number of genes. Because there is no separate scaffolding like those found in other phages, HK97 Prohead I can assemble *in vitro* with only the major capsid protein (Duda, Martincic, and Hendrix 1995; Xie and Hendrix 1995). Also, expression of the major capsid and protease proteins are sufficient to assemble Prohead II particles (Duda, Martincic, and Hendrix 1995). Like Phage P22, *in vitro* HK97 assembly is independent of the presence of the portal (Prevelige, Thomas, and King 1993; Duda, Martincic, and Hendrix 1995; King, Lenk, and Botstein 1973; King and Casjens 1974; Bazinet and King 1988). *In vitro* expression of HK97 produces a high concentration of capsid proteins, which are able to spontaneously assemble. During phage infection, it is believed that the portal acts as a nucleator of assembly (Hendrix 1998). Capsid expansion can be achieved spontaneously *in vitro* when incubated with certain solvents. For example, urea, chloroform, n-butanol, Guanidine hydrochloride, pH 4 buffer, and room temperature incubation of proheads in SDS gel buffer cause expansion and/or cross-linking (Duda, Hempel, et al. 1995). The capsid assembly process can be manipulated in multiple ways, allowing us to study different aspects of capsid assembly and maturation.

For most of the studies described here, HK97 capsid genes are expressed from a T7 promoter-containing plasmid in *E. coli* strain BL21(DE3)pLysS (Studier et al. 1990; Studier

2005). Different combinations of HK97 genes were expressed for biochemical and complementation tests. Some of the plasmids that I used for my mutational analyses are pV0 and pVP0 g4 H65A. The WT (i.e., wild type sequence for the included HK97 DNA) pV0 plasmid produces the protease and major capsid protein, which are able to produce proheads that can cleave and expand to heads. A schematic of the pV0 plasmid is shown in Figure 3. pVP0 g4 H65A is a plasmid that contains the portal, protease, and major capsid genes. However, there is an inactivation mutation (H65A) in gene 4, the protease, which prevents the cleavage event because it inactivates the proteolytic active site. Therefore, the capsids are trapped in the Prohead I stage. A more detailed description of the different plasmids that I have used can be found in the Materials and Methods section. Sub-cloning mutant fragments into our expression plasmids allows us to test the effects of delta domain mutations on capsid assembly.

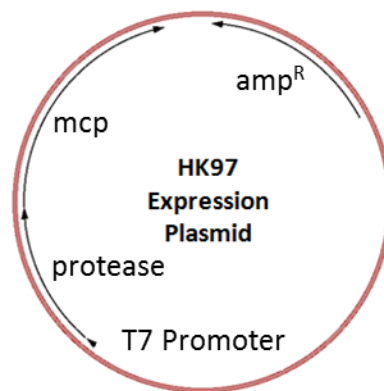


Figure 3. Schematic of WT pV0 plasmid.

Plasmid expression is driven by a T7 promoter. The protease and major capsid genes (mcp) are sufficient to produce Prohead II. This expression plasmid carries an ampicillin resistance marker (ampR). Delta domain mutations are sub-cloned into the expression plasmid and tested in protein preps. Plasmids including the portal gene, and/or having an inactivated protease are also used to test the effects of mutations on capsid assembly.

A useful biochemical tool that we use to study capsid mutants is gel electrophoresis. Capsid assembly intermediates can be differentiated on native agarose gels; free capsomers, proheads, and heads run at different mobilities (Figure 4). Mutant phenotypes are easily discernable from WT phenotypes. If a mutant produces only capsomers, we can predict that the mutation has disrupted the ability of the capsid proteins to assemble correctly. If only proheads are present, then we can predict that the mutation has disrupted the cleavage of the delta domain. Denatured protein samples electrophoresed on SDS gels provide useful information about mcp processing. Full length mcp is 42 kDa, while properly cleaved and processed mcp runs at 31 kDa. We can compare mutant and WT protein samples to see if a mutation has affected delta domain cleavage. SDS gel data is complementary to agarose gel data to show how a mutation affects capsid assembly. Along with these biochemical tests, complementation assays using expression plasmids and phage with amber mutations allow us to test for mutant protein functionality. Negative stain electron microscopy is also used to assay the assembly state of mutants.

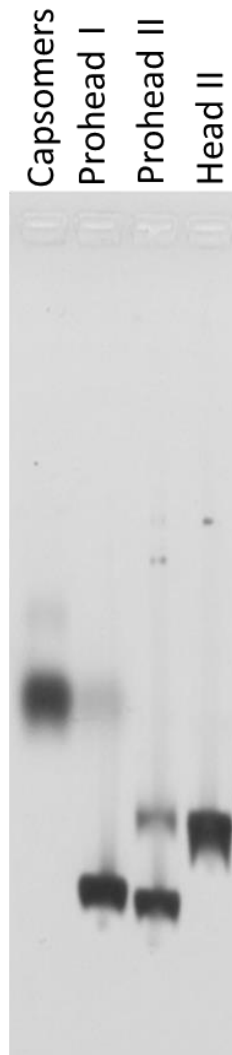


Figure 4. Representative native agarose gel of HK97 protein expressed from plasmids

Purified HK97 protein assemblies have different mobilities on native agarose gels. This representative 0.8% agarose gel contains purified capsomers, Prohead I, Prohead II, and Head samples. Capsomers (hexamers and pentamers) form a fuzzy round spot, which runs slower than assembled particles in this gel. Prohead I and Prohead II bands have similar mobilities and run faster. Some of the Prohead II sample has expanded to form Heads. Heads particles run slightly slower than Proheads.

Using this HK97 plasmid expression system, we can manipulate the delta domain and gain insight about the initial capsid assembly process. HK97 capsids have 415 delta domains, one connected to each capsid subunit. How do these 415 domains interact inside the capsid? Does the delta domain play a scaffolding like role? And if it does, how does it coordinate the interaction of 500+ copies of capsid, protease, and portal proteins to form an icosahedral capsid. How does one protein function in the assembly of a macromolecular structure? By studying how the delta domain functions, we can learn more about the specific characteristics of scaffolding proteins which allow them to help form large protein complexes.

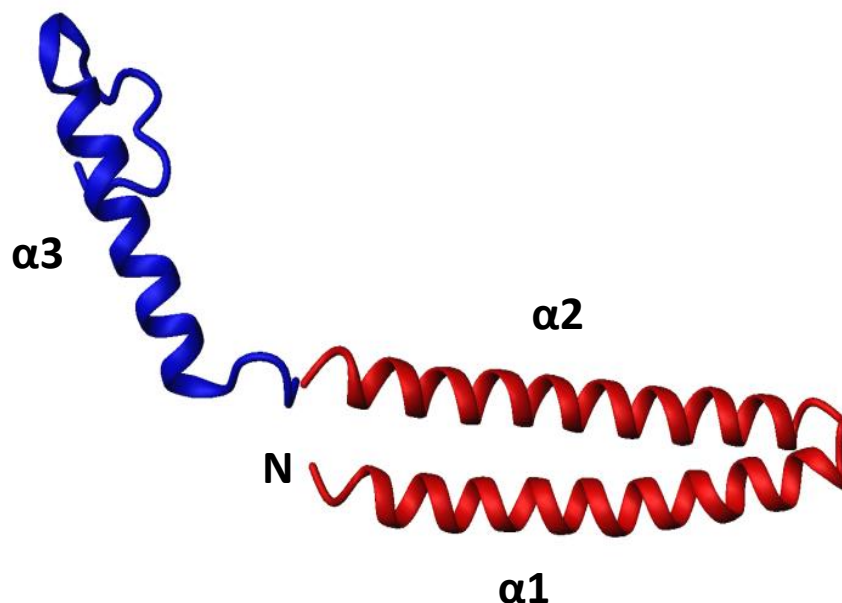


Figure 5. Proposed model of the HK97 Delta Domain

This model shows the three predicted helical regions of the delta domain, labeled $\alpha 1$, $\alpha 2$, and $\alpha 3$. The two red helices are pictured in a coiled coil conformation because these two helices have a high predicted propensity for making coiled coil interactions (Conway et al. 1995) (Model courtesy of Alasdair Steven). N: N-terminal, C: C-terminal.

In this document, I will describe the different types of mutations made in the delta domain and how they affect capsid assembly. The effects of a series of deletions, point mutations, and small insertions in the delta domain will be discussed. From these mutational studies, it is clear that the delta domain plays multiple roles in assembly. Not only is this domain required for capsid protein solubility, it is important for ensuring proper size and shape of the capsid. Like other scaffolding proteins, the delta domain plays a role in the incorporation of other proteins into the capsid. Interestingly, different regions of the domain are responsible for these different roles. Chapter 2 discusses how delta domain deletions and linker insertion mutations show that the delta domain is important for proper protein expression and assembly. Also, point mutations and a 'hinge' region deletion near the C-terminal end of the delta domain show that the delta domain is important for proper capsid geometry and size. Chapter 3 discusses how mutations in the N-terminal region of the delta domain affect the incorporation of the protease proteins and mutations in the middle or 2nd predicted helical region of the delta domain affect the incorporation of the portal into the capsid. The different roles of the delta domain map to specific regions, showing that the delta domain is very dynamic, allowing it to play multiple functional roles during assembly. The structure of the delta domain and the specific interactions that it is involved with allows it to function and interact with a variety of different proteins to ensure proper assembly. The appendices will include details on a point mutation of the delta domain that has a unique phenotype, and touch briefly on studies of delta domain stabilization.

2.0 THE DELTA DOMAIN IS REQUIRED FOR CASPSID PROTEIN SOLUBILITY, CAPSID ASSEMBLY, AND SIZE

2.1 INTRODUCTION

It has been shown in other dsDNA phages and herpesviruses that scaffolding proteins are required to assemble the proper sized and shaped capsid. In studies where the scaffolding protein is absent, the major capsid protein (mcp) assembles incorrectly and forms abnormal structures (Cerritelli and Studier, 1996; Earnshaw and King, 1978; Hagen et al., 1976). The common structural characteristics between delta domains and scaffolding proteins lead us to hypothesize that the delta domain is playing a scaffolding like role in assembly. One fundamental question that we want to answer is whether the delta domain is required for capsid assembly? In order to answer this, we can remove the delta domain and test if the capsid protein can still function correctly to assemble proheads.

Crystal Moyer, a previous student in the lab, deleted the delta domain from the capsid protein in the HK97 expression plasmid construct (pV0), which contains the protease and capsid genes. The first deletion, which we call pNoDelta1 is a full length deletion of the delta domain. The Methionine start codon was moved directly upstream of Serine-103 in the expression plasmid. Upon protein expression, radiolabelling experiments were conducted and the pellet and supernatant samples were collected over time (1, 5, 45 minutes) to test for mcp expression and

processing. The resulting soluble and pellet fractions were also collected and analyzed by electrophoresis. Although WT capsids are well expressed and fully cleaved (31 kDa band), pNoDelta1 showed barely detectable protein on the SDS gel, even after 45 minutes (Figure 6B). A second construct, pNoDelta2, was made which included the T7 ribosome binding site and the first four codons (MASMT) of the bacteriophage T7 major capsid protein sequence just directly upstream of the relocated start codon (Figure 6A). These additions have been previously shown to enhance protein production in plasmid expression studies (Olins and Rangwala 1989; Olins et al. 1988). In the radiolabelling experiments, WT showed cleaved and soluble mcp. pNoDelta2 showed a 31 kDa mcp band, which was mostly present in the pellet fraction (Figure 6B) (Oh et al. 2014), suggesting it is insoluble. These radiolabelling experiments suggest that the delta domain may play some chaperone-like function with regards to proper capsid protein folding. To delve more deeply into the role of the delta domain in capsid assembly, I studied the effects of different mutations on assembly in a plasmid-based system. In total, 63 distinct mutations have been made in the HK97 delta domain; a majority of these are single point mutations, but some are small insertions and deletions. About half of these mutations cause major defects in regards to protein solubility, capsid structure and assembly, or portal and protease incorporation, indicating that the delta domain plays major multiple roles in capsid assembly.

A.

aaggagatatacat MASMT

SLGSDAD	SAGSLIQPMQ	IPGIIMPGLR	RLTIRDLLAQ	GRTSSNALEY	150
VREEVFTNNA	DVVAEKALKP	ESDITFSKQT	ANVKTIAHWV	QASRQVMDDA	200
PMLQSYINNR	LMYGLALKEE	GQLLNGDGTG	DNLEGLNKVA	TAYDTSLNAT	250
GDTRADIIAH	AIYQVTESEF	SASGIVLNPR	DWHNIALLLK	NEGRYIFGGP	300
QAFTSNIMNG	LPVVPTKAQA	AGTFTVGGFD	MASQVDRMD	ATVEVSREDR	350
DNFVKNMLTI	LCEERLALAH	YRPTAIKGT	FSSGS		385

B.

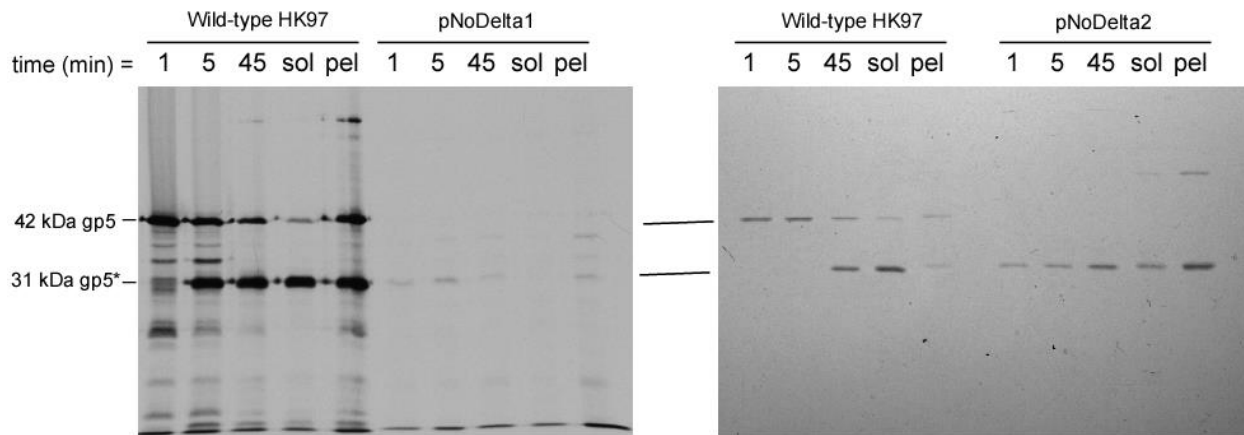


Figure 6. Radiolabelling data of full length deletions (pNoDelta1, pNoDelta2) of the delta domain

A) Sequence of the pNoDelta2 deletion mutant. The T7 RBS (underlined) and tag upstream was added upstream of the mature capsid protein sequence. B) Radiolabelled protein gel comparing WT major capsid protein (mcp) (gene product 5= gp5), pNoDelta1, and pNoDelta2 expression. Samples collected 1, 5, and 45 minutes after induction, along with the soluble and pellet fractions, were loaded on an SDS gel. WT showed cleaved (31 kDa) mcp appearing after 45 minutes, which was mostly in the soluble fraction. pNoDelta1 produced barely detectable protein that was mostly in the pellet fraction. pNoDelta2 produced higher levels of 31 kDa protein but was found mostly in the pellet fraction. The other bands visible in the gel may be from non-specific binding from the labeling experiment

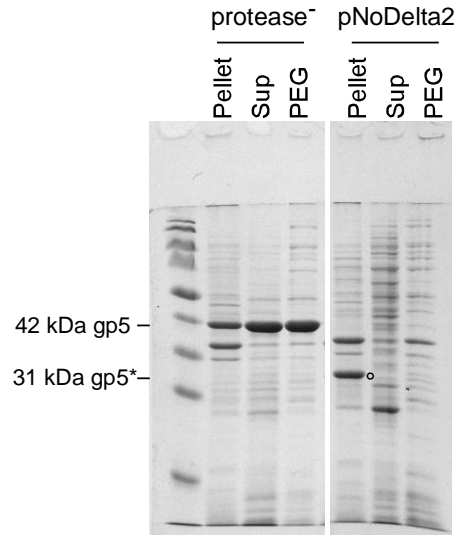
2.2 RESULTS

2.2.1 Full length delta domain is required for capsid protein solubility, assembly, and size

Radiolabelling experiments of the pNoDelta plasmids provided incomplete evidence that HK97's delta domain is essential for assembly. To pursue this further, I conducted small scale protein expression experiments (miniprohead preps) to test the full length deletion construct, pNoDelta2. The miniprohead preps are based on F. William Studier's method of auto-induction (Studier 2005). Three samples were collected from each construct: pellet, supernatant, and polyethyleneglycol (PEG) precipitate. A plasmid with the protease gene knocked-out (pVB) was used as a control. The control and mutant samples were loaded on a 12% low cross-linking SDS gel. The control produced uncleaved mcp as expected. pNoDelta2 produced an uncleaved mcp band in the pellet fraction only (indicated by circle) (Figure 7A). On native agarose gels, the control produced proheads. pNoDelta2 did not produce any obvious prohead or head bands (Figure 7B). There were also no capsomers visible on the agarose gel, suggesting that the delta domain is responsible for facilitating the formation of the earliest assembly form, capsomers.

Spot complementation tests were performed to test protein functionality. By comparing the mutant complementation results to the WT control, we can see how well the protein expressed from the plasmid is able to complement phages with an amber mutation in their capsid or protease genes. Dilutions of different phage mutants are spotted on soft agar lawns of cells expressing WT and mutant HK97 proteins. WT phage serve as a positive control and should be able to efficiently form plaques at all dilutions. A capsid gene amber mutant phage (*am1*) is used

A.



B.

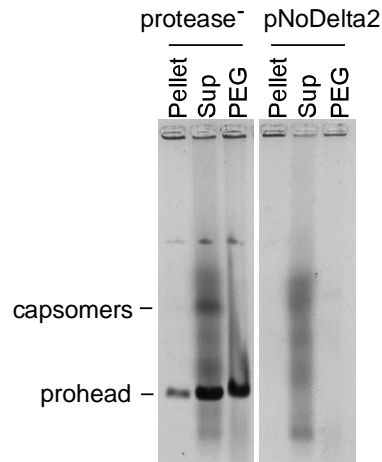


Figure 7. Miniprohead prep results of pNoDelta2 deletion

A) Pellet, supernatant, and PEG samples were run on an SDS gel. The protease⁻ control has a knocked-out protease gene, which produced only uncleaved mcp (42 kDa gp5) in all three fractions. pNoDelta2 produced cleaved mcp (31 kDa gp5*) in the pellet fraction only (indicated by circle). B) On a 0.9% agarose gel, protease⁻ produced prohead and capsomer bands (in the supernatant only). pNodelta2 did not produce any obvious HK97 structures. The smear of protein in the supernatant fractions correspond to cell host proteins and is commonly found in these crude preps.

to test if the capsid protein expressed from the plasmid is able to complement and efficiently form plaques. A protease gene amber mutant phage (*amU4*) is used to test if the protease protein expressed from the plasmid is able to complement and efficiently form plaques. An amber phage mutant in an unrelated gene (*amC2*) is used as a control. With pNoDelta2, the spot complementation tests show no detectable complementation (Table 1). Negative stain transmission electron microscopy (TEM) of the pNODelta2 pellet sample does not show any soluble assembly products, only cell debris, which supports the biochemical evidence that no soluble capsid products are expressed from this deletion mutant.

2.2.2 Different sized deletions prevent capsid protein expression and functionality

We know that the full length delta domain is required for capsid assembly, but will the delta domain be able to function with smaller deletions? Small deletions could show whether specific regions of the delta domain are important for specific aspects of capsid assembly. Four different sized deletions were made using the pV0 plasmid construct, all with a common starting point. Del1 removes residues 4-13, a portion of the first predicted helix. Del2 removes residues 4-29, a majority of the first predicted helix. Del3 removes residues 4-50, the first predicted helix and about half of the second predicted helix. Del4 removes residues 4-62, the first predicted helix and a majority of the second predicted helix. A schematic of the deletions are shown in Figure 8A.

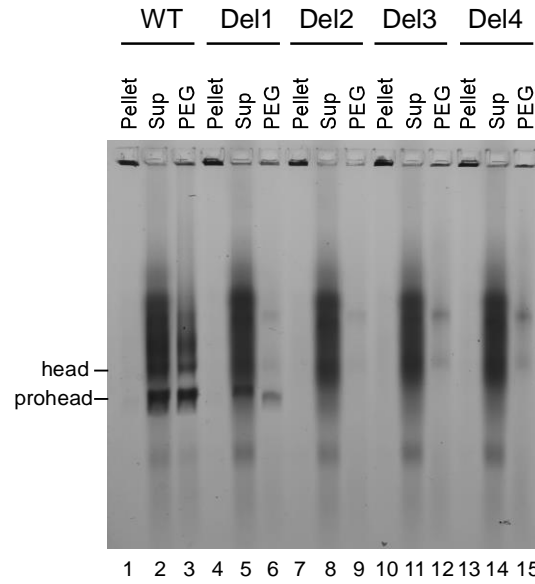
Miniprohead preps were again used to analyze the mutants. The pellet, supernatant, and PEG samples were run on agarose and SDS gels (Figure 8B, C) The WT control produced proheads and heads as shown in the agarose gel. Del1 was the only deletion which produces an

identifiable product on the agarose gel- a light prohead band. The other three larger deletions, Del2, 3, and 4, did not produce any obvious assembled structures in the agarose gel (Figure 8B). On the SDS gel, small circles denote the predicted band sizes for the deletion mutants. The WT control produced cleaved mcp. Del1 produced uncleaved mcp in all three fractions. Del2 did not produce any HK97 bands in any fractions in this experiment and when repeated (not shown). Del3 and Del4 produced mcp (of their expected sizes, denoted by circles) in their pellet fractions only (Figure 8C). In the spot complementation tests, all four deletion mutants were defective in complementing capsid gene amber phage, suggesting that these deletions are detrimental to capsid protein function (Table 1). Selected fractions containing truncated mcps from these deletions were examined by TEM. Del1 produced WT like procapsids whereas the other deletions did not produce any assembled structures. Even though Del1 is able to produce WT like proheads, the capsid protein made is nonfunctional and unable to incorporate into viable phage particles. The anomalous phenotype of Del1 will be discussed in further detail in Chapter 3. All four different-sized deletions in the delta domain render the capsid protein non-functional, suggesting that the full length of the delta domain is required for capsid protein solubility and proper capsid assembly. The next question we want to answer is if there are particular regions or residues of the delta domain that are critical for its function during capsid assembly.

A.



B.



C.

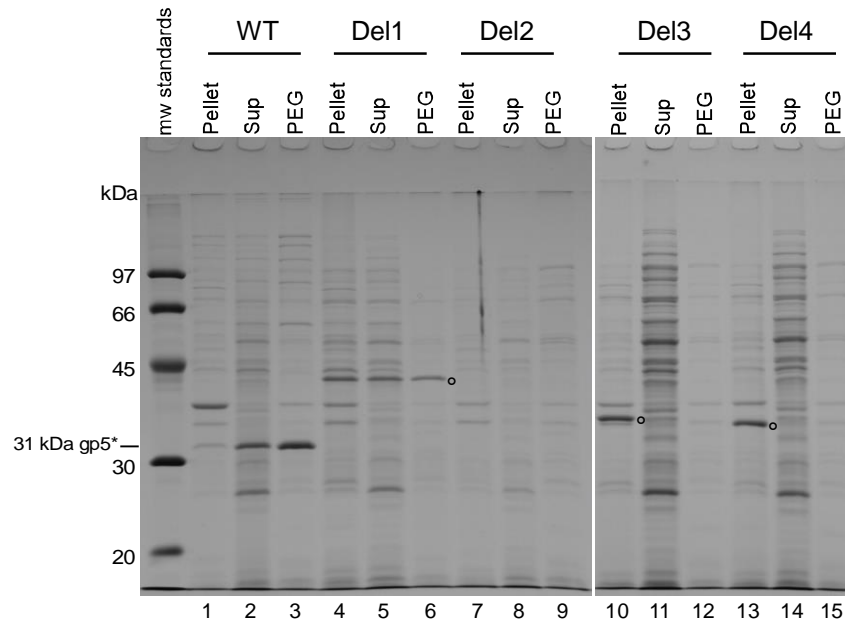


Figure 8. Different sized delta domain deletions are deleterious to capsid assembly

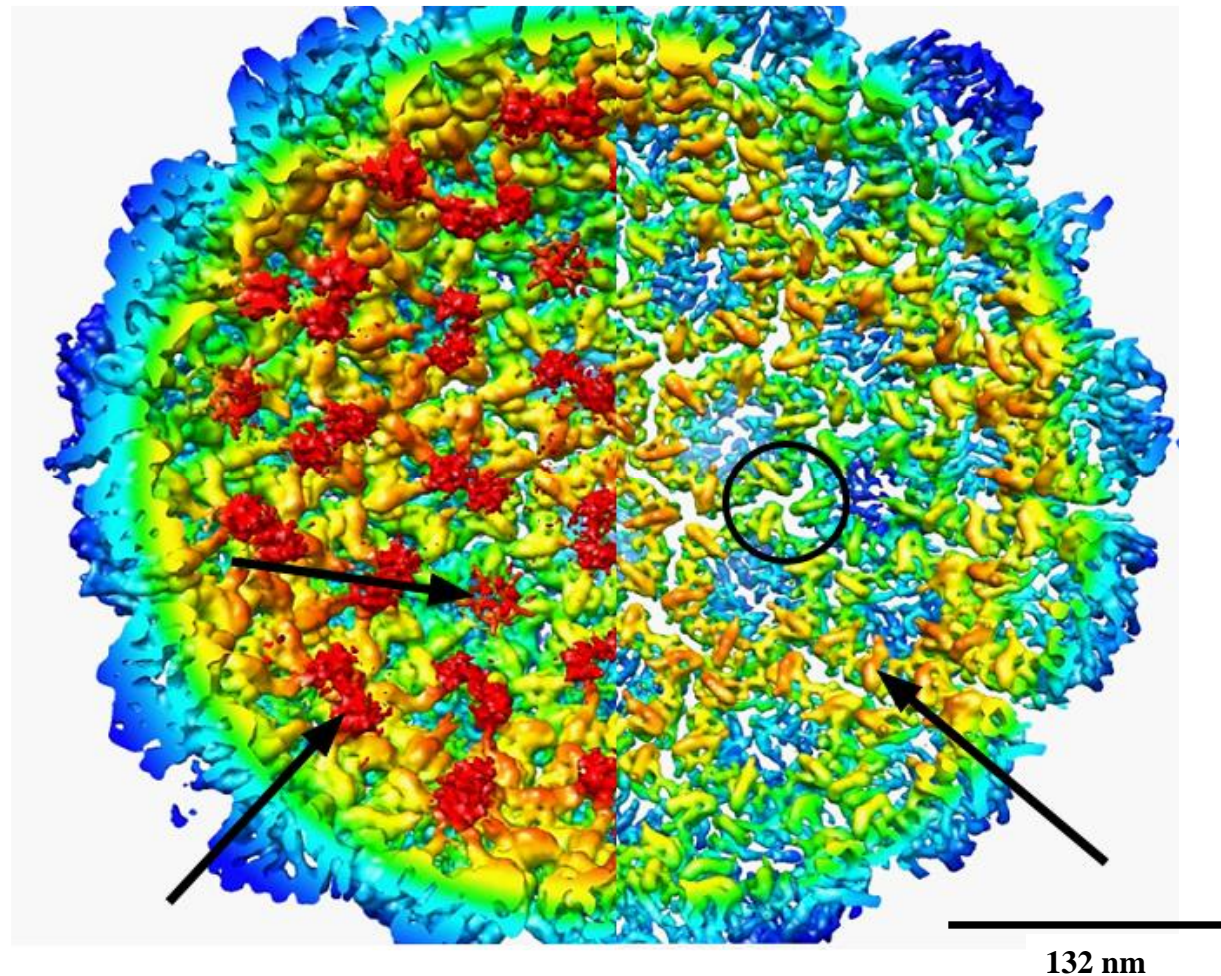
A) Schematic of the different sized deletions and the predicted secondary structure of the delta domain. B) 0.9% non-denaturing agarose gel of miniprohead prep samples of WT and deletions. WT produces proheads and heads. Del1 is the only deletion that was able to assemble into prohead like capsids. Del2, 3, and 4 did not produce any obvious structures. C) Pellet, supernatant and PEG fractions were precipitated with 10% TCA and run on a 12% low cross-linking SDS gel and stained with commassie. WT produced cleaved 31 kDa mcp, which was mostly in the PEG. Del1 produced only uncleaved mcp in all fractions (denoted by small circle in lane 6). Del2 was never able to express mcp, even after multiple trials. Del3 and Del4 show uncleaved mcp at their expected sizes in the pellet fractions only (small circles in lane 10 and 13).

2.2.3 Mutations in the delta domain's C-terminal region affect capsid assembly and geometry

Available structural information was used to design informative mutants in the delta domain. An HK97 Prohead I X-ray model (3QPR, pdb) with 5.2Å resolution was available (Huang et al. 2011), however, the delta domain was not ordered in the crystal and is therefore not present in the model. A Prohead I density map (unpublished) reconstruction made by James Conway can be used to identify potential mutant targets. Figure 9 shows an internal view of the capsid, as if it were cut in half. The red blob-like clusters underneath each pentamer, and the dimer of blobs underneath each hexamer represent the delta domain densities. Compared to the rest of the capsid protein, the delta domain is less dense in density maps because it is less ordered. In the Prohead I reconstruction, there are tubes of density, one per subunit, which lie against the internal capsid surface and are arranged in a spoke-like pattern (highlighted in Figure 9A). We call these densities 'spokes' and believe them to contain the C-terminal end of the delta domain. It is possible they also represent part of the N-arm of the major capsid protein, a region which is also not present in the X-ray model. While the majority of the delta domain is less ordered and only partly visible as the 'blob' density, the spoke region that is interacting with the internal surface of the capsid subunit is apparently more stable. We believe these to contain part of the delta domain because they are present in the Prohead I structure, but absent in the reconstructed Prohead II (Steven et al. 2005).

The densities visible on the interior of the Prohead I map allow us to infer delta domain residues which could be responsible for making contacts between capsomers. Upon inspection of these spokes, there appears to be a possible 3-spoke interaction between a pentamer and two

A.



B.

MSELALIQKA	IEESQQKMTQ	LEFDAQKAEIE	STGQVSKQLQ	SDLMKVQEEL	50
aa	aa	aa	aa	aa	
TKSGTRLFDL	EQKLAGSAEN	PGEKKSFSER	AAEELIKSWD	GKQGTFGAKT	100
aaaaaaaaaaaaaaaaaaaaaaaaaaaaaaaa	aaaaaaaaaaaaaaaaaaaaaaaaaaaaaaaa	aaaaaaaaaaaaaaaaaaaaaaaaaaaaaaaa	aaaaaaaaaaaaaaaaaaaaaaaaaaaaa↑↑	bbbbbbb	
FNK					
bbbb					

Figure 9. Internal spoke like densities may be possible inter-capsomer interaction sites.

A) Cut-away view of the internal densities of the Prohead I reconstruction (James Conway). This density map is contoured so that the left half of the radially colored surface is rendered using a lower cutoff value to include less dense (less ordered) parts of the map. The yellow and orange spoke-like regions and the spidery blobs represent the delta domain densities (arrows). The rest of the major capsid protein is much more ordered compared to the delta domain. It is possible that the 3rd predicted helical region is responsible for some of the spoke density. A possible inter-capsomer 3-spoke interaction site is highlighted by the circle. B) The delta domain protein sequence with predicted secondary structure. Residues W89 and D90 lie directly after the 3rd predicted helix (arrows) and are large or charged residues which may be involved with the 3-spoke interaction between capsomers. (a=predicted alpha helix, b= predicted beta sheet). The scale bar represents 132 nm.

hexamers and between three hexamers (circle in Figure 9A). If the spoke density correlates with the C-terminal end of the delta domain, then we can hypothesize which residues are interacting at this predicted inter-capsomer interaction site. In the delta domain sequence, there are some charged and aromatic side groups near the end of the 3rd predicted helix and the beginning of the predicted β -sheet region (arrows, Figure 9B). Tryptophan 89 (W89), and aspartic acid 90 (D90) reside in this region and could be participating in important hydrophobic or charged interactions at the 3-spoke interaction sites. These residues were mutated to alanines and tested for assembly defects. For example, if these residues are important for intercapsomer interaction, then these mutations might only produce capsomers, with no higher order structures being made.

W89A and D90A were tested against three different controls using miniprohead preps. The pellet, supernatant, and polyethyleneglycol (PEG) precipitation protein samples were run on native agarose gels and SDS gels to study the resulting assembly products. WT produced prohead and head bands in the PEG sample lane (Figure 10A). D231E is a control that only produces capsomers, which is detectable in the supernatant fraction. W89A and D90A did not produce any obvious structures in the agarose gels (Figure 10A, B). On the SDS gels, WT produced cleaved mcp in all fractions. D231E produced uncleaved mcp in all fractions. W89A and D90A produce uncleaved mcp in the pellet fraction only. There were also higher molecular weight bands present in the pellet fractions, which are usually indicative of crosslinking induced by premature expansion (Figure 10C, D). In normal capsids, the delta domain must be cleaved before it can be fully cross-linked (Duda, Martincic, et al. 1995). Expansion and cross-linking have begun before mcp cleavage in the mutant sample. This is seen when abnormal tube-like structures are formed. The mutants were tested using spot complementation to test for protein functionality.

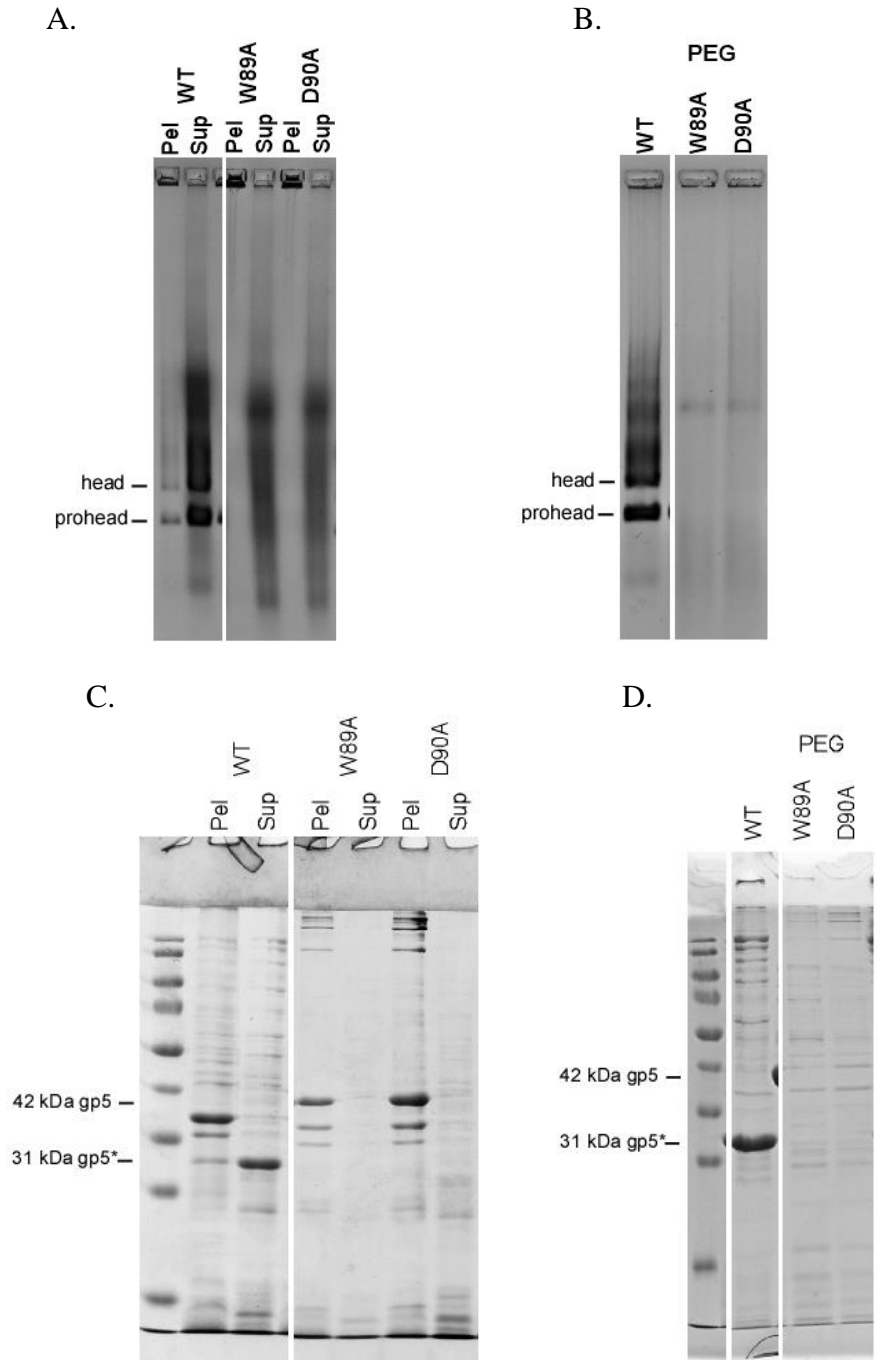


Figure 10. Miniprohead prep results of W89A and D90A show cleavage defects

A and B) Pellet, supernatant (left gel) and PEG (right gel) samples were run on agarose gels. WT control produced proheads and heads. W89A and D90A did not produce any obvious assemblies. The smears are nonspecific cell proteins. C and D) Pellet, supernatant (left gel), and PEG (right gel) samples were run on SDS gels and stained with Comassie. WT showed cleaved 31 kDa gp5* in the supernatant and PEG lanes. W89A and D90A mostly showed uncleaved 42 kDa gp5 in the pellet lanes along with higher molecular weight bands.

Both W89A and D90A were unable to efficiently complement phage with amber mutations in the capsid gene as indicated by a 3-4 log reduction in complementation. Interestingly, these mutants were also unable to complement phage with an amber mutant in the protease gene (Table 1).

To identify whether there were any assembled forms of HK97 major capsid protein present in the pellet fractions of W89A and D90A, we imaged the samples using TEM. Figure 11 shows representative images of the W89A and D90A samples, compared to WT Prohead I. In the agarose gels, there was stained protein present in the pellet fraction wells. The proteins that did not enter the gel could be the abnormal spontaneously cross-linked structures which were indicated by the higher molecular weight bands in the SDS gels. The electron micrographs show that W89A and D90A pellet samples contained round abnormal structures, some open, some closed and some open short tubes. There were large clusters of these abnormal structures, making it difficult to tell if some of the tubes are closed on both ends (Figure 11). Using the program ImageJ, I measured the sizes of some of the tube assemblies. The diameter of the tubes is similar to the diameter of WT proheads. The presence of tubes suggests a lack of pentamers.

The two point mutations from the suspected C-terminal spoke region, W89A and D90A, have very interesting assembly defects. Are there other residues in this region of the delta domain which play a similar role in capsid assembly? Five point mutants were tested: F77S, L85R, D90G, and F96L. Some were mutants that had been previously made in the lab, others were mutated based on the sequence alignment and changed to a residue with a drastically different property. These mutants showed similar phenotypes to W89A and D90A. In the agarose gels, F77S produced a very light but fuzzy prohead band only. L85R, D90G, and F96L did not produce any prohead or head bands. (Figure 12A). In SDS gels, the mutants all produced

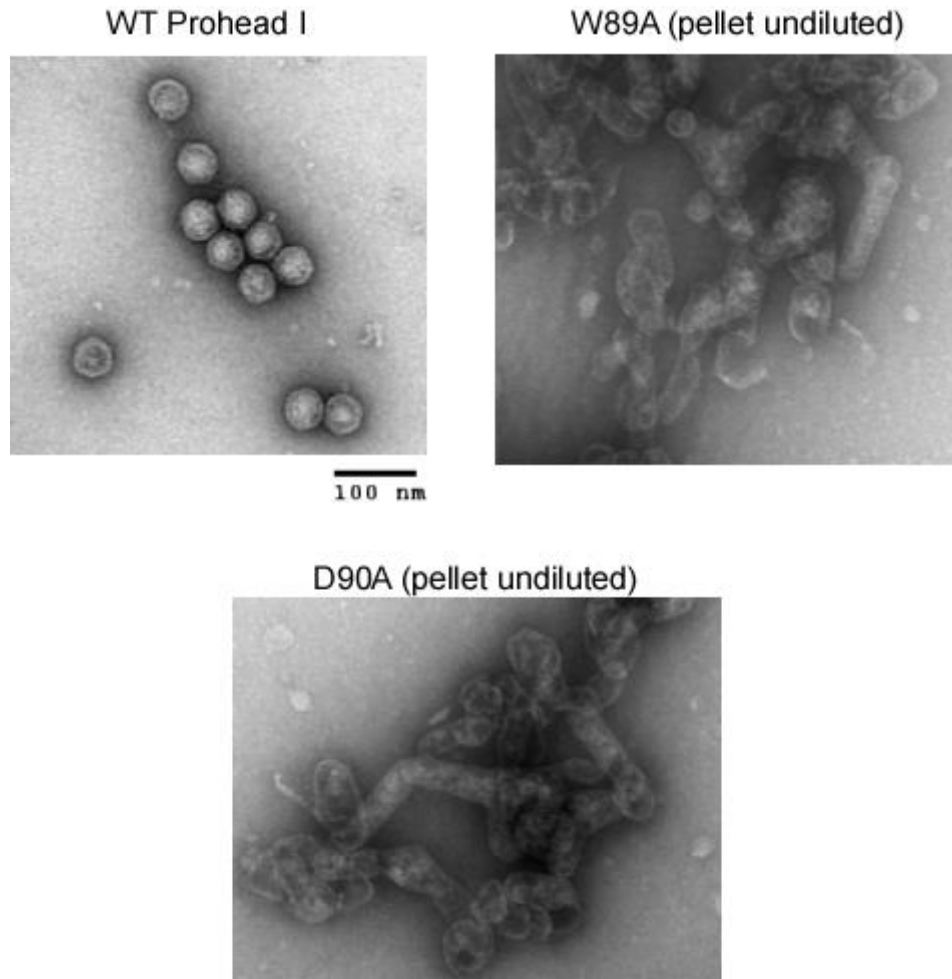


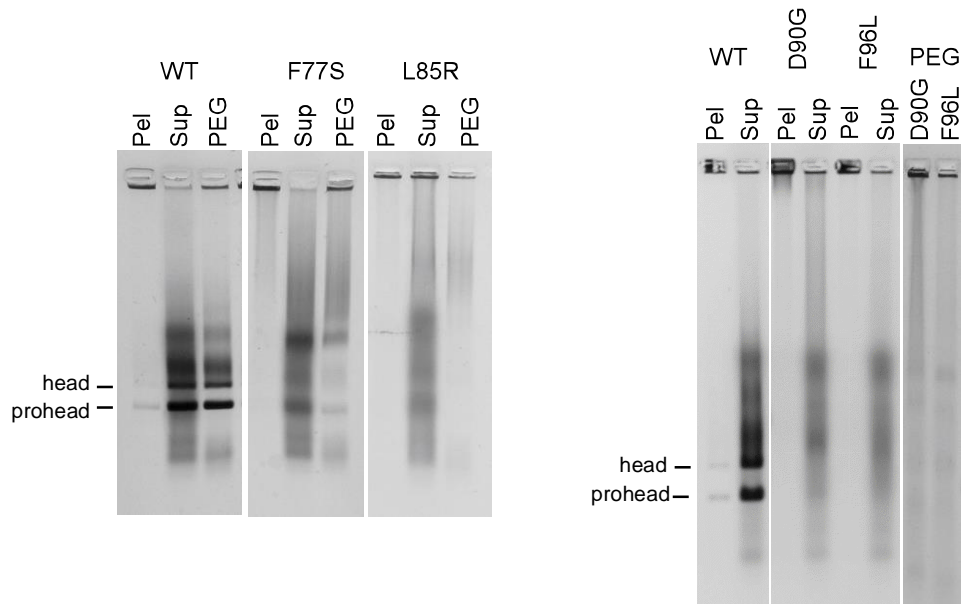
Figure 11. Representative EM images of W89A and D90A pellet samples.

WT Prohead I is shown for comparison. W89A and D90A pellet samples show that these mutant proteins assemble into abnormal and tube like structures, and that are sometimes kinked or bent. All samples were either undiluted or diluted 1/10 in 1x Calorimetry buffer and stained with 1% uranyl acetate. All images are taken at 56,000x magnification. Scale bar: 100 nm.

uncleaved mcp, mostly present in the pellet fraction. D90G had uncleaved mcp in both the pellet and PEG fraction. Each mutant also produced high molecular weight bands near the top of the gel, leading us to believe there were tubes or premature cross-linking occurring (Figure 12B).

In the spot complementation tests, they were 3-4 logs down in major capsid gene amber phage complementation indicating they all produced non-functional capsid protein. L85R, D90G, and F96L were also defective in protease amber complementation while F77S was about 1 log down (Table 1). When the PEG and pellet fractions were studied by TEM (Figure 13), it was obvious that these mutants produced abnormal products, which correlates with the gel data. F77S, L85R, and D90G produced abnormal round structures, which tended to aggregate, and very few WT like proheads. F96L produced abnormal tube like structures, which also tended to aggregate.

A.



B.

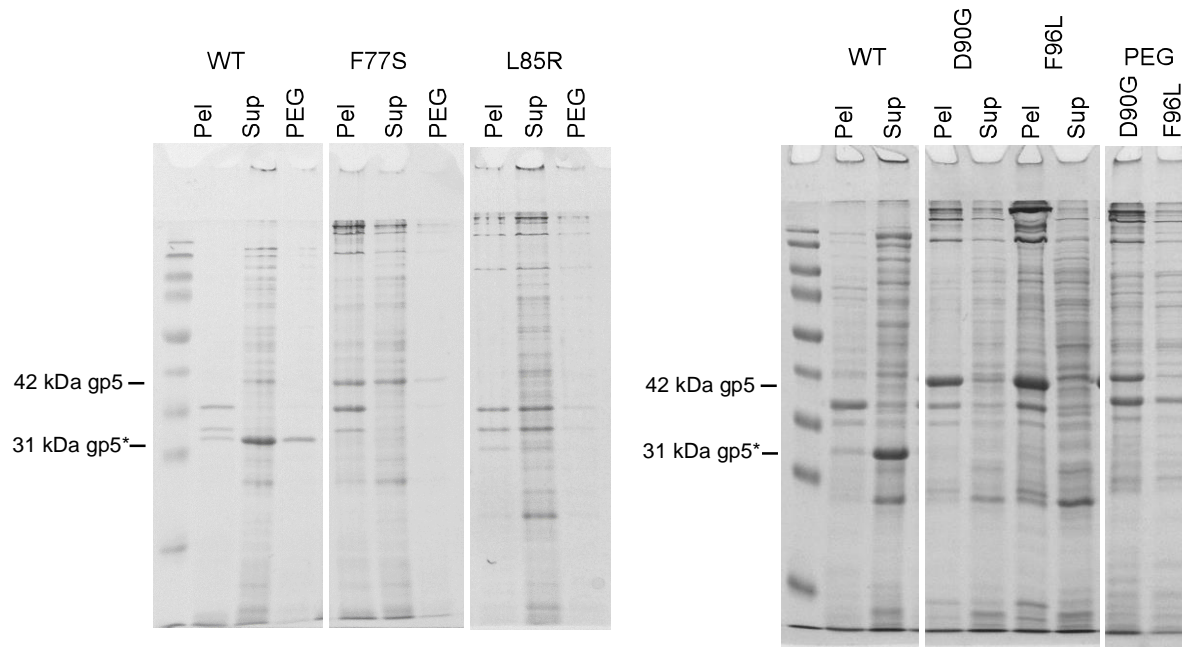


Figure 12. Miniprohead prep results of C-terminal mutations.

A) Pellet, supernatant, and PEG samples were collected and run on a agarose gels. WT produced proheads and heads. F77S produced a very light prohead band. L85R, D90G, and F96L did not produce any detectable HK97 assemblies B) On SDS gels, WT showed cleaved 31 kDa mcp. F77S produced uncleaved mcp that was mostly in the pellet and supernatant fraction, with very little in the PEG fraction. D90G produced uncleaved mcp and higher molecular weight bands (indicative of premature expansion and cross-linking) which was strongly present in both pellet and PEG fractions. F96L produced a strong uncleaved mcp band in the pellet fraction only, along with higher molecular weight bands.

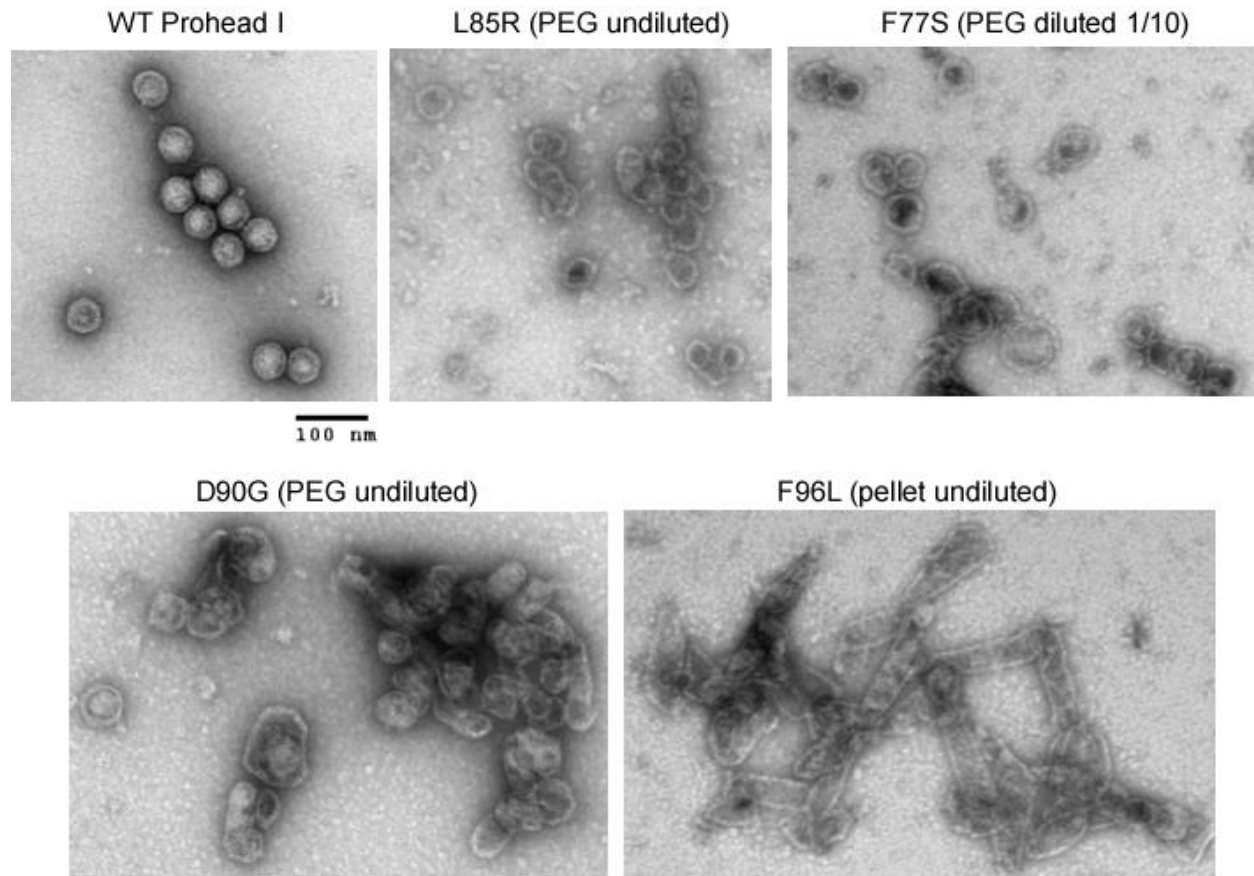


Figure 13. Representative EM images of C-terminal point mutations

WT Prohead I is shown as a control. Miniprohead preps samples were stained with 1% uranyl acetate. Undiluted PEG sample of L85R shows small round abnormal assemblies, aggregating. There were very few regular looking capsids. A 1/10 diluted PEG sample of F77S shows abnormal assemblies and some WT like proheads. An undiluted PEG sample of D90G shows mostly abnormal assemblies, some tubes, and very rarely, WT like proheads. An undiluted pellet sample of F96L shows abnormal tube like structures, which are slightly longer than other tube forming mutants. Scale bar: 100 nm. Images taken at 56,000x magnification.

Charged and bulky residues play an important role in the delta domain C-terminus

Seven mutants located near the C-terminal end of the delta domain show assembly defects by causing premature cross-links and forming abnormal and tube like structures. Does the delta domain require bulky, aromatic sidechains or charged residues in this region to ensure proper assembly? For example, is a large bulky group like tryptophan required at residue 89? Four of these tube mutants were changed to other amino acids with similar characteristics to the WT residue to test if it would recreate a WT like phenotype. L85V, W89Y, D90E, and F96Y were made in the pv0 expression plasmid and tested in miniprohead preps.

On the agarose gel, F96Y had WT-like phenotypes, and produced proheads and heads. L85V and W89Y also produced proheads and heads, but at less than WT levels. D90E showed a very light prohead band only (Figure 14). On the SDS gel, L85V showed mostly uncleaved mcp in the pellet fraction and mostly cleaved in the PEG fraction. W89Y showed mostly uncleaved in all three fractions. D90E produced uncleaved mcp, mostly in the pellet fraction with barely any detectable cleaved mcp in the PEG sample. L85V, W89Y, and D90E also showed higher molecular weight bands, indicative of premature expansion, cross-linking, and abnormal structures. F96L showed a WT phenotype with cleaved mcp (Figure 14). These mutants were tested for protein functionality with spot complementation tests. L85V and F96Y both have WT-like spot complementation for both protease and capsid gene amber phage. W89Y complements phage with an amber mutation in the capsid gene like WT and is about ½ a log down in protease amber phage complementation. D90E produces non-functional capsid protein because it is unable to complement capsid gene amber phage. D90E is also about 1 log down in protease

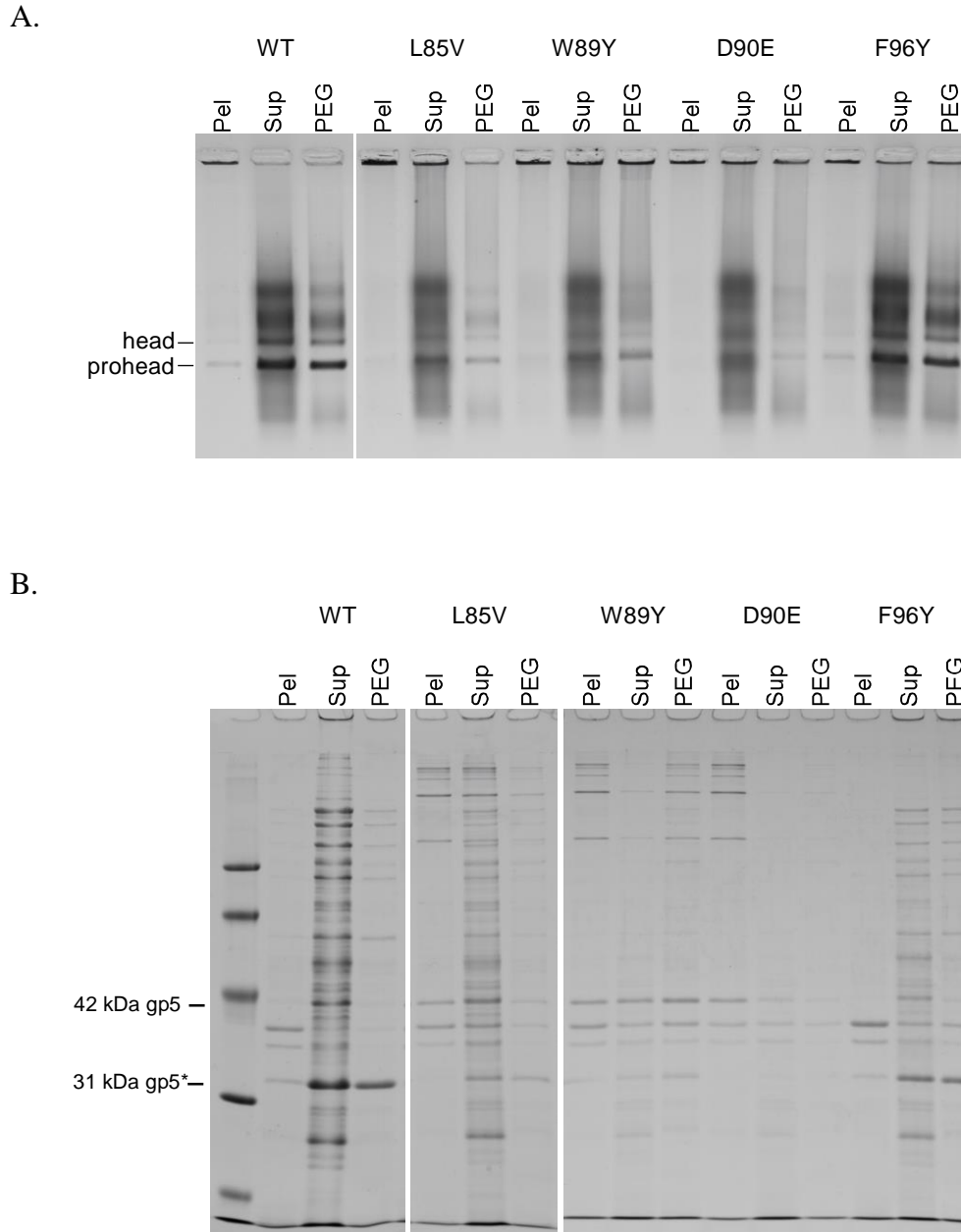


Figure 14. Miniprohead prep results of C-terminal mutants that ‘mimic’ the WT residue

A) Pellet, supernatant, and PEG samples were run on an agarose gel. L85V and W89Y produced prohead and head bands, but at less than WT levels. D90E produced very light prohead and head bands. F96Y produced proheads and heads, like the WT control. B) In the SDS gels, L85V and W89Y produced both uncleaved and cleaved mcp, but at a lower than WT level of protein expression. D90E produced mostly uncleaved mcp which was mostly in the pellet fraction. There were very light uncleaved and cleaved mcp in the PEG lane. L85V, W89Y, and D90E also had higher molecular weight bands. F96Y showed cleaved mcp, like WT.

amber phage complementation (Table 1). The PEG or pellet fraction protein samples were diluted 1/10 and visualized by TEM (Figure 15). L85V showed proheads, heads, and a few abnormal structures. W89Y showed proheads, heads, and some abnormal and tube like structures. D90E showed proheads, tubes, and abnormal structures. F96Y showed WT like prohead and head particles.

It is very interesting that multiple mutations made in this region of the delta domain cause the formation of tube-like structures, which may be cross-linked. Wild-type capsids have a ratio of 6:1 hexamers to pentamers. Tubes contain a larger ratio of hexamers to pentamers than icosahedral capsids. In order to see if the ratio is different with these point mutants, we can dissociate the capsids and visualize the hexamer and pentamer bands on 6% native polyacrylamide gels using capsid dissociation buffer. Prohead I as a positive control produces two bands on this native gel: a pentamer band, and a higher molecular weight stronger hexamer band. Prohead II does not dissociate due to its increased stability. Also, cross-linked capsids, like Head, do not dissociate in this buffer. L85R, L85V, W89A, D90A, and D90E were incubated with capsid dissociation buffer for 4.5 hours and the samples were run on a gel. Compared to the Prohead I control, none of the abnormal tube mutants dissociated into hexamers and pentamers, indicating that these abnormal structures are more stable (Figure 16). The lack of dissociation does not mean that they are not cross-linked, but it does mean that the mutant subunits have a similar stability as WT Prohead II. To assay for cross-linking, the residues in the capsid protein required for covalent cross-linking (K169 and N256) (Wikoff et al. 2000) could be mutated in these tube mutants. These double mutants can be expressed to test if their abnormal structures are held together by crosslinks.

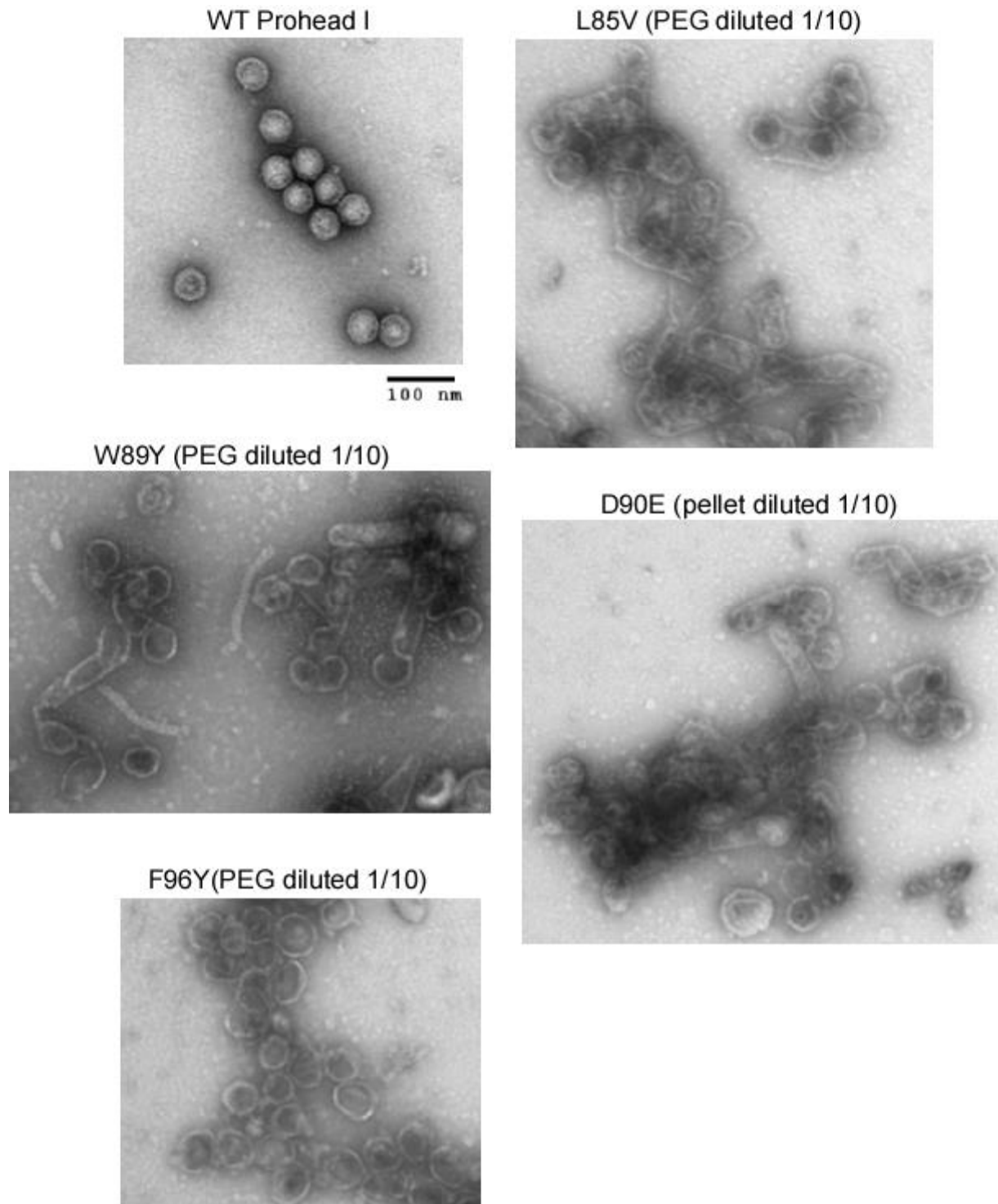


Figure 15. Representative EM images of C-terminal mutants that ‘mimic’ the WT residue

WT Prohead I is shown as a control. Mutant samples are from miniprohead preps and were diluted 1/10 in 1x Calorimetry PBS. L85V, W89Y, and D90E all produce some prohead head particles but also abnormal and tube like structures. F96Y produced WT like proheads and heads, but they look fragile compared to WT. All samples were stained with 1% uranyl acetate and all images were taken at 56,000x magnification. Scale bar: 100 nm.

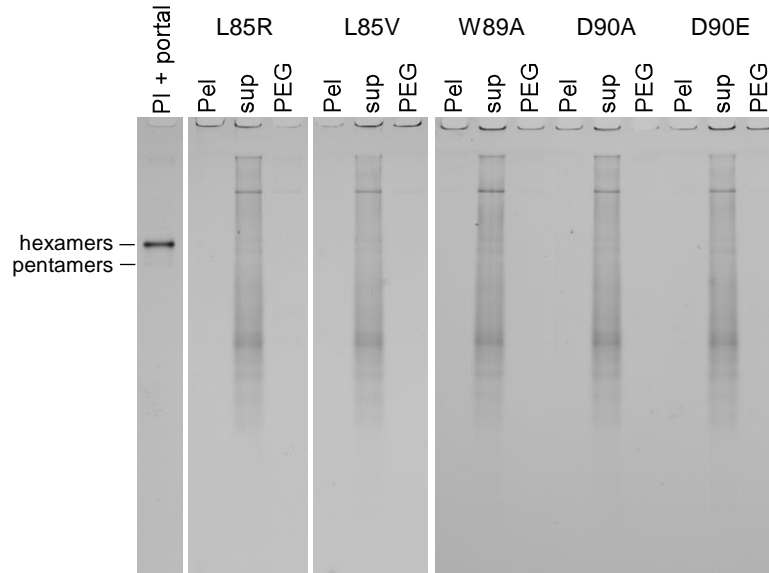


Figure 16. C-terminal point mutant protein products may be cross-linked and do not dissociate

Miniprohead prep pellet, supernatant, and PEG samples were incubated with capsid dissociation buffer for 4.5 hours before loading on a 6% native acrylamide gel. Prohead I with portal was used as a positive control to show the dissociation into hexamers and pentamers. Hexamers and pentamers are in a 6:1 ratio in the capsid and hexamers have a slower mobility than pentamers. None of the C-terminal mutants which make tubes and/or abnormal structures dissociated into hexamers and pentamers.

2.2.4 The search for 2nd site suppressors of W89A

These protein expression studies provided a great biochemical method of understanding how delta domain mutations affect capsid assembly and processing. We can expand the study and characterization of these mutations by moving interesting (lethal) mutations into an HK97 prophage and testing for the presence of 2nd site suppressors in the genome. This genetic method could provide support for our biochemical results or shed new light on the kinds of interactions the delta domain can make. If we can identify 2nd site suppressors in the phage genome of our initial lethal mutation, we can learn more about how the delta domain could be interacting inside the capsid. Recombineering (homologous recombination mediated genetic engineering) can be used to move lethal mutants into a prophage (Marinelli, Hatfull, and Piuri 2012). This method uses homologous recombination and a positive and negative selection system to integrate mutations into a region of interest. Recombineering has been used successfully to mutate regions of interest in bacteria by taking advantage of phage Lambda's recombination system. (Court, Sawitzke, and Thomason 2002; Oppenheim et al. 2004; Sawitzke et al. 2007; Thomason et al. 2007).

The Lambda recombination genes are *beta*, *exo*, and *gam*. *Beta*, a ssDNA binding protein, helps complementary strands of DNA anneal to the 3' overhang and binds to *Exo*. *Exo*, a dsDNA-dependent exonuclease degrades the 5' end of the dsDNA constructs to allow for complementary ssDNA to anneal to the 3' single strand overhangs that are generated. *Gamma* is a protein which protects DNA from nuclease degradation by RecBCD (Court, Sawitzke, and Thomason 2002). With recombineering, these recombination genes can be expressed under a *lac* promoter on a multicopy plasmid to manipulate bacterial or phage genes *in vivo* (Thomason et

al. 2007; Sawitzke et al. 2007). Recombineering was optimized for studying *E. coli*. However, this system can also be applied to studying *E. coli* phage (Court, Sawitzke, and Thomason 2002). Recombineering involves a two-step positive and negative selection system to select for possible recombinants. The first (positive) selection replaces the gene of interest with a selectable marker. The second (negative) selection replaces the first marker with a mutation of interest in the target gene (A schematic of galK recombineering is shown in Figure 17). This produces positive recombinants, containing the mutation of interest that can be used for further studies.

To study the delta domain, I can use this method to move a lethal mutation into a HK97 prophage. A gene fragment of interest requires only 35-50 base pairs of homology flanking either end for recombination to occur (Court, Sawitzke, and Thomason 2002). Using a PCR fragment of a mutation of interest flanked by homology arms, I can transform the recombineering cell line for the negative selection process. The genotype of the recombineering strain BW25113 is F-, $\Delta(araD-araB)567$, $\Delta lacZ4787(::rrnB-3)$, λ , *rph-1*, $\Delta(rhaD-rhaB)568$, *hsdR514* ((Datsenko and Wanner 2000). Danju Tso, a previous graduate student, modified this strain to contain an HK97 prophage and the Lambda Red recombination plasmid, pKD46. She used positive selection to recombineer the galactokinase gene, galK, into the major capsid gene (Tso 2010; Warming et al. 2005). I used this galK-containing prophage for the negative selection process. I prepared a linear dsDNA construct of my delta domain mutation of interest containing 200 base pairs of homology arms on either end. These long homology arms were designed to increase recombination. 200-400 ng of mutant fragment DNA was transformed into cells expressing the recombination genes and were plated on 2-deoxygalactose (2-DOG) plates. Galactokinase phosphorylates the galactose analog, producing a product that cannot be metabolized, resulting in cell toxicity. Cells that have undergone homologous recombination

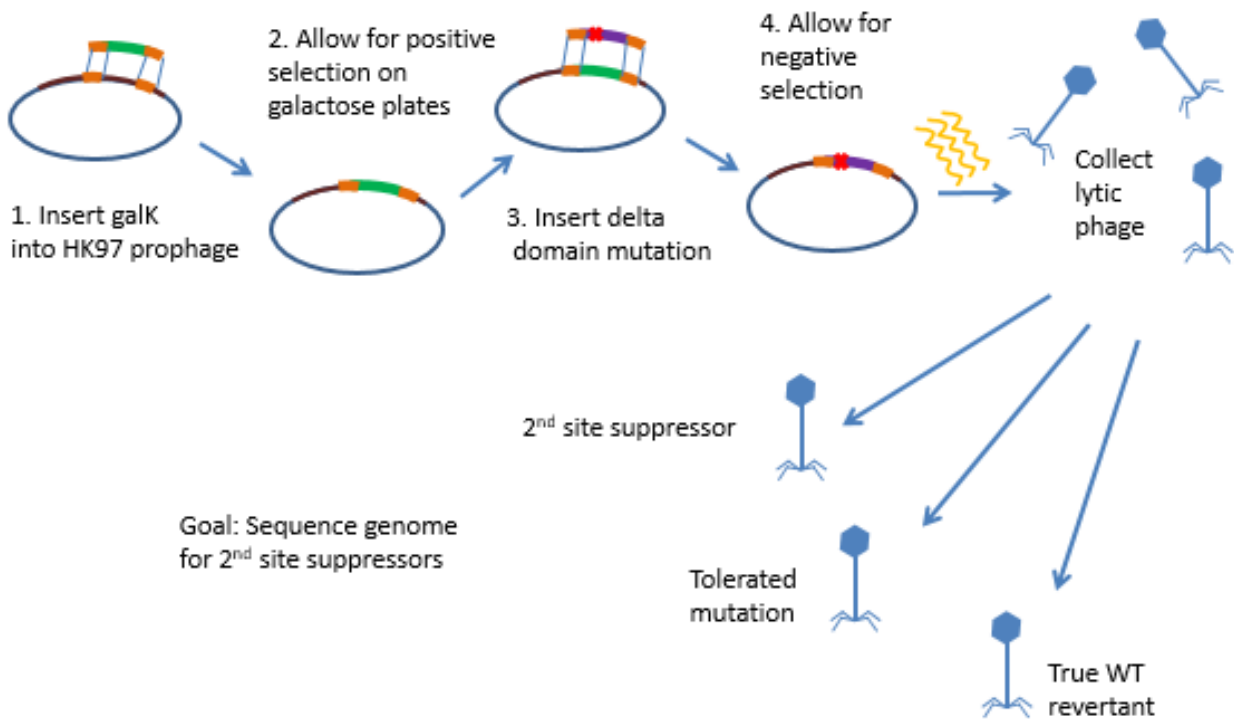


Figure 17. Schematic of galK Recombineering and sequential steps to isolate 2nd site suppressors

The recombinering strain (BW25113 HK97 galK pkD46) that was used in the initial experiments was prepared by Danju Tso. She inserted the galactose kinase gene into the major capsid gene in a HK97 prophage. Positive recombinants were selected on galactose plates. A delta domain mutation with homology arms to the HK97 sequence was used to replace the galK gene. This mutant fragment was transformed into competent cells (made from the recombinering cell line) expressing the Lambda Red recombination genes on plasmid pKD46. Positive recombinants were selected on 2-deoxygalactose (2-DOG) plates. After one round of re-streaking on selection plates to purify the colonies, colony PCR was conducted to identify possible recombinants. Restriction digestions were performed on possible recombinants. Once a recombinant is identified, a cell culture is grown, suspended in induction buffer and exposed to UV light to induce lytic growth. Phage are collected by centrifugation and plaques are isolated for sequencing. There are different possibilities to the phage that can be made: 1) WT revertant that has changed the mutation of interest back to WT, 2) tolerated mutant phage that are viable, and 3) phage containing a 2nd suppressor elsewhere in the genome. This suppressor has rescued the initial lethal mutation that was inserted and the two residues are likely in close contact.

with my mutant fragment will have lost the *galK* gene, allowing for cell growth on DOG plates (Warming et al. 2005).

This negative selection process allows for the identification of positive recombinants. In order to ensure a pure recombinant colony, individual colonies are picked and re-plated on selection plates to purify. Streak tests of colonies across a line of WT phage confirmed that the colonies I picked were indeed lysogens. An issue that I encountered was the high level of background colonies on the selection plates. The transformation efficiencies were not optimal, at an average of 10^6 cfu/mL transformants. Different delta domain mutations were tested using this method. All mutations contain a unique restriction site that can be used to identify their presence in the genome. When tested with PCR and restriction digestion, no positive recombinants were ever identified.

I then began recombineering using Tetracycline resistance selection in the same BW25113 HK97 lysogen strain with pKD46. Using PCR and fragment ligation, I prepared a gene fragment containing the tetracycline resistance gene flanked by HK97 homology arms. In the positive selection process, I was able to isolate a positive recombinant from colonies grown on tetracycline plates. Using this HK97 lysogen tetR pKD46 cell line, I transformed in lethal delta domain mutants and plated the cells onto Bochner-Maloy plates. These selection plates contain Chlorotetracycline, Fusaric Acid, and Zinc Chloride. The exact mechanism is still unknown but the chelating action of the Fusaric Acid with the Zinc allows for the negative selection of colonies that have lost the tetR gene (Bochner et al. 1980; Maloy and Nunn 1981). After multiple recombineering experiments, I was unable to isolate any recombinants. Therefore, I decided to try using a LE392 *E. coli* strain for tetracycline recombineering. I transformed the pKD46 recombineering plasmid into a LE392 HK97 lysogen strain. Using this, I was again

successful in inserting the tetR fragment, creating the recombineering line. I then began testing with D90A and W89A. These were two point mutations that produce abnormal tube like structures. Colony PCR and restriction digestions were done to identify colonies containing the delta domain mutation. I was able to identify one positive recombinant from a W89A recombineering experiment. Sequencing for the HK97 capsid gene in the lysogen showed that this lethal mutation was successfully moved into the prophage.

Now that a positive W89A prophage was identified, I proceeded to induce lytic phage growth to collect the phage for sequencing. My goal was to identify 2nd site revertants or suppressors in the phage genome which would represent an interacting partner with W89. I used WT HK97 phage as a control during the UV light induction tests. The lysogens were grown to an OD₅₅₀~0.2. The cells were then spun down and resuspended in induction buffer. The cells were exposed to low wavelength UV light for 0, 10, and 20 seconds. After induction, the cells were shaken at 37°C for 1.5 hours. Chloroform was added for the last 30 minutes to help with lysis. Phage supernatants were collected and plated on LE392 plates to test for plaque growth. For the WT control, plaques were produced. However, after multiple tests, I was never able to produce plaques with the W89A prophage.

2.2.5 Linker Insertion Mutations (LIMs) affect capsid assembly

Linker Insertion Mutations are 12 base pair oligo (four amino acids) insertions made in HK97. These mutations were randomly made throughout the major capsid gene in order to study their effects on capsid assembly. While these LIMs were made previously in the lab, I tested four that were located in delta domain using the miniprohead expression method. LIM 20 (GLES), LIM 33 (WTRV), LIM49 (GLES), and LIM82 (GLES) (letters represent the amino acid linker) are

mapped onto the delta domain protein sequence (Figure 18A). The number corresponds to the amino acid directly preceding the insertion sequence. Each LIM contains a unique restriction site.

Pellet, supernatant, and PEG samples were collected and separated by electrophoresis through SDS and agarose gels. On the agarose gels, WT produced proheads and heads. LIM 20 produced a light prohead band. LIM 49 produced a prohead band which runs slightly slower than WT. LIM 33 and LIM 82 did not produce any discernable products (Figure 18B). All four LIMs produced uncleaved mcp, which mostly resided in the pellet fractions (Figure 18C). LIM 49 showed a fairly strong mcp band in the PEG fraction also. LIM 20 and LIM 82 had lighter uncleaved mcp bands in their PEG fractions. Higher molecular weight bands are present in LIM 20, LIM 49, and very strongly in LIM 82 fractions, indicative of premature expansion and crosslinking or abnormal structures (Figure 18C). While some of these insertions were able to produce WT like capsids, in complementation tests, none were able to complement phage with an amber mutation in the capsid gene, showing that they all produced non-functional capsid protein. LIM 20 and LIM 33 were 1 log down while LIM 49 and LIM 82 were multiple logs down in complementation against phage with an amber mutation in the protease gene (Table 1). Undiluted pellet or PEG samples of these mutants were visualized in the TEM (Figure 19). LIM 20 showed few prohead like structures, and some abnormal assemblies. LIM 33 did not show any regular HK97 products, mostly very small round assemblies. LIM 49 showed prohead like structures. LIM 82 produced round, abnormal structures, and some tubes, which aggregate together with cell debris. Most of the miniprohead prep samples contain cell debris due to the crude purification steps. WT Prohead I containing portals are shown as a control. LIM20 and LIM49 will be studied in further detail in Chapter 3.

Figure 18. Miniprohead preps of the Linker Insertion Mutants (LIMs)

A) Protein sequence of delta domain showing predicted secondary structure and the positions of the LIMs B) Pellet, supernatant and PEG samples were run on a 0.8% agarose gel. WT produced proheads and heads. LIM 20 produced a very light prohead band. LIM 49 produced a prohead band that ran slightly slower than WT. LIM 33 and LIM 82 did not produce any detectable assembly products. C) The pellet, supernatant, and PEG samples were prepared for SDS gels. WT samples showed cleaved 31 kDa mcp. Each LIM produced mostly uncleaved mcp, which mostly ended up in the pellet fraction. LIM 13, 49, and 82 produced some uncleaved mcp in the PEG fractions. LIM 82 also showed strong higher molecular weight bands, while LIM 49 showed weaker higher molecular weight bands. LMW: lower molecular weight marker.

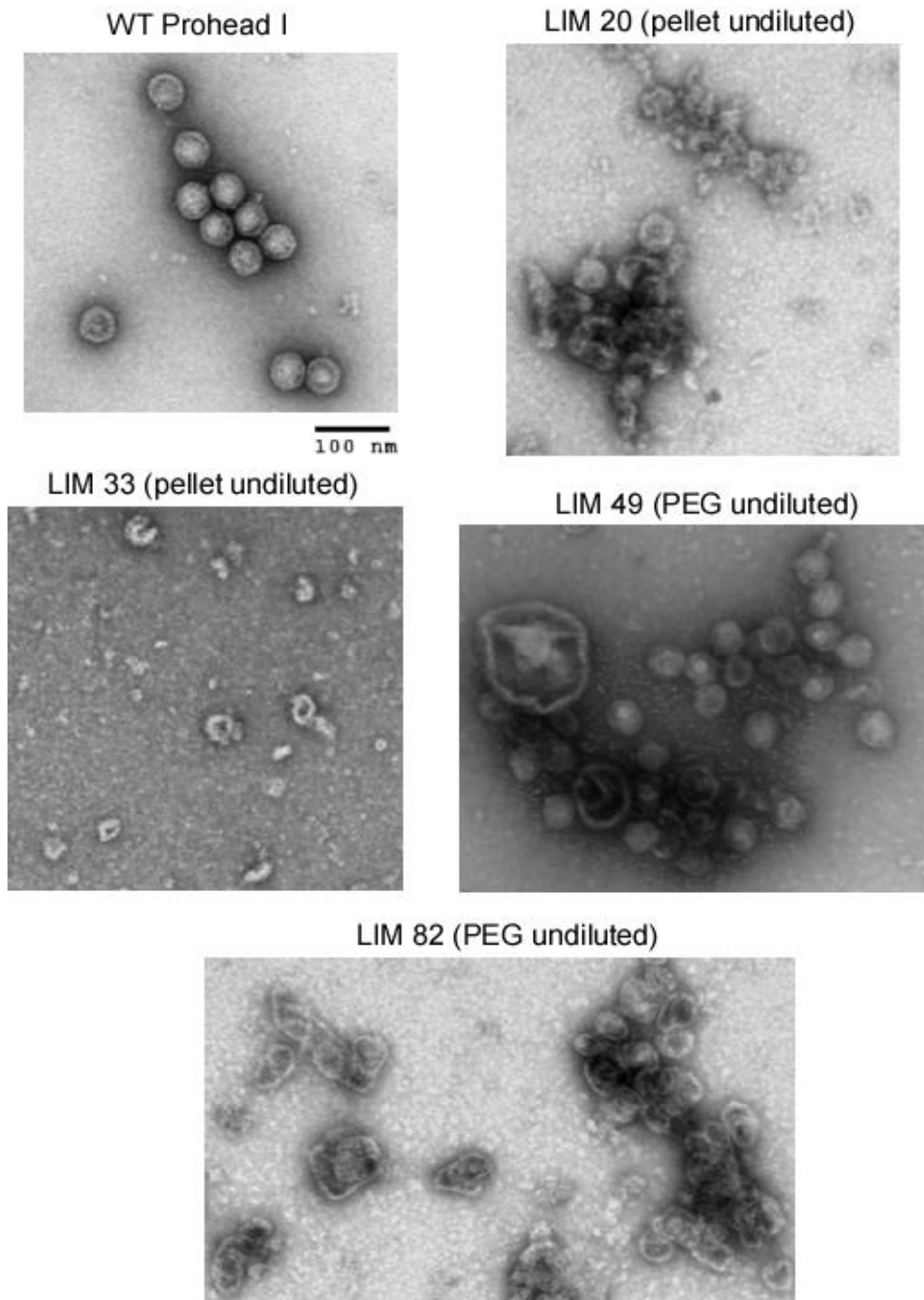


Figure 19. Representative EM images of Linker Insertion Mutations (LIMs)

Purified WT Prohead I is shown for comparison. Undiluted pellet or PEG samples from the miniprohead preps were stained with 1% uranyl acetate and visualized with transmission electron microscopy. LIM 20 produced very few WT like particles and some abnormal structures. LIM 33 did not produce any detectable WT like products, but small round assemblies. LIM 49 produced WT like proheads. LIM 82 produced abnormal round assemblies and some small tube like structures. All images were taken at 56,000x magnification. Scale bar: 100 nm. Cell debris is present in these crude purification samples (as seen by large vesicles in LIM 49 image).

2.2.6 ‘Hinge’ deletions affect capsid assembly and size

The cryo-EM density map of the HK97 Prohead I shows the delta domains as blob-like structures. We believe that it is the inherent flexibility of the delta domain that prevents high resolution visualization. This flexibility may play an important role during capsid assembly. Secondary structure prediction algorithms suggest that the delta domain has three helical regions. It is possible that the regions between these predicted helices, which we will call ‘hinge’ regions, are responsible in part for the flexibility of this domain. In addition, the first two predicted helical segments are predicted to form coiled coils (Conway et al. 1995). By deleting these ‘hinge’ regions, we can study whether they are important for delta domain function. Two deletion mutants were made: Del1stHinge, which deletes residues S31-S36 and Del2ndHinge, which deletes residues G67-E73 (Figure 20A). These deletion mutants were analyzed using our miniprohead expression system, as described above. Del1stHinge did not produce any discernable assembly products (Figure 20B). In contrast, Del2ndHinge produced a weak prohead band (denoted by circle), a stronger band that ran slightly faster than WT proheads, and a fuzzy capsomer band (Figure 20B). Del1stHinge produced apparently insoluble uncleaved mcp, which was found in the pellet fraction only. Del2ndHinge produced uncleaved mcp in all fractions; the mcp band in the PEG fraction suggest some protein was soluble (Figure 20C).

Complementation tests showed that these two deletions were 3 orders of magnitude down in their ability to complement phage with an amber mutation in the capsid gene. Unexpectedly, the WT control phage and the protease amber mutant phage were 1 log down in complementation for Del2ndHinge (Table 1) suggesting a possible dominant negative effect of the mutant. Previous work with mutant M357G showed that smaller proheads run slightly faster

A.

Del 1st Hinge

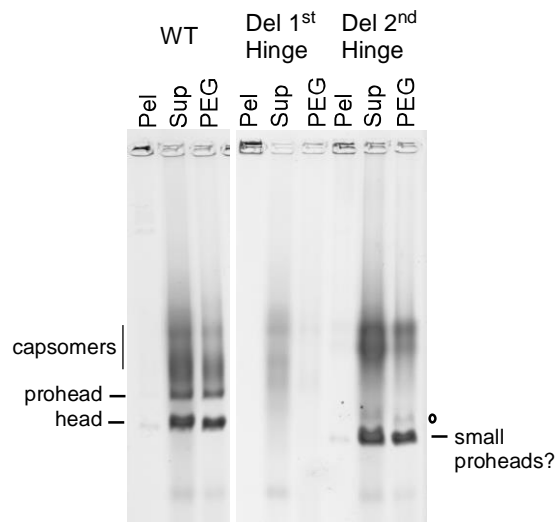
MSELALIQKA IEESQQKMTQ LEFDAQKAEIE STGQVSKQLQ SDLMKVQEEL **50**
 aa aaaaaaaaaaaaaaaaaaaaaaaaaaaaaa

Del 2nd Hinge

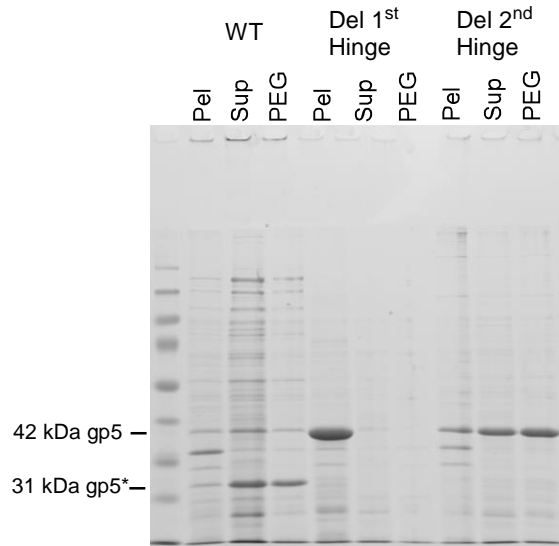
TKSGTRLFDL EQKLAGAEN PGEKKFSER AAEELIKSWD GKQGTFGAKT **100**
 aaaaaaaaaaaaaaaaaaaaaaaaaaaaaa aaaaaaaaaaaaaaaaaaaaaaaaaaaaaa bbbbbbb

FNK
 bbbb

B.



C.



D.

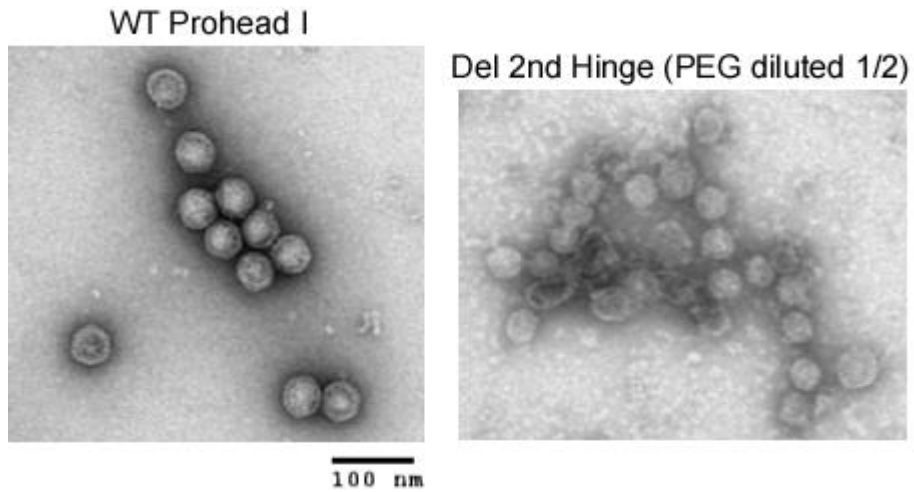


Figure 20. Del 1st and 2nd Hinge mutants affect capsid assembly

A) Delta domain protein sequence showing predicted secondary structure and regions of ‘hinge’ deletions. B) Pellet, supernatant, and PEG samples from miniprohead preps were run on a 0.8% native agarose gel. WT produced proheads and heads. Del 1st Hinge did not produce any discernible products. Del 2nd Hinge produced a fuzzy capsomer band, a very weak prohead band (denoted by circle), and a strong prohead band that ran faster than WT. Other HK97 studies have shown that protein bands with faster mobilities than WT could be indicative of smaller than normal particles. C) In the SDS gel, WT produced cleaved 31 kDa mcp. Both ‘hinge’ deletion mutants created uncleaved mcp. Del 1st Hinge’s 42 kDa mcp was exclusively in the pellet fraction while Del 2nd Hinge mcp was present in all fractions. D) Representative EM image of Del 2nd Hinge (diluted 1/2 in 1x calorimetry buffer) shows abnormal structures, a few WT sized proheads, and smaller than normal capsids. WT Prohead I is shown for comparison. Samples were stained with 1% uranyl acetate and all images were taken at 56,000x magnification. Scale bar:100 nm. Del 1st Hinge produced inclusion bodies (not shown).

than normal sized proheads on agarose gels (Duda, Maurer, Conway, Hendrix, unpublished). The agarose gel data suggests that this mutant may produce small capsids. The TEM data supports this as we were able to visualize a variety of structures: WT-like proheads, proheads which appear smaller than normal, and abnormal round and tube assemblies. When compared to WT Prohead I, a few particles were WT sized while the rest were smaller. Del1stHinge pellet samples only showed inclusion bodies and cell debris when visualized (Figure 20D).

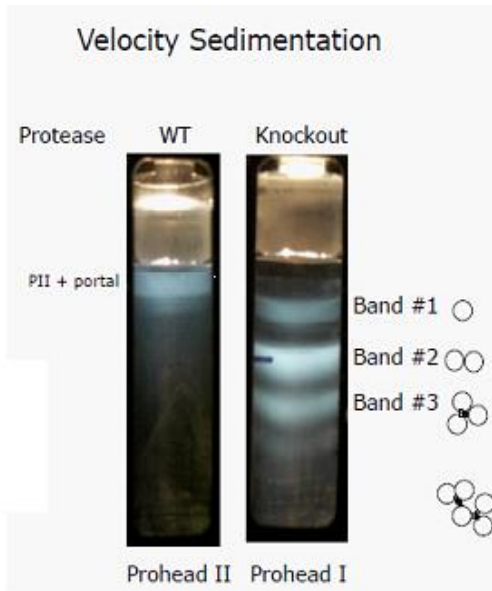
To further study Del2ndhinge, this deletion was moved into a plasmid that contains the portal and inactivated protease genes (pVP0 g4 H65A) to allow us to test for portal and protease incorporation and determine the T-number of the small particles. This plasmid would show if these mutant capsids are unable to cleave or unable to complement amber phage due to a protease or portal incorporation defect. The active site mutation H65A in the protease gene inactivates the protein, allowing for proper protein expression and incorporation, but no protease activity (Duda, Oh, and Hendrix 2013). This plasmid provides a sensitive assay to test for portal incorporation.

Capsids containing the WT portal and capsid genes but the inactivated protease only produce Prohead I. When Proheads containing the portal and inactivated protease are purified through sucrose or glycerol gradients (as is done with our large scale Prohead preps), a unique banding pattern emerges. We can see multiple prohead bands compared to the single prohead band in a Prohead II containing portal prep (Figure 21A) (Crystal Moyer, unpublished results). These multiple bands correspond to proheads with and without the portal. The top band correlates with portal-less proheads, while the bands below correlate with portal containing proheads. These portal containing proheads are creating prohead dimers and trimers because the

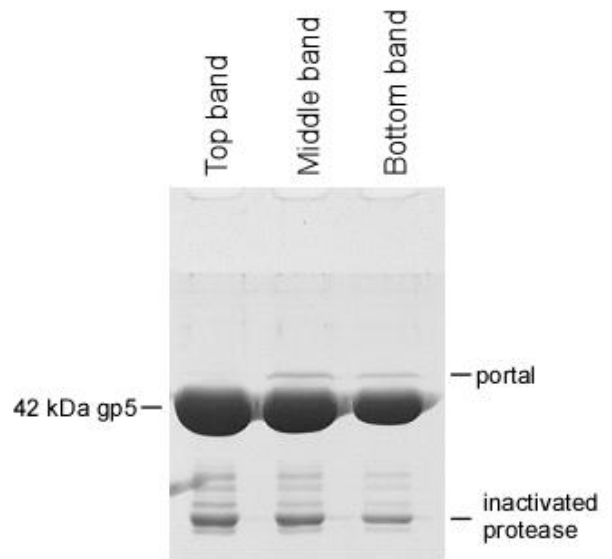
multiple capsids adhered to cell membrane fragments by their portals, causing them to band together as dimers, trimers, etc. in the gradient.

For preps with Prohead I containing the portal, we run the samples on special SDS gels made with twice the normal concentration of bis-acrylamide, which clearly separates the portal and uncleaved mcp, which migrate almost identically in normal SDS gels. An SDS gel shows the absence of the portal in the top band fraction, and the presence of the portal in the middle and bottom band fractions (Figure 21B). This is supported by a representative agarose gel showing the presence of these prohead dimers in the middle and bottom band fractions whereas the top band only contains prohead monomers (Figure 21C). We can also visualize these prohead dimers and trimers with TEM, as shown in Figure 21D. The arrows are pointing at pieces of cellular membrane that are connecting these portal-containing capsids. It is commonly believed that capsid assembly may occur on the cellular membrane with the phage portal acting as the initiator of capsid assembly (Simon 1969; Simon 1972; Murialdo and Becker 1978). With the portal at the cell membrane, capsid proteins assemble around the portal and create Prohead I. After delta domain cleavage and processing by the protease, we believe that there are conformational changes that allow the portal to detach from the membrane. Then, DNA can be packaged through the portal and phage assembly can progress. This hypothesis also ensures that there is only one portal per capsid. During our purification steps in the Prohead prep, our inactivated protease capsids are trapped on the cell membrane. When lysis occurs, the capsids are still attached to pieces of membrane, which have been released by treatment with detergent during lysis, allowing for the formation of prohead dimers and trimers. While this dimer and trimer phenomenon is not biologically relevant during phage infection and assembly, this provides us with a unique and sensitive assay to test for portal incorporation.

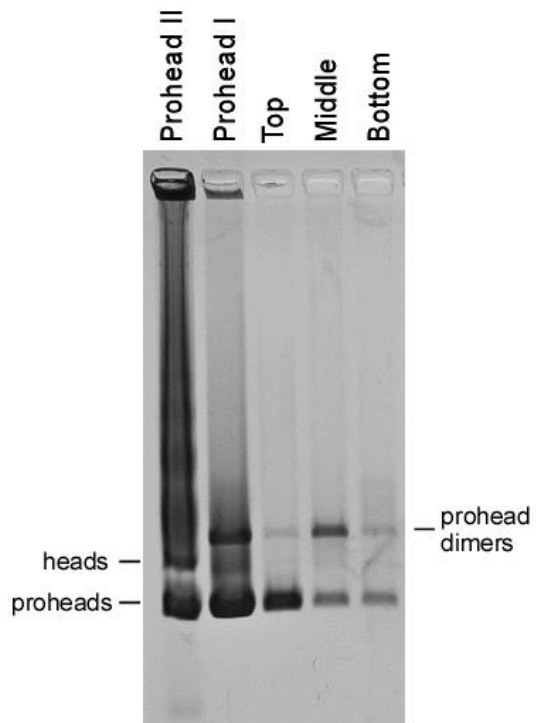
A.



B.



C.



D.

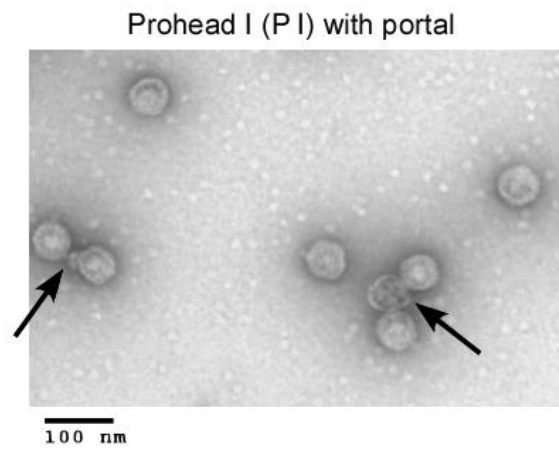


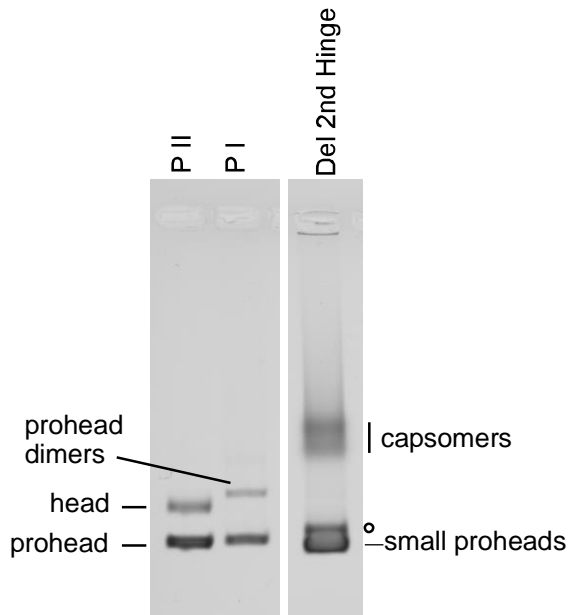
Figure 21. Prohead I with portal and inactivated protease (pVP0 g4 H65A) used to test for portal and protease incorporation

A) Sucrose gradient image by Crystal Moyer. Prohead II (WT protease) creates one band in gradient purification. Prohead I (inactivated protease) creates multiple bands due to portal incorporation. The top band correlates with proheads with little to no portal, the middle band correlates with prohead dimers - two proheads sticking to bits of cell membrane by their portals, and the bottom band correlates with trimers of proheads and lower bands with larger complexes. B) Prohead I samples pulled from a top, middle, and bottom band of a glycerol gradient were prepared and run on a 12% SDS acrylamide gel containing 1.6% (double the normal amount) bis-acrylamide. The top band contains no detectable portal while the middle and bottom bands contain portal. The 25 kDa protease band is present in all fractions. C) PII and PI containing portal controls and top, middle, and bottom band samples were run on a 0.9% native agarose gel. P II produced proheads and heads. PI produced proheads and prohead dimers. The top band produced mostly proheads and some prohead dimers. The middle band produced more prohead dimers than prohead monomers. The bottom band produced proheads and prohead dimers. D) Representative TEM image of PI with portal capsids showing prohead dimers connected by bits of cellular membrane (arrows). Scale bar: 100 nm. Image was taken at 56,000x magnification.

Del 2nd Hinge is defective in portal and protease incorporation

Assembled particles were purified from a 1 L culture of the Del 2nd Hinge mutant in the portal and defective protease plasmid. In the glycerol gradient (Figure 22A), there was a strong band and a smear of protein underneath. The top portion and smear were separated into two fractions, which I will refer to as the top band and bottom band. The top band was used in the gel analyses. In the agarose gel, Prohead II and portal control showed prohead and head bands. Prohead I with portal showed proheads and prohead dimers. Del2ndHinge did not show any dimer or trimer bands. Instead, there was a strong prohead band that ran faster than WT, along with a weaker prohead band that ran at the same molecular weight as the WT prohead (denoted by circle) (Figure 22A). The extra band with faster mobility suggests the presence of smaller-than-normal capsids. In the SDS gel, Prohead II control produced cleaved mcp, while Prohead I with portal showed portal, uncleaved mcp, and protease bands. Del2ndHinge showed uncleaved mcp (as expected with the inactivated protease) and a light protease band. There was no detectable portal band present (Figure 22B).

A.



B.

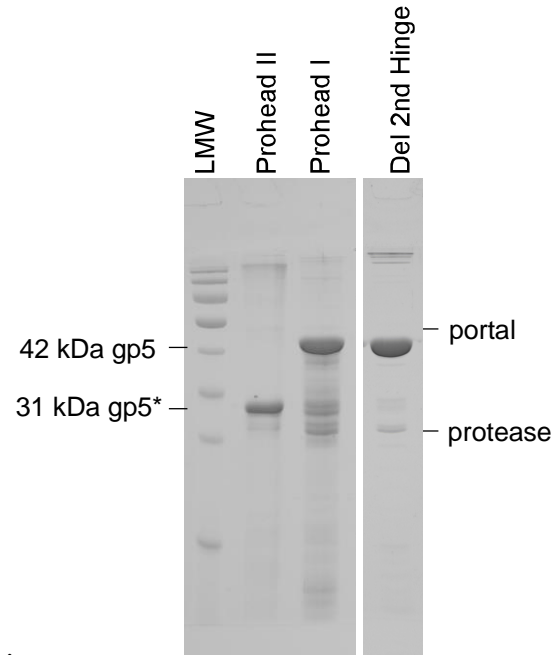


Figure 22. Del 2nd Hinge is defective in portal and protease incorporation

A) Del 2nd Hinge was expressed in the pVP0 g4 H65A plasmid to test for portal and protease incorporation. A larger Prohead Prep was conducted and samples were purified using a glycerol gradient. On the native 0.9% agarose gel, WT Prohead II and WT Prohead I with portal are shown as controls. Prohead II produced proheads and heads. Prohead I with portal produced proheads and prohead dimers. Del 2nd Hinge produced a prohead band (WT, denoted by circle), capsomers, and a band of faster mobility which may be smaller than normal proheads. B) On the SDS gel, Prohead II showed cleaved mcp while Prohead I showed portal, uncleaved mcp, and an inactivated protease band. Del 2nd Hinge showed an uncleaved mcp band, and a weaker protease band.

Del 2nd Hinge produced capsids of different sizes

The initial micrographs and gel data showed the presence of smaller than normal capsids. In order to determine the T number of these mutant small proheads, higher resolution data was needed. Both top and bottom band samples collected from the Prohead prep were further purified using an HQ20 anion exchange column and separated into multiple peaks. Graphs of the absorbance (280 nm) peaks detected over time are shown in Figure 23A and B. Both top and bottom band samples separated into five peaks. The bottom sample contained less protein, as shown by the lower levels of absorbance. The peak fraction numbers are labeled for each sample and the asterisks denote the fractions collected for agarose gel analysis. The first peak consisted of capsomers. The 2nd peak showed a smear of protein and a band, which is believed to be abnormal expanded prohead I particles (Duda, Maurer, Hendrix, unpublished data). The 3rd small peak did not show any discernable protein products on the agarose gel. The large fourth peak consisted of small proheads and some capsomers. The last peak/shoulder of the graph consisted of mostly WT proheads and some small proheads (Figure 23C). Peak fraction #14 from the top band sample contained a strong band of small proheads. This fraction was pelleted in the ultracentrifuge and resuspended in a small volume to ensure a high concentration.

The purified Del2ndHinge #14 prohead sample was visualized by cryo-EM using a FEI Polara microscope and a Falcon 2 direct detection camera (James Conway). Figure 24 shows a representative micrograph, which confirms that this mutant does indeed produce smaller-than-normal capsids. A preliminary reconstruction (Conway, unpublished) using only 23 particles showed that the smaller-than-normal particles express a T=4 triangulation number. Along with a large number of abnormal structures, there were few 'normal' T=7 sized particles (Figure 24).

Figure 23. Purification of Del 2nd Hinge isolates different sized particles

Top and bottom band samples were run on an ion exchange HQ20 column. A) and B) show the absorbance peaks over time from the top and bottom sample fractions, respectively. The samples produced a complicated five peak pattern. The peak fraction numbers are labeled, and the fractions used for gel analyses are denoted with an asterisk. C) The main peaks were collected and run on a 0.9% agarose gel. Both samples displayed a similar peak pattern, but the bottom band sample had a smaller amount of protein, shown by the lower absorbance levels. The first peak (fractions 6, 19) was made of capsomers. The 2nd peak (fractions 8, 22) showed a band and smear, which could possibly be expanded Prohead I particles. The 3rd small peak (10, 25) did not contain any obvious assemblies. The 4th peak (fractions 14, 29) contained small proheads and some capsomers. The last peak/shoulder (fractions 15, 30) was made of mostly WT sized proheads and some small proheads.

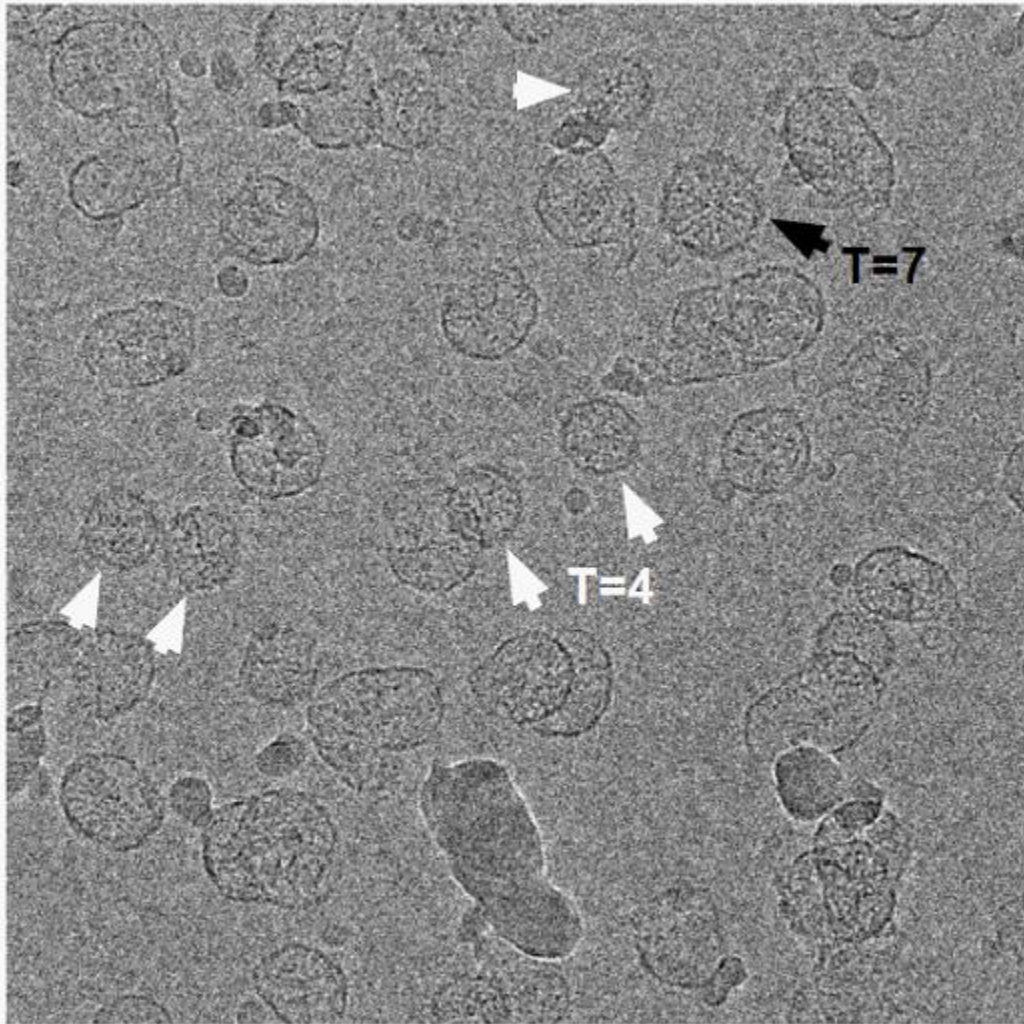


Figure 24. Cryo-Electron Micrograph of a purified Del 2nd Hinge small prohead band sample

A) Using a FEI Polara cryo-electron microscope, James Conway took this representative micrograph of the purified mutant sample. A majority of the protein products are abnormal assemblies. The second most abundant products are the small capsids, and the rarest structures were the WT sized capsids. From a preliminary reconstruction, he determined that the small capsids have a triangulation number of 4. White arrows point out some of the small capsids. Black arrow points out a rare T=7 capsid. Radial lines of internal density are visible in the small and larger icosahedral capsids. These densities are possibly the delta domains.

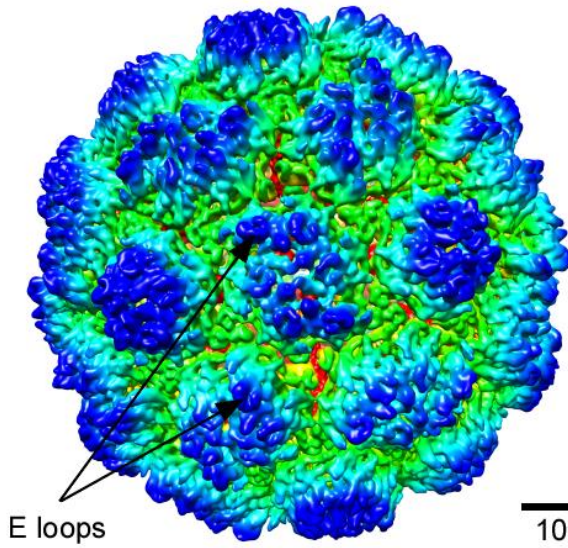
Del 2nd Hinge T=4 and T=7 capsids have more stable delta domains than WT

This reconstruction using 850 Del 2nd Hinge small particles from 151 micrographs produced a 8.7 Å resolution map (Figure 25A-C). Figure 25A shows an external view of the T=4 capsid density map, with a skewed hexamer in the middle. This map was also able to resolve the E-loops protruding from each subunit. Figure 25B shows an interior view of the T=4 capsid, revealing tall towers of density from underneath the pentamers, which protrude towards the center of the capsid. These stable towers are the delta domains, in a very different conformation from WT delta domains (compare to interior view of T=7 ‘normal’ capsid, Figure 25D). Along with the elongated delta domain towers, there are pairs of smaller delta domain protrusions underneath each hexamer. Unlike the stronger spoke densities in the WT T=7 density map, there are varying degrees of spoke densities in the hexamers of the T=4 mutant (weaker spoke densities highlighted with ovals in 25B and C). Much more of the delta domains (red colored densities) are visible in these mutant Del 2nd Hinge particles compared to WT. Figure 25C shows an interior view of the T=4 mutant capsid using a different contour density level to highlight the spoke regions (yellow and orange densities). The small capsids have a triangulation number of 4, so each asymmetric unit is composed of half of a hexamer (three subunits) and one subunit of the adjacent pentamer. Therefore, the two halves of the skewed hexamer are equivalent and opposite so each pair of opposing spoke densities are equal. The spokes of a hexamer that are in an interface between three hexamers along the 3-fold symmetry axis are the strongest (highlighted by circle). The spokes of a hexamer that are interacting with a spoke from a pentamer are weaker. The weakest hexamer spoke densities are highlighted by ovals (Figure 25B, C) and do not contribute to the delta domain bundles on each half of the skewed hexamer (Figure 25B)

In a pentamer, the spoke densities are relatively equal due to the five-fold symmetry imposed. The WT Prohead I reconstruction shows relatively equal spoke density in each capsid subunit (Figure 25D). A slice of the mutant T=4 capsid with an increased contour density level shows the less dense areas of the map (Figure 26). We can visualize the delta domains from each pentamer joining together to form what we hypothesize is a stable and elongated five helix bundle. We can also see that in a hexamer, a bridge-like density appears to make a connection between the two small delta domain protrusions (Figure 26).

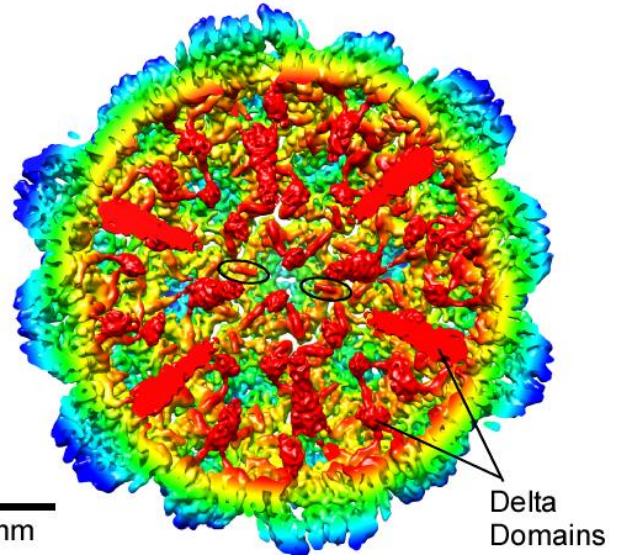
A.

Del 2nd Hinge T=4
external view



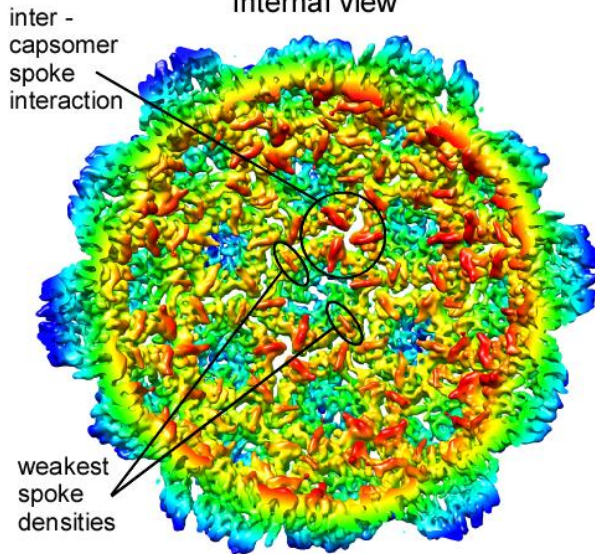
B.

Del 2nd Hinge T=4
internal view



C.

Del 2nd Hinge T=4
internal view



D.

WT HK97 T=7
internal view

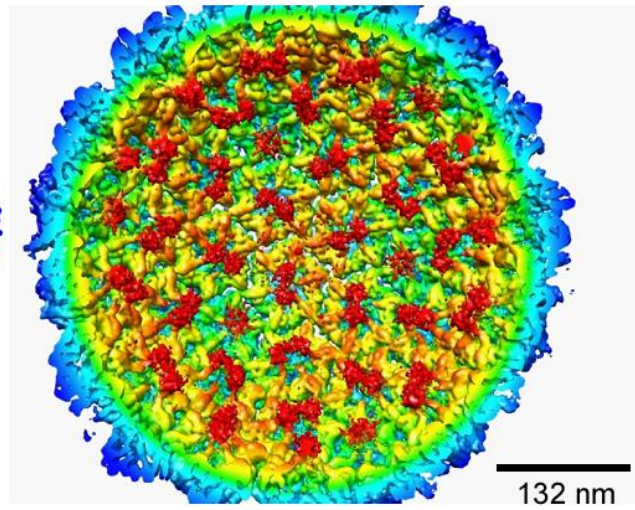


Figure 25. 8.7 Å map of Del 2nd Hinge T=4 capsid compared to WT T=7

A) External view of mutant T=4 capsid. Using 151 micrographs, 850 particles were used to create this reconstruction. Hexamers are skewed, just like they are in the WT capsid. The E-loops (the slightly protruding loops on the outer surface of each subunit) are visible. B) An internal view of the T=4 mutant capsids show much more of the delta domains (red blobs) than the WT T=7 capsids (D). The delta domains of the pentamers assemble into a more stable tower like protrusion towards the capsid center. The hexamer delta domains assemble into two bundles, similar to the WT capsid. In WT T=7 capsids (D), each spoke (orange/yellow colored) is mostly equal in density to contribute into the red blobs of the delta domains. C) The internal view of the T=4 capsid has been contoured to highlight the spokes (orange/yellow colored). Possible inter-capsomer spoke interaction site is shown. The pentamer spokes are relatively equal in density. Under the hexamers, different spokes have different densities. The weakest of the spoke densities are highlighted. D) The internal view of a WT T=7 capsid is shown for comparison. The scale bar for the T=4 capsids represents 102 nm. The scale bar for the T=7 capsid represents 132 nm. (Images from James Conway)

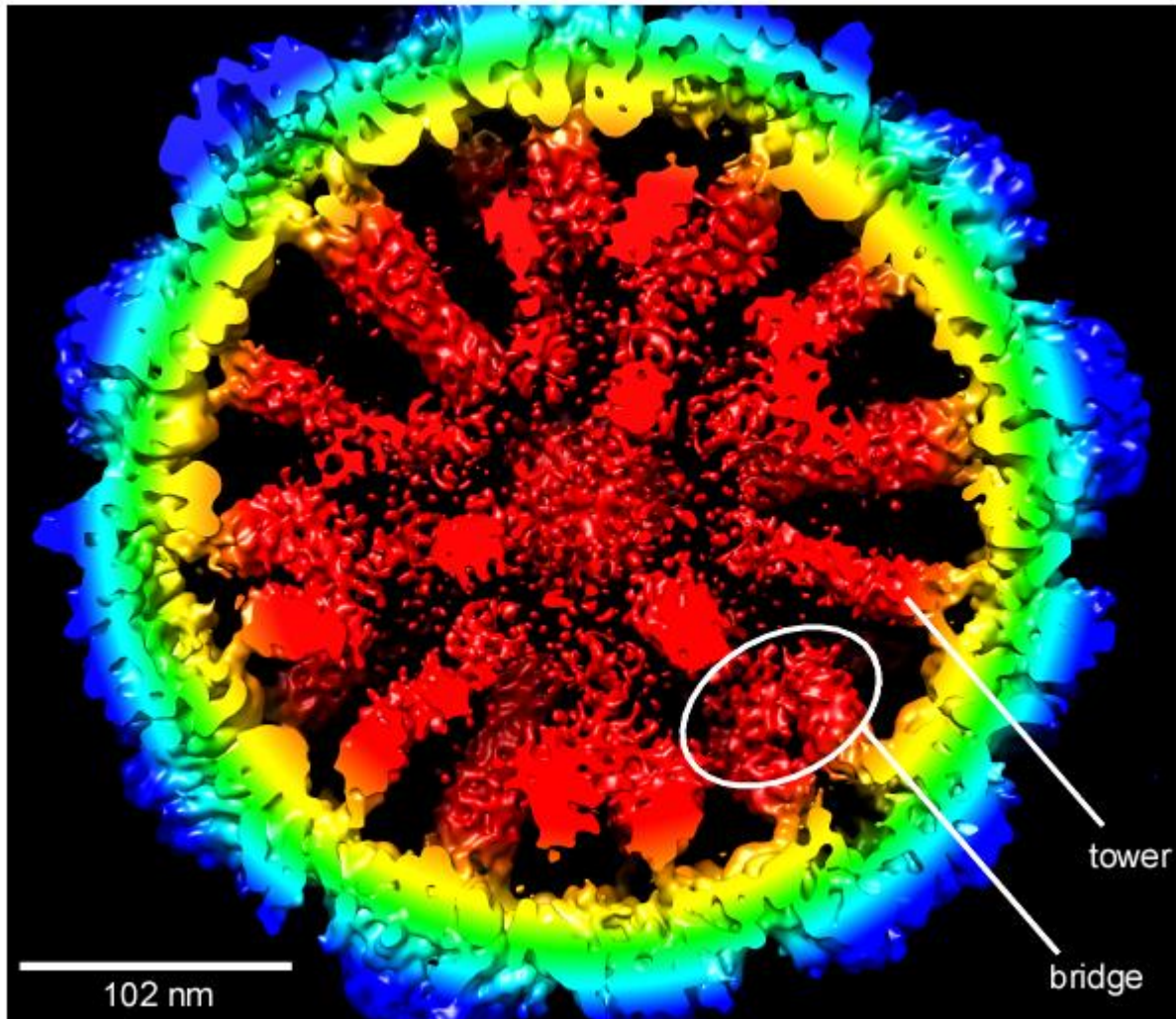


Figure 26. Slice of the Del 2nd Hinge T=4 capsid density map

The delta domains are more stable in this mutant compared to WT. The strong tower like densities of the pentamers could be forming a stable and elongated 5 helix bundle. At this lower contour level, the less dense areas of the map are visible, showing a possible connection of the two bundles in the hexamers, forming a 'bridge' like connection (highlighted by oval). Scale bar represents 102 nm.

Deleting seven residues in this predicted ‘hinge’ region has altered the stability of the delta domain, allowing us to visualize more of this flexible protein. To see if there were any differences in the predicted secondary structure of the delta domain, the mutant sequence was put through PSIPRED’s structure prediction program (<http://bioinf.cs.ucl.ac.uk/psipred/>). From this program, Del2ndHinge contains two predicted helices compared to the WT three predicted helices (Figure 27). The deletion removes exactly seven residues between two regions that are strongly predicted to be α -helical. This change could have caused the elongation and stabilization of the delta domain to form the conformations seen in the density maps.

Del2ndHinge produced a low frequency of WT sized capsids. For about every 50 small particles there was only one T=7 sized capsid. In the unprocessed electron micrographs, tower like internal densities inside the T=7 capsids are also visible, suggesting that these larger capsids might be forming similar tower structures as seen in the mutant T=4 capsids. These internal densities are not visible in micrographs of the WT capsid. Using about 100 T=7 sized particles, James Conway and Alexis Huet created a reconstruction of the mutant T=7 Del2ndHinge capsid (Figure 28A, B). The delta domains possess similar characteristics that were seen in the smaller mutants: towers underneath the pentamers and two smaller protrusions under the hexamers (Figure 28B). Compared to WT HK97 (Figure 28C), more of the delta domains are visible in the T=7 mutant particle.

WT delta domain

Del 2nd Hinge delta domain

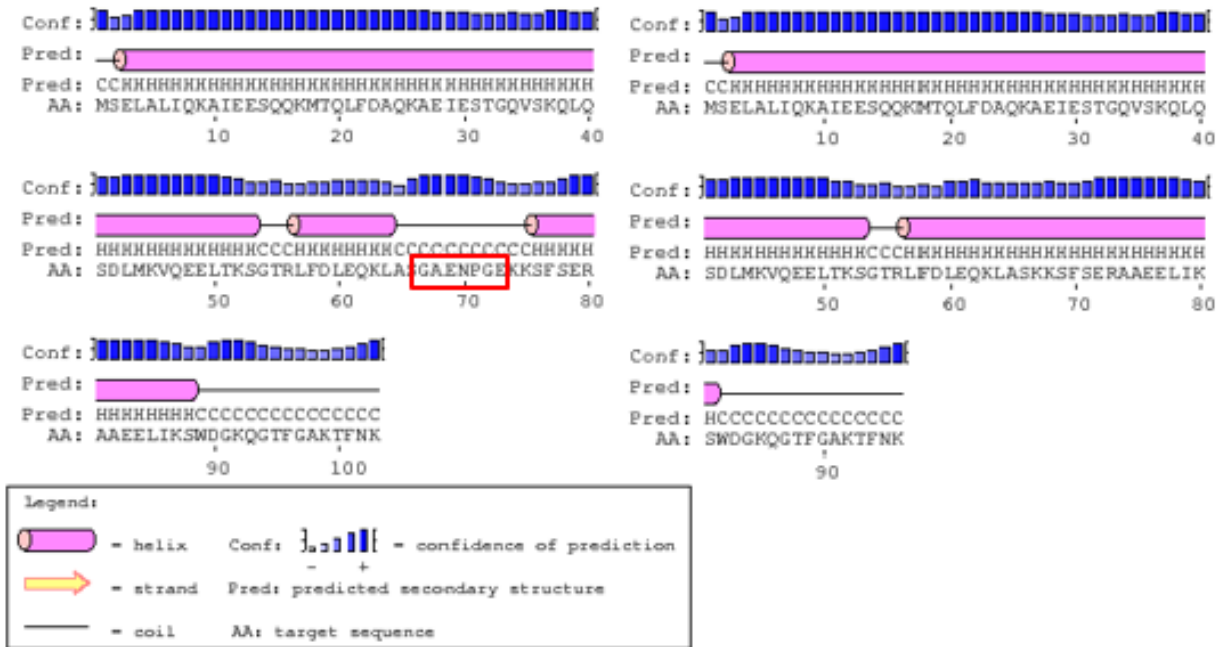


Figure 27. PSIPRED secondary structure prediction of Del 2nd Hinge sequence compared to WT

This secondary structure prediction program predicts the WT delta domain to have three helical regions (left). After the Del 2nd Hinge (deleted residues highlighted in red box), the program predicted this mutant delta domain to only have two helical regions.

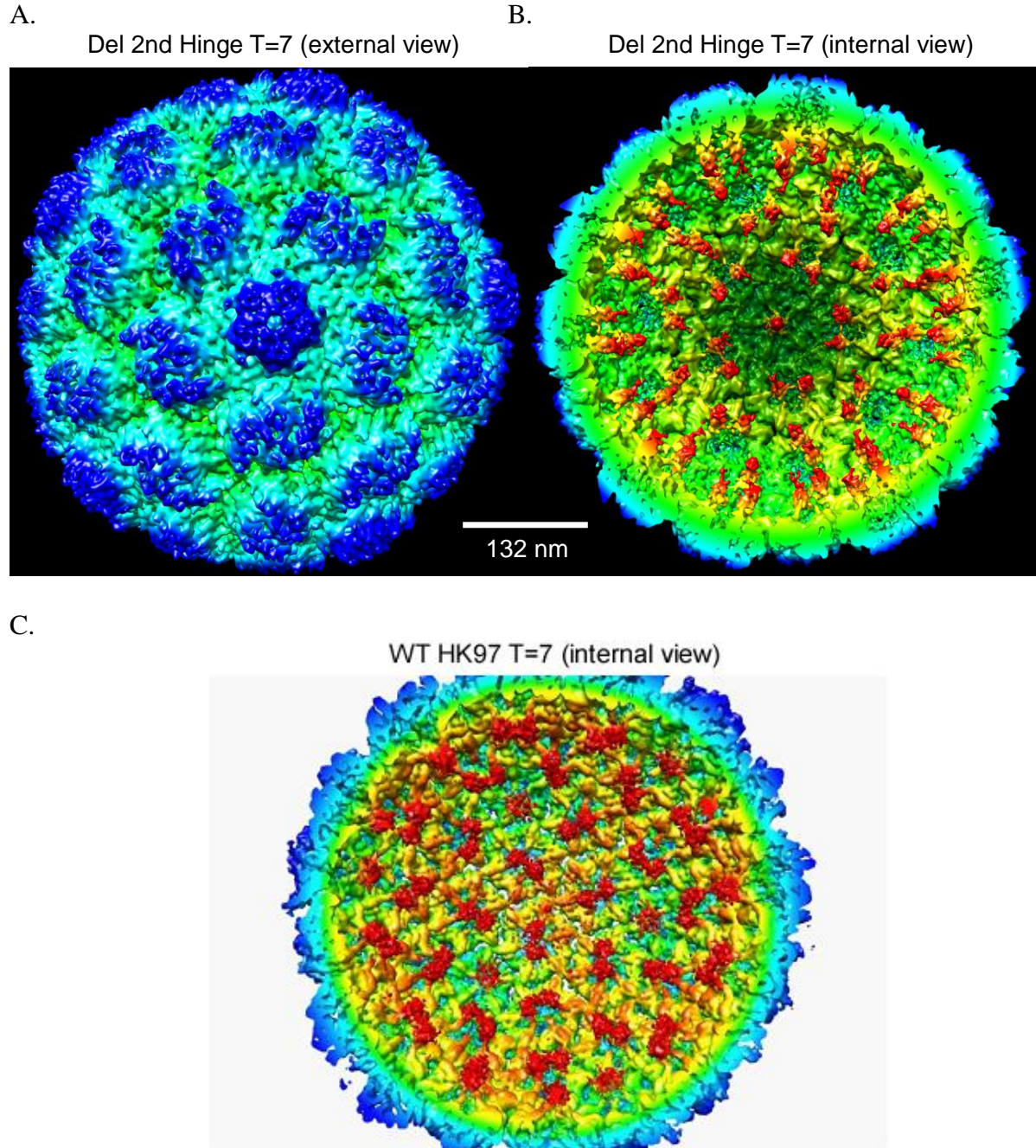


Figure 28. Density map of Del 2nd Hinge T=7 capsids compared to WT HK97

Using about 100 particles, a reconstruction of this mutant T=7 capsid was made. A) An external view of the capsid looks similar to WT. The hexamers are skewed as is seen in WT Prohead I. B) An internal view of the mutant capsid shows the delta domains as red blobs and the spoke regions as yellow-greenish. Like in WT, there is one group of delta domains per pentamer and two blobs per hexamer. However, even at this lower density contour, the pentamer delta domains are more extended towards the center of the capsid than they are in WT. Similar to the T=4 capsids, the delta domains seem to be more stable in this mutant. C) Internal view of WT HK97 capsid is shown as a comparison. The scale bar represents 132 nm.

Figure 29A shows the mutant capsid using a reduced contour level to show less dense regions of the map, so we can visualize more of the delta domains. At this level, we can again see the stable towers of a possible 5 helix bundle underneath the pentamers and we can hypothesize that the two bundles underneath the hexamers may connect to form a bridge across the skewed hexamer. In a slice through this mutant capsid, we can see that the pentamer delta domain densities are very strong, showing a drastic difference in stability between this mutant and the WT (Figure 29B)

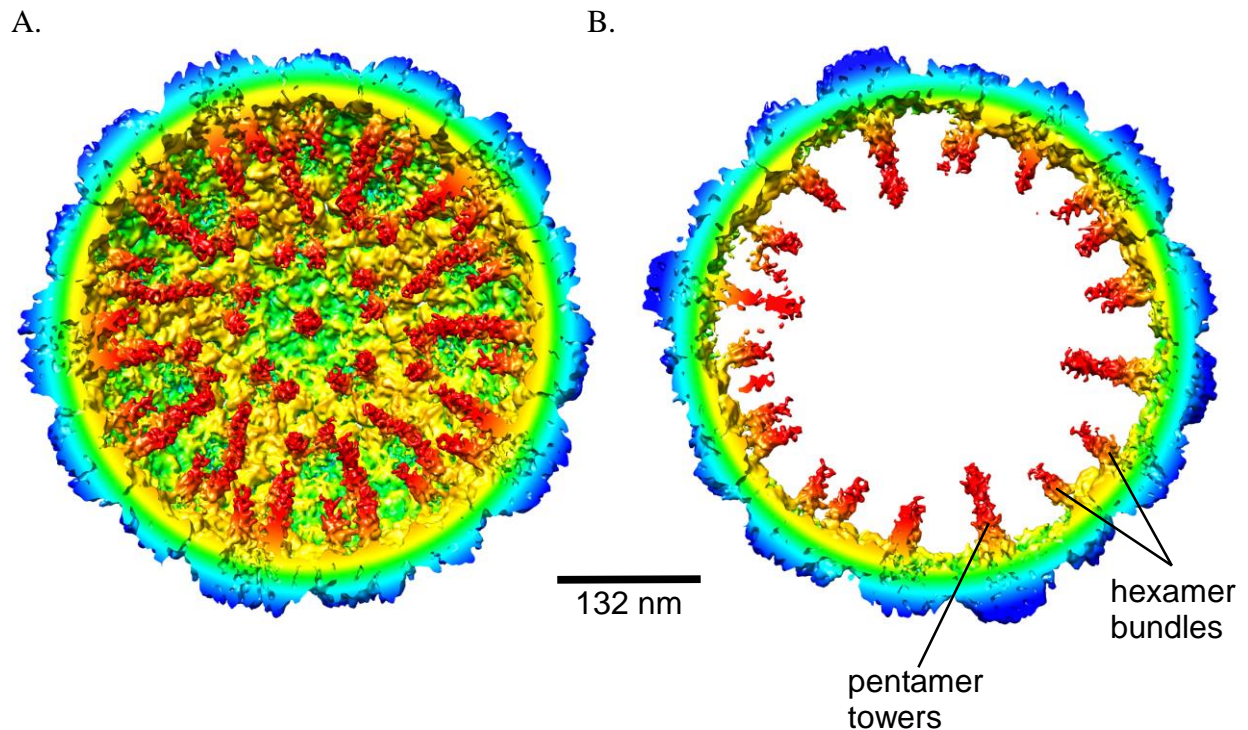


Figure 29. Density map of Del 2nd Hinge T=7 particles show similar delta domain conformations as T=4 mutant particles.

A) An internal view of the T=7 mutant capsid shows the dimers of delta domain from each hexamer and the tall tower from each pentamer. B) A cross-section through the capsid highlights the elongated towers of density in the pentamers. We can hypothesize a five helix bundle is formed. In the hexamers, there is a more stable and elongated delta domain density as well. At even lower contour density levels, it is possible that the two hexamer delta domains form a bridge connecting the two bundles, similar to what is seen in the T=4 mutants.

A noticeable difference between the three different types of capsids lies in the spoke densities. As mentioned before, in the WT T=7 Prohead I, there is a distinct spoke density underneath each capsid subunit and they are mostly equal in strength (Figure 30A). With Del2ndHinge T=4 mutant capsids, there are spokes underneath each capsid subunit, but they are not all at equal densities. The pentamer spokes show relatively equal densities because of the five-fold symmetry imposed. These spokes also visibly show a connection into the rigid pentamer towers. In the hexamers, different spokes have different densities. The weakest spoke densities (highlighted by ovals) do not have an obvious connection towards the ‘bridge’ bundles. As mentioned earlier, the strongest spokes interact at the 3-fold symmetry axis between three adjacent hexamers (highlighted by circles) (Figure 30A, B). With Del2ndHinge T=7 mutant capsids, there are again equal density spokes underneath each pentameric subunit due to the imposed symmetry. In the hexamers, the spokes of the subunits that are in direct contact with spokes of a pentamer are not visible (ovals). The other four adjacent spokes of the hexamers are strong and we can see their connections to form the ‘bridge’ bundles (Figure 30C). This deletion mutant has created a drastic assembly defect that can produce different sized capsids. Because of this change, the delta domains are more stable, allowing us to visualize more of this region of the major capsid protein. The different point mutations, insertions, and deletions have shown that the delta domain not only plays a role in capsid protein solubility and capsid assembly, but in capsid size determination as well.

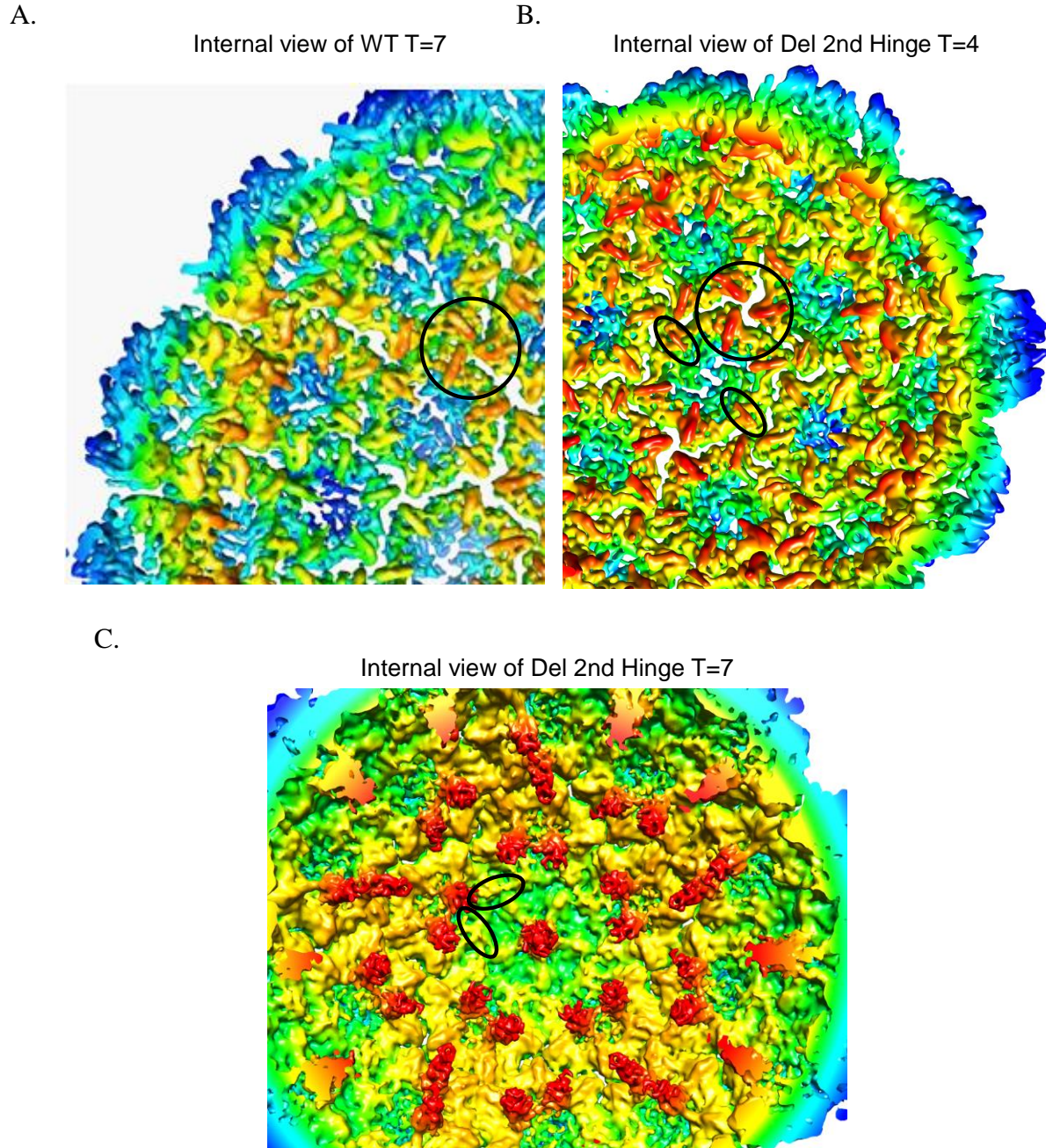


Figure 30. The spoke densities are different between all capsids (WT T=7, Del 2nd Hinge T=4, and T=7)

Cropped sections of the internal densities of the WT and mutant capsids are shown. A) In the WT capsid, the spoke densities are mostly equal in strength in each subunit. B) In the Del 2nd Hinge T=4 capsids, the spoke densities are equal in each subunit of the pentamer. In the hexamers, one opposing pair of spokes are less dense than the other four (highlighted with ovals). There also seems to be one dominant pair of spokes at the 3 fold symmetry axis. C) In the Del 2nd Hinge T=7 capsid, the spokes of the pentamer subunits are equal in density. In the hexamer, there are also a pair of adjacent, weaker, barely visible spokes (highlighted with ovals). The missing spokes are also only located at a pentamer-hexamer interface. The capsid subunits in the hexamers surrounding the pentamers are missing their spokes. The four visible spokes continue to form the red colored densities of the delta domain. Capsids are not to size.

2.3 DISCUSSION

The full length delta domain is required for capsid protein expression

Previous lab members and I have conducted a large number of mutational analyses to better understand the role that the delta domain plays in capsid assembly. Our initial deletion experiments were done to answer an important question: is the delta domain required for HK97 capsid assembly? Our full deletion studies show that the delta domain is required for capsid protein expression solubility. Even when plasmid expression was enhanced by the addition of the T7 RBS and tag sequence with the pNoDelta2 construct, the capsid protein was still mostly insoluble. These results show that the delta domain, like other known viral scaffolding proteins, plays an important role in capsid assembly. The capsid protein cannot function properly without the delta domain. This domain could be acting as a chaperone in regards to capsid protein folding upon translation. The delta domain's presence as part of the capsid protein is somehow aiding its folding and solubility. From the experiments with different sized deletions, we learn that the full length delta domain is required. Even Del1, a deletion of just 9 residues near the N-terminal region of the delta domain, produced non-functional capsid protein. It was not able to complement phage with an amber mutation in the capsid gene. This slightly shortened delta domain is unable to carry out its roles to ensure proper capsid assembly. More in-depth studies of the Del1 mutant proheads, presented in Chapter 3 identify the reason behind its inability to form viable phage particles. Del2 never made detectable HK97 protein products suggesting that this deletion reduces expression or makes the protein very unstable. The larger deletions (Del3 and Del4) produced insoluble protein, similar to the results with the full length deletion. These general deletions show us that the delta domain plays a critical role in capsid assembly.

The C-terminus of the delta domain is involved with specifying proper capsid geometry

In the WT Prohead I reconstruction, spoke like densities are visible which are not seen in the Prohead II reconstruction. We hypothesize that these densities may contain parts of the delta domain that are lying against the internal surface of the capsid proteins. The C-terminal region of the delta domain was targeted for mutations because we believed this region may be a part of the spoke interactions. Two point mutations in the C-terminal segment of the delta domain, W89A, and D90A showed drastic capsid assembly defects. Further biochemical tests show that a total of five point mutants (included W89A and D90A) cause similar abnormal assembly phenotypes. L85R, W89A, D90A, D90G, and F96L all produce uncleaved mcp, which resides mostly in the pellet fractions, along with higher molecular weight bands, indicating possible cross-linking due to premature expansion and/or the formation of tube like structures. All of these point mutants produce abnormal assembly products. These mutations prevent the capsid from assembling correctly into T=7 icosahedral capsids. They mostly made irregular round structures or short tube like structures which aggregated with cellular debris. This aggregation explains their strong presence in the pellet fractions. These mutants were still able to produce soluble capsids subunits which could form hexamers and pentamers. The folding of the subunits appears to be correct, but the interaction of the subunits is somehow altered. In some cases, it seems that capsid assembly begins normally, as many of the tubes have at least one closed end and some of their diameters are similar to the diameter of WT capsids. As assembly progresses, however, the capsid proteins begin to spontaneously expand before cleavage has occurred, leading to the monster or tube formation. If these C-terminal residues are located in the spoke region, then a mutation could be disrupting the interactions between the delta domain spoke and the internal surface of the rest of the mcp. Adding a charged group or removing a large or charged group in this region could

affect the conformation of the mcp subunit, triggering the formation of abnormal or tube like structures and resulting in loss of functional protein. This loss of function is confirmed by spot complementation tests.

The mutated mcps are unable to complement amber phage to produce viable phage. However, these mutants were also decreased in complementation efficiency for protease amber phage. The protease produced from the plasmid is wild-type, so in theory, the protein should be able to complement and form plaques at all dilutions. If a mutation shows a defect in protease complementation, then this could indicate an interaction between the mutant capsid protein and the WT protease that are expressed from the plasmid. The mutant protein is sequestering the WT plasmid-expressed protease, which prevents the protease from fully being able to complement the amber phage. This suggests that the abnormal and tube like assemblies might still be capable of binding and incorporating the protease, but due to the altered capsid protein conformation and premature expansion and cross-linking, the protease cannot activate and function to cleave the delta domain. This inability of the protease to function correctly and at the correct time could explain why all these mutants produced uncleaved mcp. Also, the assembly efficiency of these abnormal structures could be drastically decreased, allowing for protease degradation before the structures finish assembling. A way of testing for protease incorporation is to express the mutation with the inactivated protease, which would be visible on an SDS gel if incorporated. However, our purification protocols are optimized for soluble products that are precipitated by PEG. These tubes are present and aggregate in the pellet fractions, preventing proper purification away from cell debris. Therefore, I am unable to determine if these tubes are able to incorporate the protease like WT.

Charged, and bulky side chains in the C-terminus make crucial interactions to ensure proper capsid geometry

Perhaps the deleterious assembly affects were due to the drastic changes in amino acid at these locations. If we change, for example, the hydrophobic Leucine 85 to another similar hydrophobic residue, or Phenylalanine 96 to another bulky sidechain residue, would the capsid protein be functional and able to assemble properly, like WT? Are these particular residues or types of residues required at these locations to ensure proper capsid geometry? Four new point mutations were created in this C-terminal region: L85V, W89Y, D90E, and F96Y to try and conserve the original amino acid properties. In three of these mutants, L85V, W89Y, and F96Y, protein functionality was restored to or very close to WT levels. Even though L85V and W89Y now showed a partial mcp cleavage defect, and produced a few abnormal or tube like structures, they were able to complement major capsid gene and protease gene amber phage like WT (W89Y had a half log decrease in protease complementation). These mutations which were made to similar residues showed WT like phenotypes. These results show that large, aromatic residues at 89 and 96 are required to make the necessary interactions to ensure proper capsid protein conformation, assembly, and maturation. Mutant studies in the C-terminus of the internal scaffolding protein of phiX174 showed that aromatic side chains were important for making contact with capsid protein (Dokland et al. 1999). It is possible that W89 and F96 make contacts with the interior of the capsid shell. When this interaction is disrupted, the capsid shell takes on the wrong geometry.

D90E, on the other hand, still has a mcp cleavage defect. This mutation creates abnormal and tube like structures and very few Prohead I like structures. D90E is still defective in capsid gene amber complementation and shows a 1 log decrease in protease gene complementation. Even though Glutamic acid is a negatively charged residue, position 90 seems to require the

negatively charged properties of Aspartic Acid in order for proper assembly to occur. Aspartic Acid is slightly smaller than Glutamic Acid, so perhaps its size is important for the electrostatic interactions in this location. The major changes that were created in this region significantly altered capsid geometry suggesting that large aromatic, hydrophobic, and charged residues are important in this region of the delta domain. Perhaps mutating this region of the delta domain forced the capsid subunits to interact in a way that favors the assembly or interaction of hexamers, thus causing the formation of tubes. The capsid subunits appear to spontaneously expand before the delta domain is cleaved by the protease. A 42 kDa ladder of uncleaved mcp formed as a result of their premature expansion. Are these C-terminal changes favoring hexamer conformations, thus allowing tubes to form? Due to the premature cross-linking, I was unable to dissociate these abnormal assemblies to test if the ratio of hexamers to pentamers was different than a WT capsid. One future experiment would be to mutate the cross-linking residues of the capsid protein, K169 and N356, which would prevent premature cross-linking from occurring. If the mutant tube like structures are still able to assemble into tubes or other anomalies, then we would be able to dissociate the assemblies and determine the capsomeric ratios. However, the abnormal structures may be unstable without crosslinking and easily dissociate into capsomers.

It would be interesting to learn if the hexamers that make up the tubes are symmetrical or skewed. In Prohead I and II, the hexamers are normally skewed, but in the mature capsid, through expansion, they become symmetrical. If the tube mutant hexamers are symmetrical, it would suggest that mutating the delta domain in this region pushes the capsid protein towards a mature-like conformation. If the hexamers are skewed, then it would support the idea that the removal of the delta domain must precede the maturation steps that lead to hexamer symmetry. However, the tubes are not regular in their structure, they are different lengths and some are

kinked and bend. This would make a reconstruction to visualize the state of the tube hexamers impossible.

Prohead II is more stable than Prohead I and cannot be dissociated into capsomers using glucose or salt. Studying the crystal structures of Prohead I and Head II, there is a difference in the main α -helix backbone of the mature capsid protein. In Prohead I, there is a slight bend in the helix while in Head II, the helix is straight. The delta domain may play a role in the skewing of the hexamers and cause the bend in the helix backbone. Then, once the delta domains are removed, the hexamers remain in this energetically favorable state. This is disrupted when DNA packaging occurs to cause expansion and cross-linking (Gertsman et al. 2009). The skewing of the hexamers in the prohead is an interesting mystery. Currently, we do not know if the hexamers are skewed as individual capsomers, or if the skewing is induced during capsid assembly. Does the delta domain play a role in the skewing? Do the six delta domains bundle into two groups underneath the hexamer and cause the skewing? Or is this a combination of delta domain interaction and subunit interaction between capsomers? With more studies on the interactions in the interfaces of the capsid subunits and on the delta domain's role in assembly, we can learn more about the finer details of the interesting and complex HK97 capsid assembly pathway.

The search for 2nd site suppressors of delta domain point mutations

To learn more about how the delta domain may be interacting with other delta domains or other capsid proteins during assembly, we can move mutations of interest into an HK97 prophage and induce lytic phage growth. If there are 2nd site suppressors elsewhere in the genome, then we can hypothesize that the initial mutation and the 2nd site mutation are close to each other and may interact.

Recombineering was used to move mutant fragments of DNA into the prophage. My initial attempts using galK recombineering were with LIM 49. However, I was never able to identify positive recombinants. When using tetR selection for recombineering, I was able to successfully move the C-terminal mutation W89A into a prophage. However, I was never able to produce any phage particles. W89A was made using two base pair changes in the genome. Perhaps, it was too difficult for the phage to suppress two base pair changes or revert back to WT. Also, W89A caused premature expansion and cross-linking and the formation of abnormal capsid structures. Even if there were no suppressors or reversions, it would be highly unlikely that this mutation could have been tolerated in the phage. I noticed a high level of background colonies, showing that the selection system was not very efficient. In chapter 3, I will discuss a few changes made to the recombineering protocol which resulted in a positive recombinant and phage induction.

Deleting predicted flexible regions in the delta domain disrupt capsid solubility, assembly, and affect capsid size

Based on secondary structure prediction algorithms, the delta domain is composed of three α -helical regions and one β -sheet region. If this is true, there would be possible flexible regions in between the more structured areas. The delta domain is flexible, and less ordered than the rest of the major capsid protein, which has prevented its crystallization. Perhaps its flexibility is a part of its function. If this is true, then removing its flexibility should have detrimental effects on its function and assembly. To test this hypothesis, I deleted two predicted 'hinge' regions in between predicted α -helical regions: Del 1st Hinge and Del 2nd Hinge. Del1stHinge turned out to create nonfunctional protein, which was unable to produce soluble capsid subunits. This deletion

removed a Glycine, a known player in flexible regions. The deletion of six residues in this ‘hinge’ showed that this region, and its flexible nature are important for assembly. Without this flexible region, the capsid protein precipitated out of solution. The flexibility of the delta domain could be an important role of its chaperone like qualities in regards to protein solubility. Like the previously discussed deletions: Del2, Del3, and Del4, the length of the delta domain cannot be disrupted without sacrificing functionality. This deletion showed that the flexible regions in between the predicted helical regions are just as important for protein solubility and functionality.

Del 2nd Hinge is a particularly interesting mutation, as it creates the most drastic assembly defects out of all the delta domain mutations studied so far. This deletion has created a very interesting phenotype of producing mostly abnormal structures, and two different-sized capsids with triangulation numbers of T=7 and T=4. This deletion removed seven residues in between predicted helices 2 and 3. Del 2nd Hinge deleted two glycines and a proline, which are known for their roles in flexible regions of a protein. Removing this flexible region caused a dramatic assembly defect. When I was going through the micrographs and picking particles, it was obvious that the majority of the products were abnormal assemblies. This showed that removing this region mostly affected how the capsid subunits interacted to make a capsid. This deletion was able to make soluble protein, indicating that it did not strongly interfere with protein solubility. This strongly showed that the delta domain plays an important role in proper capsid formation, and that the delta domain is like a scaffolding protein. The two different sized capsids show that this mutation can sometimes assemble into an icosahedral structure.

In some preliminary flexible fitting models, we are able to fit the HK97 crystal structure into the density maps of the T=4 and T=7 reconstructions. This demonstrates that this deletion

has not affected the overall fold of the HK97 capsid subunit. The main interactions between delta domains and adjacent subunits is affected. It is very exciting that this deletion is able to stabilize the delta domain and creates the towers of density under the pentamers and the two bundles underneath the hexamers. This is drastically different from the spidery blob like densities that are visible in the WT capsid. Del 2nd Hinge has indeed reduced the flexibility and disorder of the delta domain, allowing us to visualize more of this part of the capsid protein. We can see the spokes of density underneath each pentamer subunit connect and twist into the elongated tower. We hypothesize that the delta domains of a pentamer are capable of creating a five helix bundle.

Secondary structure prediction program PSIPRED predicts that this deletion has converted the three helix delta domain into a two helix delta domain. A deletion of seven residues, a heptad repeat, likely aided in this elongation of the helical structure of the domain. The joining/elongation of two helices into one has stabilized the delta domain and created or stabilized this tower like conformation. In the density maps, it seems that = with the hexamers, the two delta domain bundles may connect with each other across the hexamer and create a bridge of delta domain interaction. Del 2nd Hinge not only has changed the size of some of the capsids produced, but it has also changed how the delta domain is structured inside the capsid. Because the delta domain is mostly α -helical, it is highly probable that it uses coiled coil interactions to function. Perhaps these elongated delta domains are more stable because they are better able to make coiled coil interactions with neighboring delta domains. The delta domains appear to have similar structures in the T=4 and the T=7 mutant capsids. At very low frequency, the mcp is still able to assemble into the correct capsid, but is still not functional in complementation assays. This may be due to the inability of this mutant to incorporate the portal protein and a lowered ability to incorporate the protease; but the portal is a vital component of

the phage, as it is required for DNA packaging and injection. In spot complementation tests, we expect the WT phage control to produce plaques at all dilutions, but the WT phage spotted on these deletion mutation plates showed a decrease in complementation. This is suggesting that the mutant capsid protein is exerting a dominant negative effect in complementation. The mutant proteins may be interacting with or affecting the WT phage capsid proteins and creating chimeric capsids. These mixed capsids, which sequester the WT proteins prevents them from being incorporated into viable phage particles. Perhaps this deletion has removed a critical portal binding site, or because the deletion has made the delta domain elongated and more stable, it can no longer make the correct interactions with the portal. During assembly, the portal is surrounded by five hexamers and the delta domains have to be flexible enough to create a different type of interaction with the portal than it has by itself or with the protease. The rigid and protruding bundles of delta domains may completely prevent binding.

Another interesting effect of this deletion is the difference in spoke densities among all three icosahedral capsids: WT, Del 2nd Hinge T=4 and Del 2nd Hinge T=7. In Del 2nd Hinge T=4 capsids, two opposing spokes of the six spoke densities of a hexamer were reduced. This suggests that two of the delta domains in a hexamer have become more disordered than normal, possibly due to a lack of partners to interact with, and were averaged out during the reconstruction. The other four delta domains involved with creating the two bundles are more stable. In the Del 2nd Hinge T=7 capsids, the densities of two adjacent delta domains of the six delta domains in a hexamer are basically non-existent compared to the other four delta domains. There is no spoke and no connecting density into the bundle. These missing spokes are in the subunits which surround a pentamer. Perhaps these differing spoke densities in the deletion are the reason why the capsids are unstable and easily dissociate into capsomers. The different types

of capsids and the different spoke interactions that are visible inside leads to hypothesize that the spokes may play an important role in capsid stability and possibly even capsid size. It would be interesting to learn more about the specific interactions between capsomers and try to identify any differences that could help explain how it is assembling into different sized capsids.

This mutation has allowed towers and bridges of delta domain to be visible in the density map, and we can use these mutant reconstructions as models to learn about potential conformations the delta domain can make. It is possible that these structures exist in the wild-type situation, but are only transient and unstable. We can fit helical models into the strong delta domain densities to learn how the delta domain could be interacting with its neighbors to form these types of interactions. We can also learn how the delta domain could be interacting with the internal capsid surface, with the portal, and the protease proteins. It is amazing that this one little part of a capsid protein is able to play so many roles during the assembly process. This region is responsible for protein solubility and folding, capsid geometry and overall assembly, and even capsid size. The next chapter will focus on more of the specific roles that specific regions of the delta domain play during assembly.

3.0 THE DELTA DOMAIN HAS A ROLE IN PORTAL AND PROTEASE INCORPORATION

3.1 INTRODUCTION

The delta domain acts as a scaffolding protein in HK97 capsid assembly. Initial deletions and mutations show that the full length delta domain is required for proper capsid protein expression, while other mutations affect capsid assembly, and capsid size. Also, by testing point mutations, we have identified that the C-terminal end of the delta domain plays an important role in capsid geometry.

Other phage scaffolding proteins, like those in P22, have been shown to play a role in incorporating minor proteins into the capsid (Weigele et al. 2005). HK97 capsids contain two other proteins that are necessary for maturation and DNA packaging: a phage encoded protease, and a portal. The C-terminal end of the protease is believed to interact with the major capsid protein, thus allowing its incorporation into the capsid during assembly (Duda, Oh, and Hendrix 2013). The N-terminal region of the capsid protein, the delta domain, could be facilitating this interaction. The portal is a 12-subunit ring structure located at one vertex of the capsid. It is predicted that for some viruses the portal nucleates assembly. This could be a way to ensure that there is only one portal per capsid. There is evidence in Herpes Simplex Virus Type 1 (HSV-1), that the scaffolding protein plays a role in interacting with the portal during capsid assembly

(Newcomb, Homa, and Brown 2005; Lee and Guo 1995; Moore and Prevelige 2002). Previously, I have shown that the delta domain is similar to other viral scaffolding proteins in being required for proper capsid assembly. In this section, I will show evidence that the HK97 delta domain is acting to direct the incorporation of the protease and portal, as other scaffolding proteins do. Mutational studies show that distinct regions of the delta domain interact with the protease and the portal during capsid assembly.

3.2 RESULTS

3.2.1 The 2nd predicted helical region plays a role in portal incorporation

Amino acid sequence alignments were used to identify features that are conserved between the HK97 delta domain and delta domains of similar phages. Conserved patches of residues may indicate a functional importance to that region, which can be targeted for mutagenesis. An alignment of the HK97 mcp and related proteins was made using BLAST and Clustal (R. Duda, <http://gigapan.com/gigapans/b806a9da80b4a66bcb1dd1b273d5b7a4/>). A portion of the alignment is shown in Figure 31. In our alignment we see a series of hydrophobic residues that are regular intervals apart, which is a common characteristic of heptad repeats in coiled-coils (highlighted in blue). The predicted secondary structure is shown along the top of the figure. As described before, the delta domain is predicted to be mostly α -helical, separated into three helical regions, with a small predicted β -sheet at the C-terminal end. This regular pattern of hydrophobic residues is typical for helices involved in coiled-coil interactions. Besides these hydrophobic residues, there is a prominent conserved region containing the sequence EQK (E61,

Q62, and K63 in HK97). This is seen in about 50% of the sequences in the alignment. These three residues lie near the end of the 2nd predicted α -helix and could be playing a critical role in capsid assembly. Therefore, they were individually mutated to alanines and tested by complementation and for assembly defects in miniprohead expression experiments.

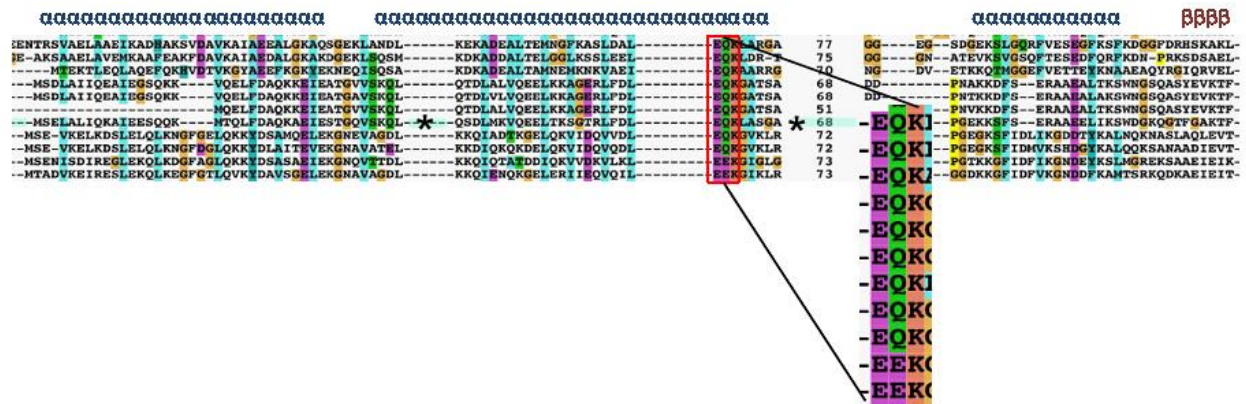


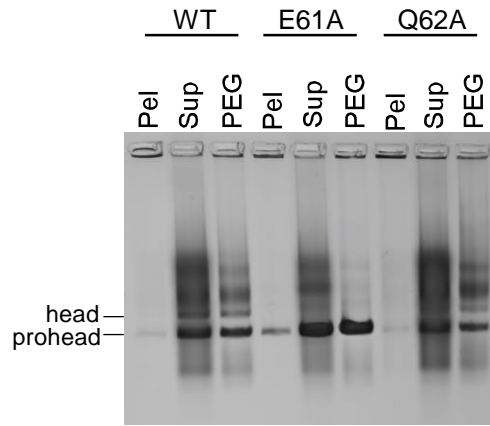
Figure 31. Portion of HK97 delta domain protein sequence alignment shows a conserved patch

A sequence alignment of the HK97 major capsid protein and related proteins was made in Clustal by Bob Duda. This portion of the alignment shows the delta domain. The sequence highlighted with the asterisks is HK97. The colors correspond to conserved residues. The predicted secondary structure is shown on top. Other than a series of hydrophobic residues, the EQK patch is present in about 50% of the aligned sequences (boxed region). These residues were mutated to alanines to test if their conservation played an important role in delta domain function and capsid assembly.

The pellet, supernatant, and PEG fractions of E61A and Q62A were run on agarose and SDS gels to determine what kind of protein assemblies are made, and if the mcp is processed correctly. On an agarose gel, E61A produced only Proheads while Q62A produced proheads and heads like WT (Figure 32A). In the SDS gel, E61A produced uncleaved mcp showing that it is defective in proteolysis, while Q62A produced cleaved mcp like WT (Figure 32B). Miniprohead prep samples were prepared for visualizing with the TEM. In the electron micrographs, E61A produced WT like proheads and Q62A produced WT-like proheads and heads. Purified portal-containing Prohead I is shown for comparison (Figure 33). K63A will be discussed in detail in a later section of this chapter (p. 106). Complementation spot tests showed that all three mutations had a three log decrease in capsid gene complementation efficiency compared to WT. E61A and Q62A were also one log down in protease gene amber phage complementation (Table 1).

The charge change mutation, E61A, in the conserved patch caused a cleavage defect. Therefore, it is not surprising that it was unable to complement phage with an amber mutation in the capsid gene. Perhaps E61A affects the interaction between the capsid proteins and the protease. On the other hand, Q62A showed WT like phenotypes in all biochemical assays. Q62A proheads were able to cleave properly and expand to form heads *in vitro*. These initial plasmid studies only expressed the protease and capsid genes; the portal gene is not included in the plasmids. Perhaps Q62A affects the interaction between the capsid proteins and the portal. These mutants were moved into a plasmid that expresses the portal and inactivated protease (pVP0 g4 (H65A)) so that we could detect incorporation of these proteins using gel electrophoresis.

A.



B.

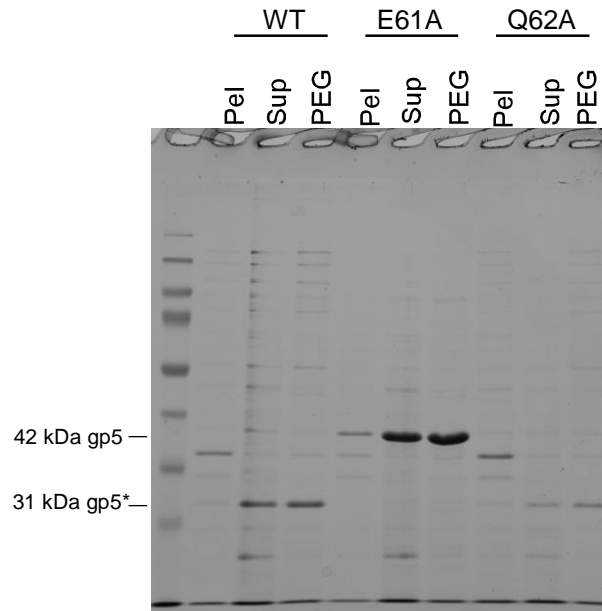


Figure 32. Miniprohead prep results of E61A and Q62A

A) Pellet, supernatant, and, PEG samples were loaded on a 0.9% agarose gel to detect assembly products. WT produced proheads and heads. E61A produced proheads only. Q62A produced proheads and heads like WT. B) On the SDS gel, WT showed cleaved 31 kDa mcp. E61A showed uncleaved 42 kDa mcp. Q62A produced cleaved mcp like WT.

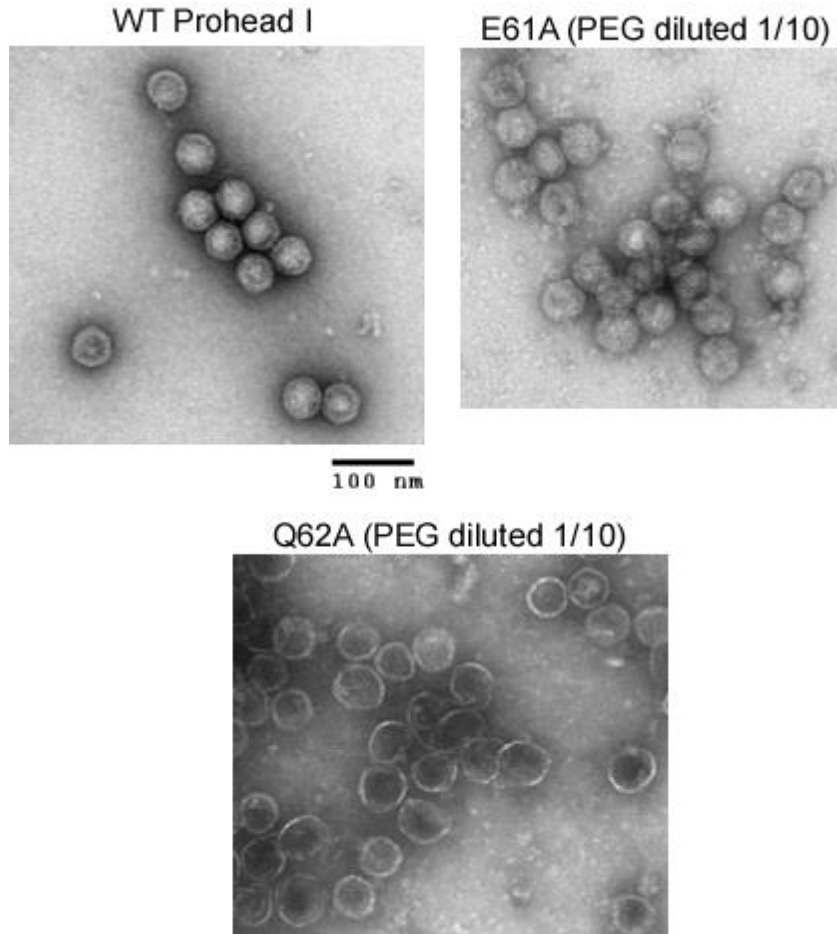


Figure 33. Representative EM images of E61A and Q62A PEG samples

WT Prohead I is used as a comparison. The miniprohead prep PEG samples were diluted 1/10 in 1x calorimetry buffer and stained with 1% uranyl acetate. E61A produced WT-like prohead particles. Q62A produced proheads and heads. Heads are visible as thinner shelled particles due to their expanded state.

E61A and Q62A show portal incorporation defects

Large scale prohead preps were made of E61A and Q62A in plasmids carrying the portal and inactivated protease genes. The purified samples were precipitated with 10% TCA and run on SDS gels to detect the presence of portal or protease bands with coomassie staining (Figure 34). The SDS gel contains Prohead II with portal and Prohead I with portal as controls. Prohead II produced a 31 kDa mcp cleaved mcp band and 47 kDa portal band. Prohead I produced an uncleaved 42 kDa mcp band, along with the portal and the 25 kDa protease. E61A produced uncleaved mcp. There was no detectable portal or protease protein in this sample. Q62A produced an uncleaved mcp and a protease band, but this mutant did not incorporate any detectable portal protein. (Figure 34A). The mutant prohead samples were run on a 0.9% native agarose gel to visualize the presence of prohead dimers or larger structures. This sensitive assay is able to detect low levels of portal incorporation, even when we cannot detect a strong portal band in the SDS gel. Prohead II control produced prohead and head bands. Prohead I control produced prohead, prohead dimer, and prohead trimer bands. E61A and Q62A produced very strong prohead bands. E61A produced very light prohead dimer and trimer bands while Q62A produced a very light prohead dimer band (Figure 34B). These weaker bands show that E61A has a protease and portal incorporation defect while Q62A has a portal incorporation defect. These results confirm that this conserved region in the delta domain plays important roles in capsid assembly.

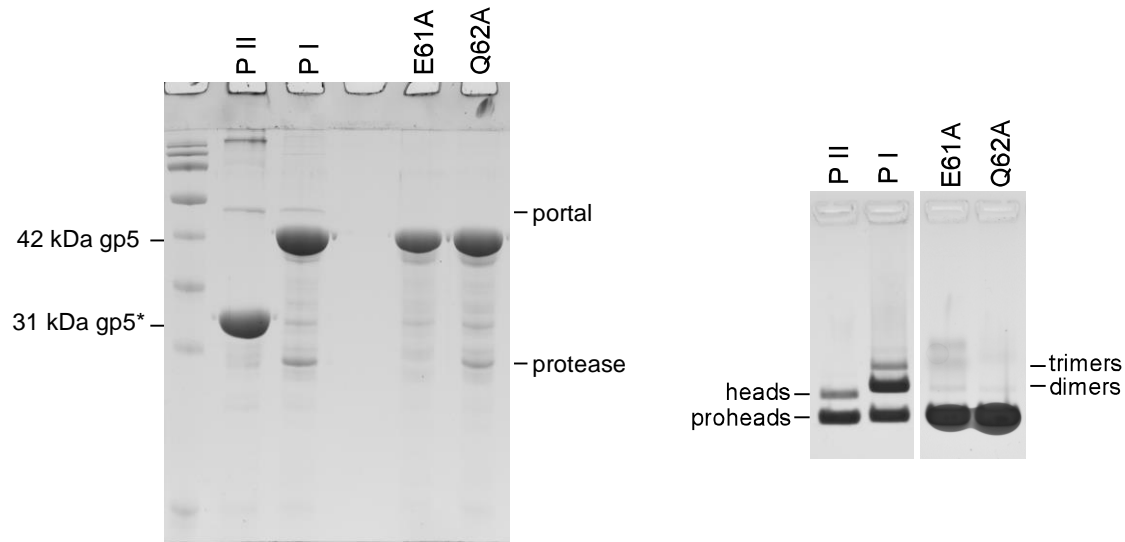


Figure 34. E61A is defective in portal and protease incorporation. Q62A is defective in portal incorporation

A) Purified prohead samples were prepared for SDS gels, and stained with coomassie. Prohead II (P II) and Prohead I (P I) with portal act as controls. Prohead II produced the portal and cleaved mcp. Prohead produced portal, uncleaved mcp, and protease bands. E61A only showed an uncleaved mcp band. There was no detectable portal or protease bands. Q62A showed an uncleaved mcp band and a protease band. B) Purified prohead samples were loaded on a 0.9% agarose gel. Prohead II produced proheads and heads. Prohead I produced proheads, prohead dimers, and prohead trimers. E61A showed a very strong prohead band, with barely detectable dimer and trimer bands. Q62A produced a very strong prohead band, and a barely detectable dimer band.

Identifying important residues in the predicted 2nd helix of the delta domain

Mutant studies on this conserved “EQK” region of the delta domain showed that it contains two neighboring residues which are important for portal incorporation: We wanted to test if there were other residues in the predicted 2nd helix which were also involved with interacting with the portal. The amino acid sequence of the predicted 2nd helix was threaded into a helical projection wheel program (<http://rzlab.ucr.edu/scripts/wheel/wheel.cgi>) to identify neighboring residues that might be on the same side of the predicted α -helix as E61 and Q62 (Figure 35). Perhaps these upstream and downstream residues also make important contacts with the portal during assembly. Arrows show the residues that were targeted for mutagenesis. Based on the helical projection wheel prediction, point mutations were designed to create drastic changes in side chain character.

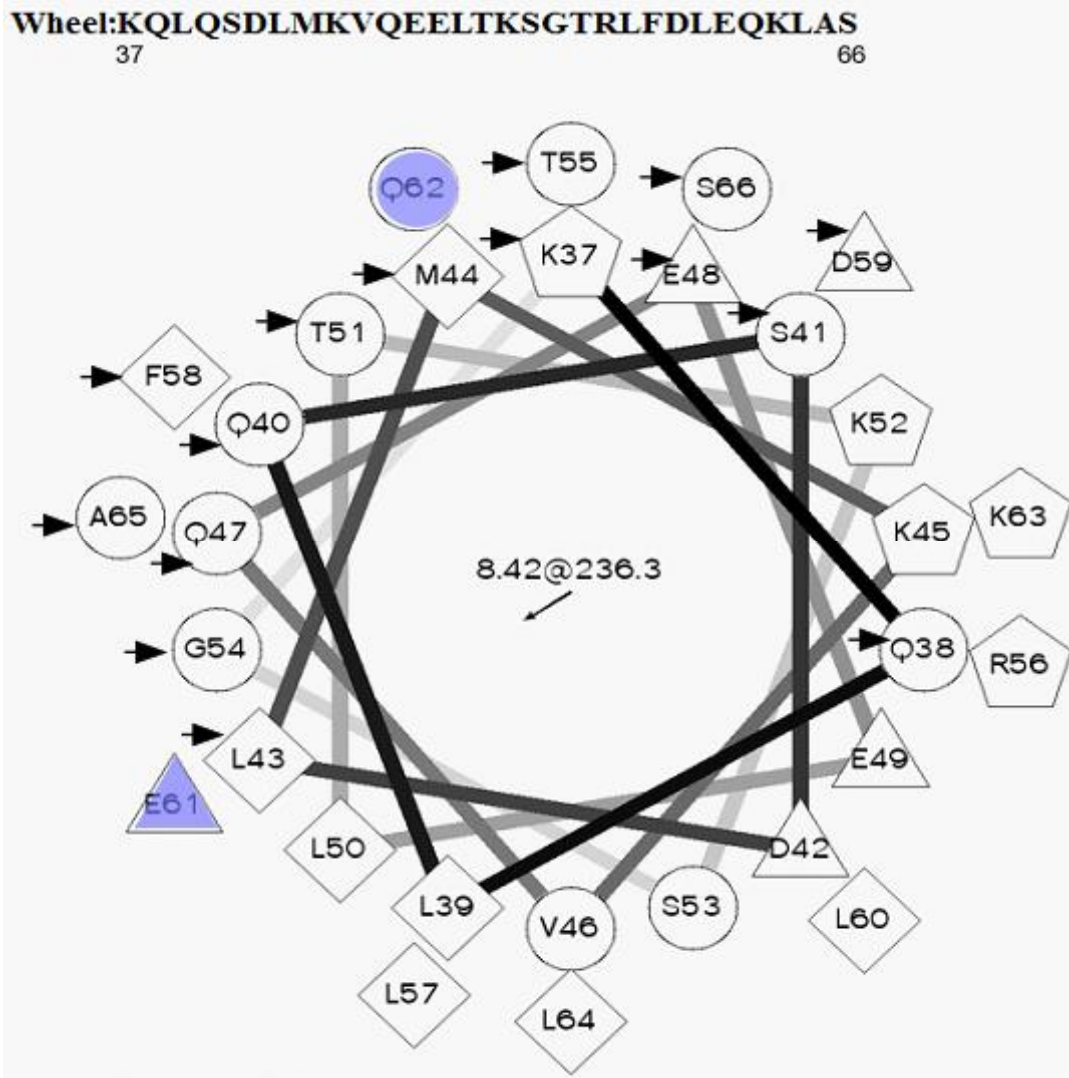


Figure 35. Helical projection wheel model of the 2nd predicted helix protein sequence

The amino acid sequence of the 2nd predicted helix of the delta domain (K37-S66) is shown at the top. E61 and Q62 are highlighted as the initial residues found to have a role in portal incorporation. The black arrows point to surrounding upstream and downstream mutations (mostly on the same side of the predicted helix) that were tested for portal incorporation defects. The circles represent uncharged polar residues. The triangles represent negatively charged residues. The diamonds represent hydrophobic residues. The pentagons represent positively charged residues.

17 new point mutations were made in this predicted helical region. The miniprohead prep results of 9 mutants (K37A, Q38A, Q40A, S41F, M44K, E48A, T51A, T55I, and T55F) produced WT-like phenotypes (Figures 36 and 37) and were able to complement amber phage like WT (Table 1). At times, K92A was used as a control in the miniprohead preps because it causes a partial cleavage defect and conveniently produces cleaved and uncleaved mcp bands in SDS gels and proheads, heads, and capsomer bands on agarose gels. K92A is discussed in further detail in Appendix A.

Eight out of the 17 point mutations (Q38P, L43R, Q47A, G54Y, F58L, D59A, A65E, and S66F) showed defects in capsid gene amber phage complementation. L43R, Q47A, and G54Y also showed slight defects in protease gene amber complementation (Table 1). The pellet, supernatant, and PEG fractions of these defective mutants were loaded on 0.9% agarose gels to detect the protein assemblies that were made (Figure 38). WT and K92A were used as controls. Q38P produced a very strong prohead band. L43R and Q47A also only produced prohead bands. F58L, D59A, A65E, and S66F produced prohead and head bands like WT (Figure 38). On SDS gels, Q38P, L43R, and Q47A produced only uncleaved mcp. F58L and D59A produced mostly cleaved mcp with very light uncleaved mcp bands in the PEG fractions. A65E and S66F show cleaved mcp like WT. However, for S66F, the mcp band is strongest in the pellet fraction (Figure 39). Q38P, L43R, and Q47A had cleavage defects, indicating a possible defect in protease incorporation. F58L, D59A, A65E, and S66F showed phenotypes similar the portal incorporation defect mutant Q62A- perhaps these mutants also affect interactions between the delta domain and the portal. The PEG fractions were visualized using the EM. Q38P, L43R, and Q47A produced proheads whereas G54Y, F58L, D59A, A65E, and S66F produced proheads and heads (Figure 40).

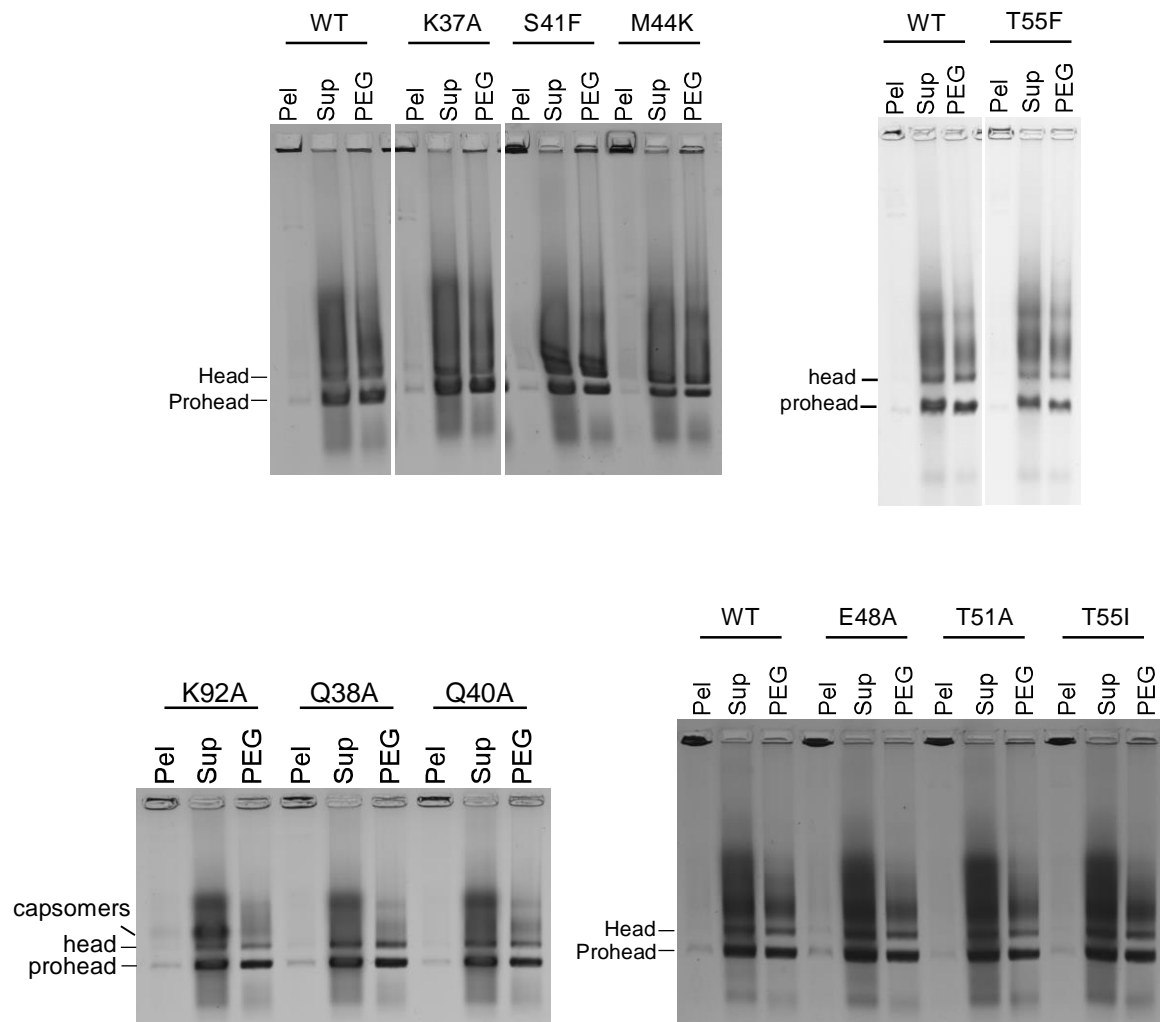


Figure 36. Agarose gels of the predicted 2nd helix mutants with WT phenotypes.

Miniprohead prep pellet, supernatant, and PEG samples were collected and run on 0.9% agarose gels for analyses. WT or K92A were used as controls. WT produced cleaved mcp while K92A produced cleaved and some uncleaved mcp. All of these point mutations produced proheads and heads on agarose gels and cleaved mcp on SDS gels like WT.

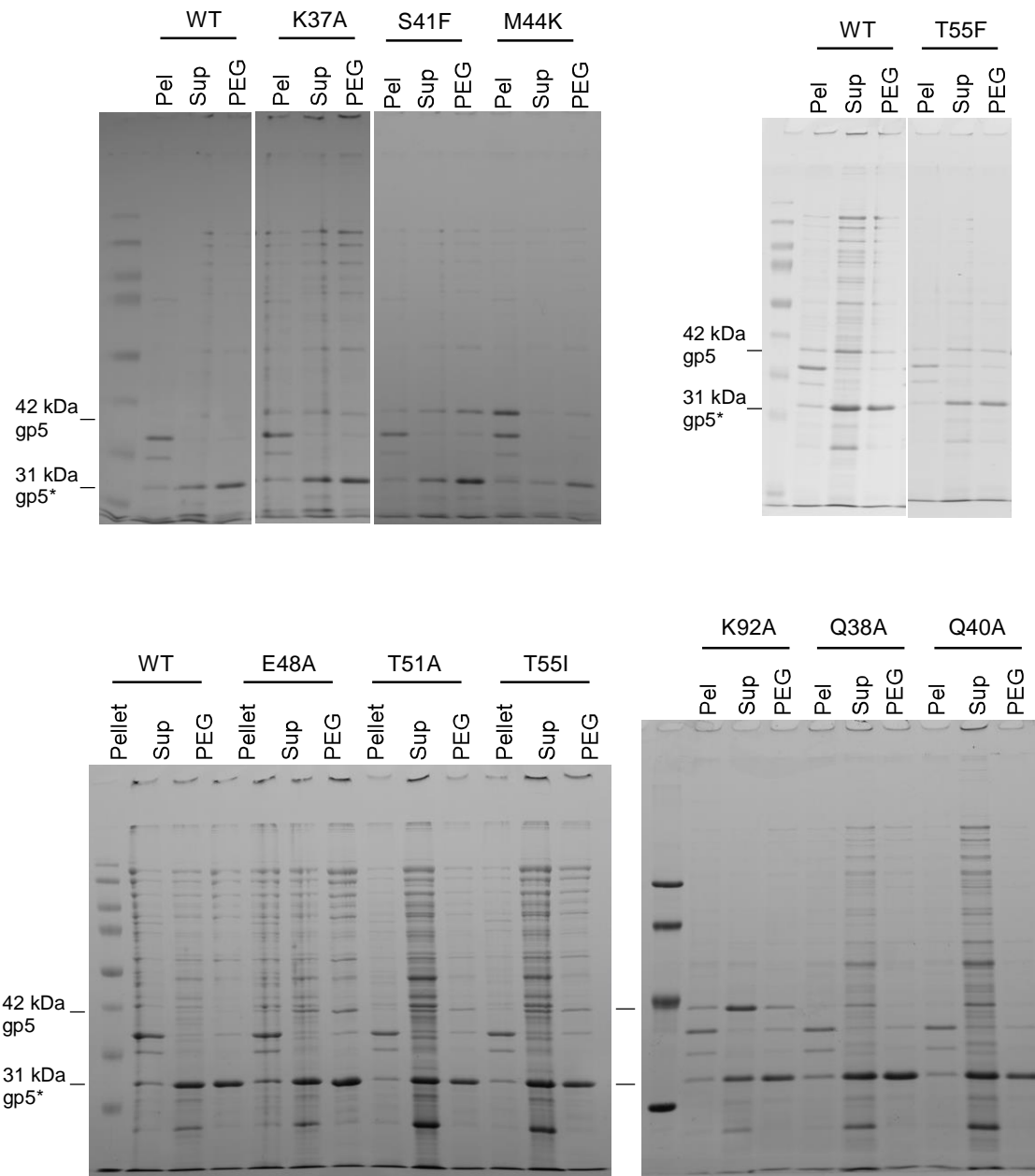


Figure 37. SDS gels of the predicted 2nd helix mutants with WT phenotypes

Miniprohead prep pellet, supernatant, and PEG samples were run on 12% low cross-linking SDS gels. WT control produced cleaved mcp while K92A produced both cleaved and uncleaved mcp. All of these mutants produced WT like phenotypes of mostly cleaved mcp.

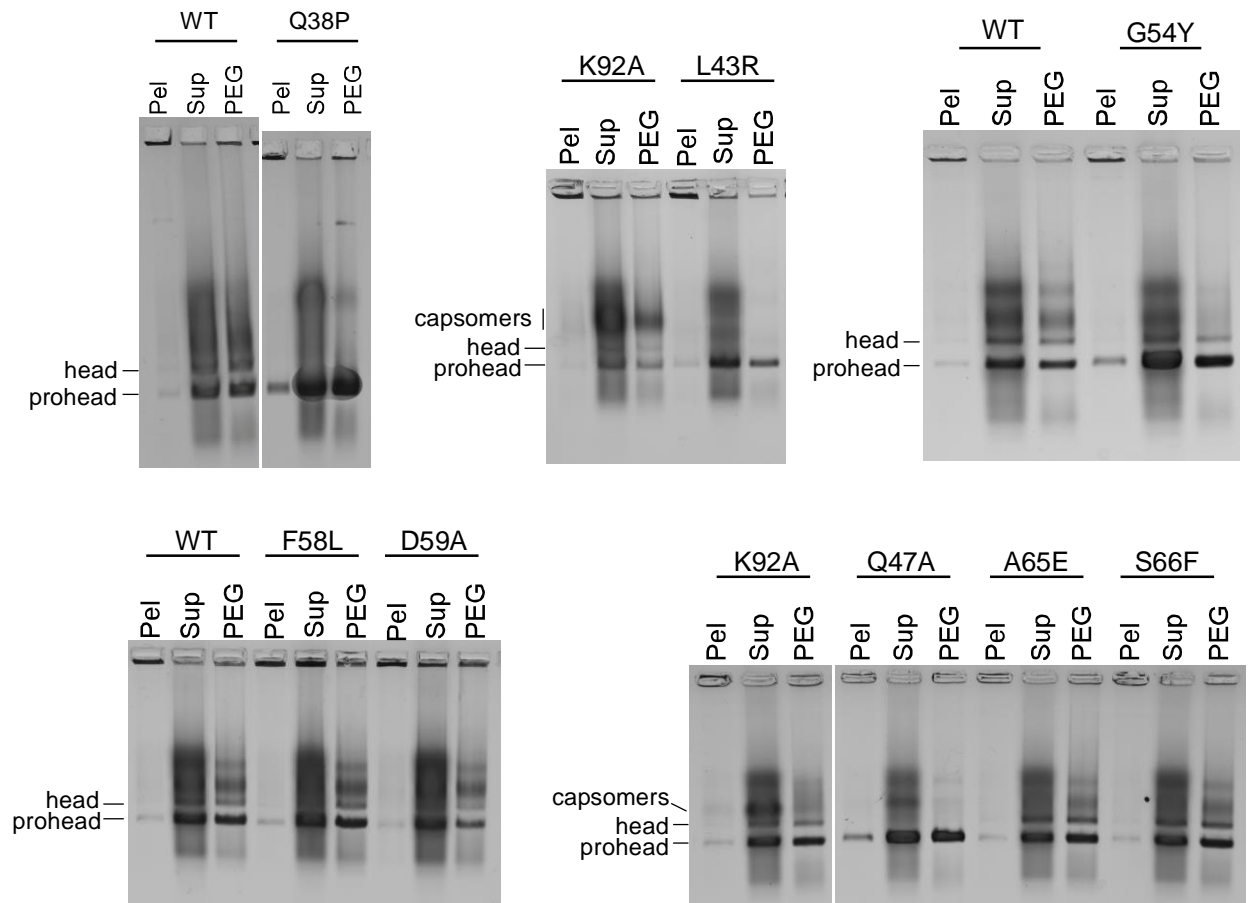


Figure 38. Agarose gel results for defective mutations in predicted 2nd helix

Miniprohead prep pellet, supernatant, and PEG samples were run on 0.9% agarose gels. WT and K92A samples were used as controls for comparison. WT produced prohead and head bands. K92A produced prohead, head, and capsomer bands. Q38P, L43R, and Q47A showed only the production of prohead bands. G54Y, F58L, D59A, A65E, and S66F showed WT like results of prohead and head bands.

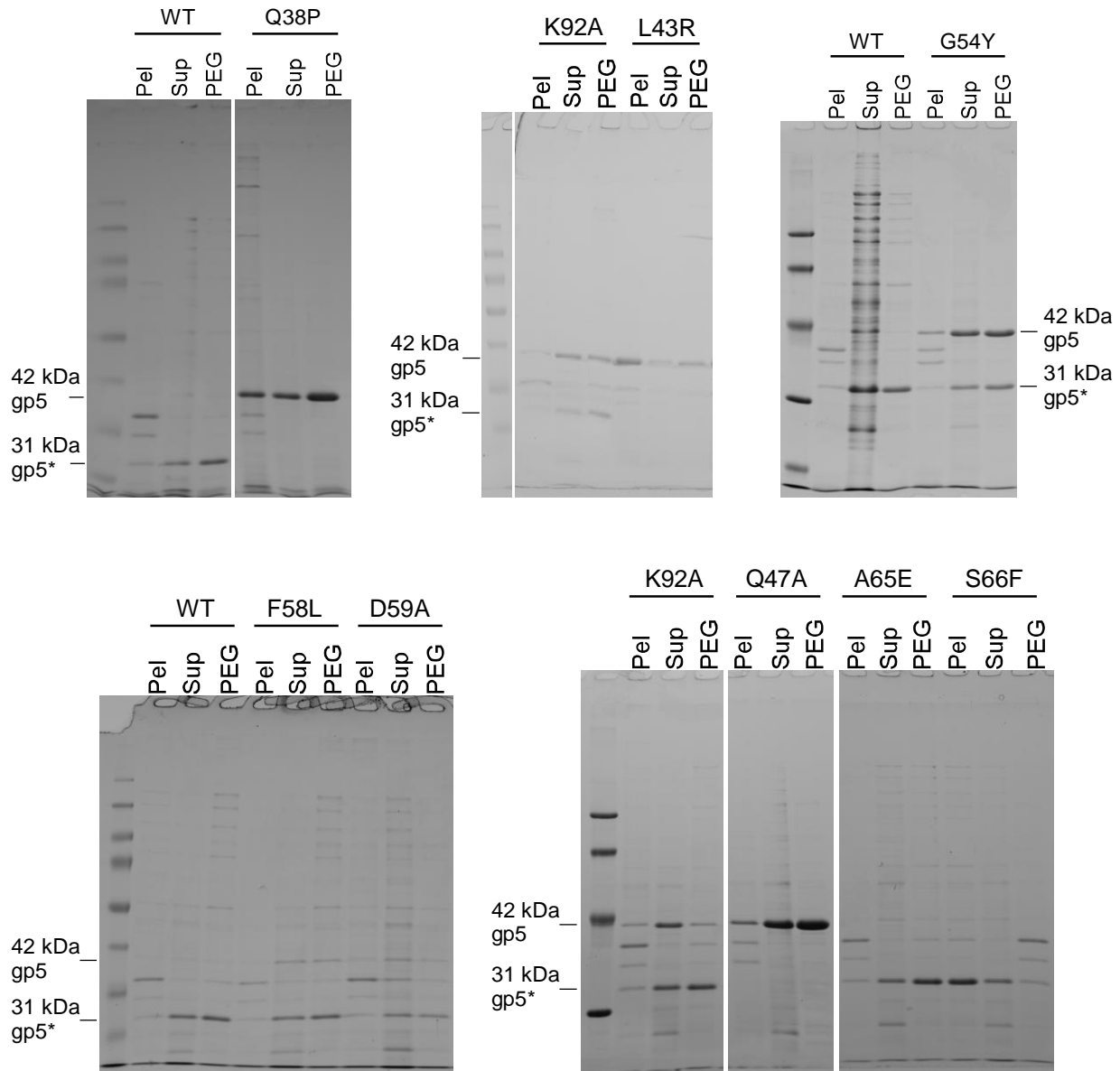


Figure 39. SDS polyacrylamide gel results of defective mutants in the predicted 2nd helix.

Miniprohead prep pellet, supernatant, and PEG samples run on SDS gels. WT and K92A samples were used as controls. WT produced 31 kDa cleaved mcp and K92A produced both cleaved and uncleaved mcp. Q38P, L43R, and Q47A produced only uncleaved mcp. G54Y showed a partial cleavage defect by producing both cleaved and uncleaved mcp. F58L and D59A produced mostly cleaved mcp, but there were very light uncleaved mcp bands present also A65E showed cleaved mcp and S66F showed cleaved mcp but, at lower expression than the control.

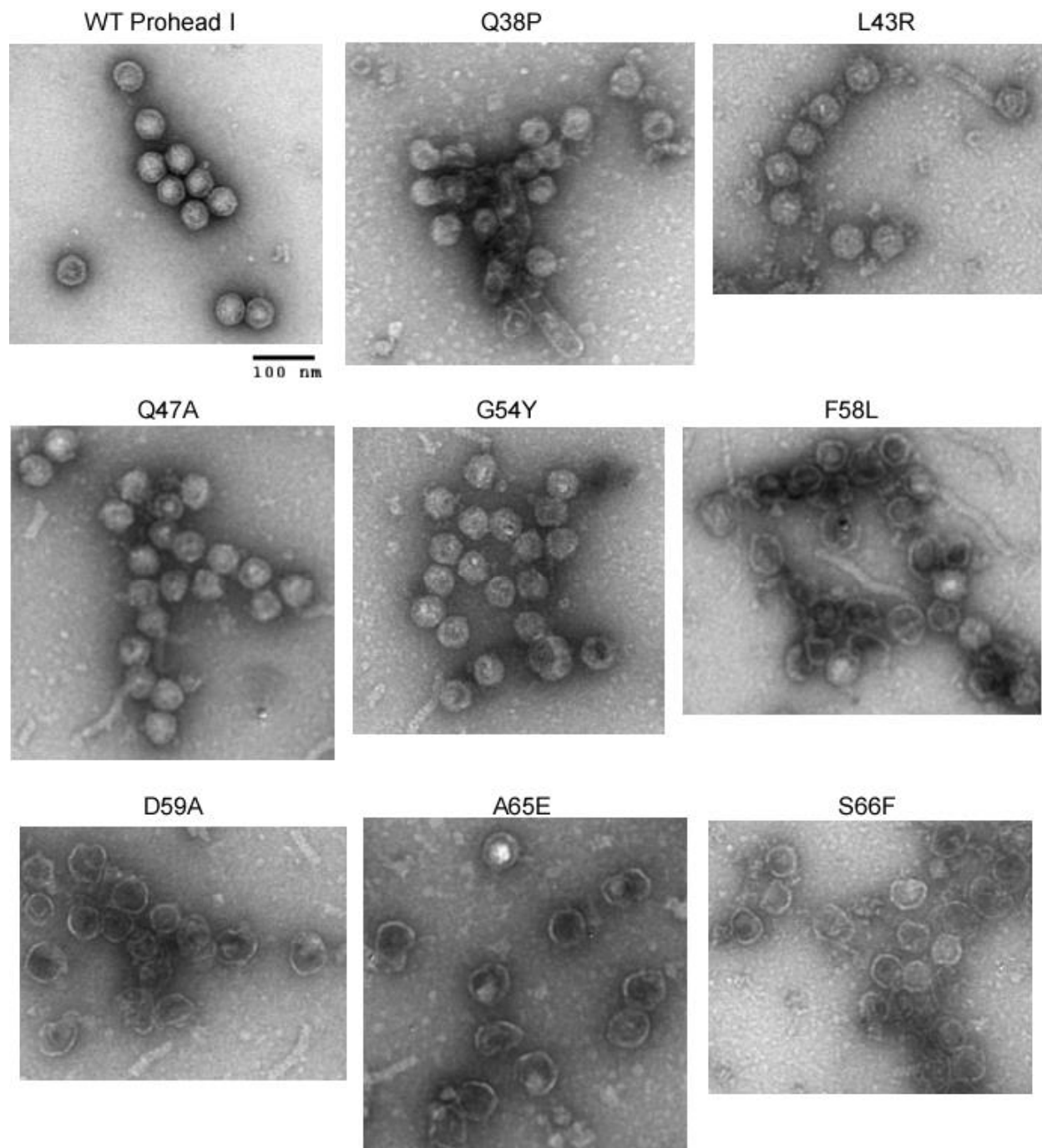


Figure 40: EM images of Q38P, L43R, G54Y, F58L, D59A, Q47A, A65E, and S66F

Miniprohead prep PEG samples were diluted 1/10 in 1x calorimetry PBS, stained with 1% uranyl acetate and imaged at 56,000x magnification. WT Prohead I is shown for comparison. G54Y, F58L, D59A, A65E, and S66F produce WT like proheads and heads. Q38P, L43R, and Q47A produce prohead like particles. Scale bar: 100 nm.

Point mutations in the 2nd predicted helical region are defective in portal incorporation

These point mutations were moved into a plasmid that makes the portal and inactivated protease (pVP0 g4 H65A) and expressed on a larger scale. After the glycerol gradients, and a final ultracentrifugation step to concentrate them, the samples were syringe filtered and run on SDS and agarose gels to detect the incorporation of portal and protease proteins. On the SDS gel, Q38P showed very light portal and inactivated protease bands, indicating less than WT levels of incorporation. For L43R there was no detectable portal band but there was a light inactivated protease band. Q47A showed a very light portal band but there was no protease band present. G54Y showed a light portal band and a WT like protease band. F58L and D59A showed a light portal band and WT like protease band. A65E was defective in portal incorporation but was able to incorporate the protease at WT levels. S66F showed a very light portal band and had WT-like incorporation of the protease. There is a unique band running at about 12 kDa in the S66F sample that is a degradation product of the mcp sometimes seen in prohead samples (denoted by asterisk) (Figure 41).

All of these point mutations show a defect in portal incorporation while Q38P, L43R, and Q47A show a double defect in portal and protease incorporation. The samples were run on agarose gels to identify any prohead dimer or trimer bands (Figure 41). Q38P produced a strong prohead band and very light dimer and trimer bands. L43R only produced proheads. Q47A, A65E, F58L, and D59A produced proheads, along with weak prohead dimer and trimer bands. S66F produced proheads, and less than WT levels of prohead dimers and trimers (Figure 42). Even though some of these mutants showed no detectable portal bands in the SDS gel, the agarose gel was able to visualize the small number of proheads that do incorporate the portal,

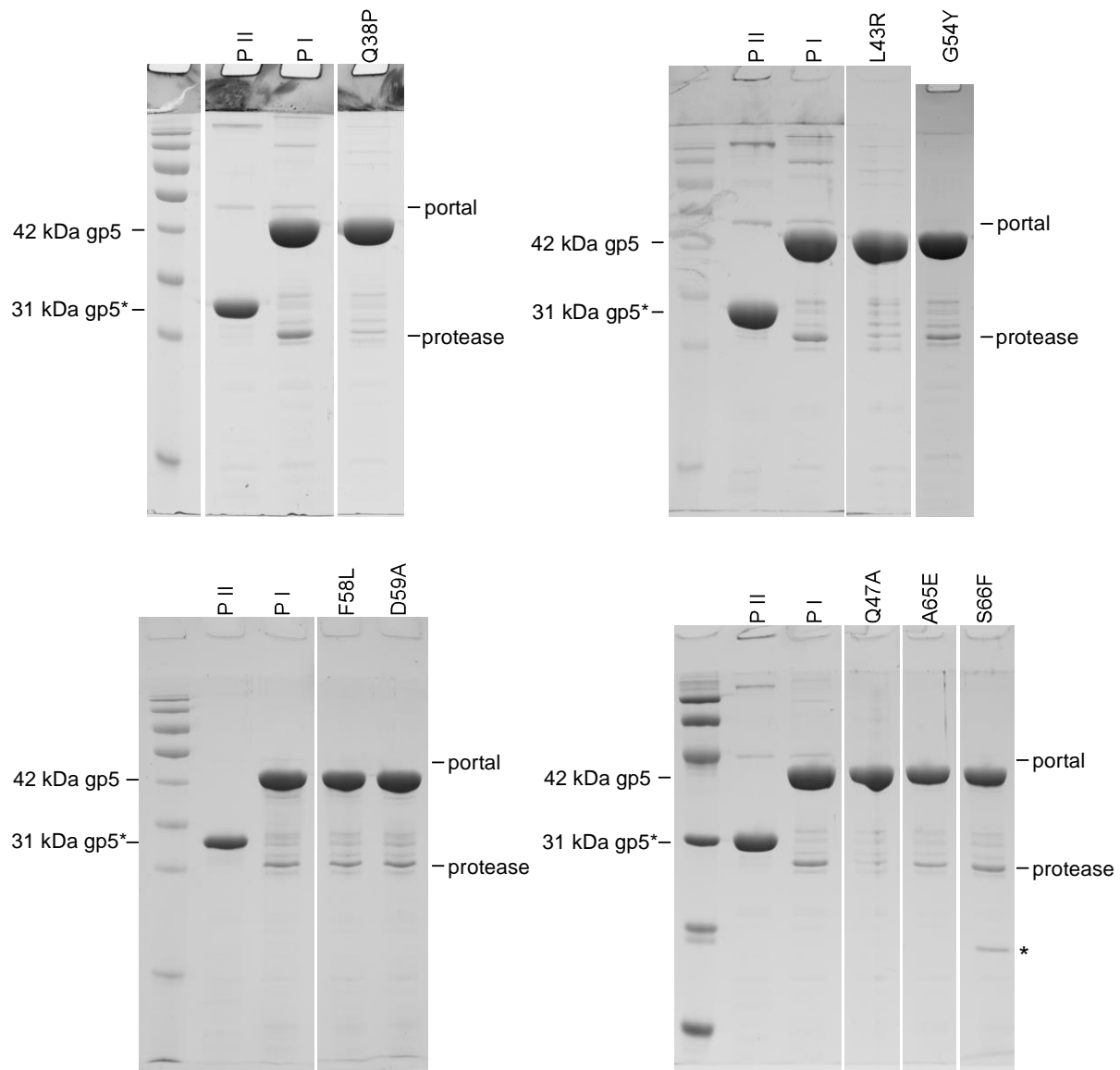


Figure 41. Prohead prep SDS gel results of mutants expressed with the portal and inactivated protease.

Purified and syringe filtered proheads were prepared for SDS gels. Prohead II and Prohead I with portal were used as controls. Prohead II had portal and cleaved 31 kDa mcp bands. Prohead I control had portal, uncleaved 42 kDa mcp, and inactivated protease bands. Q38P and L43R had uncleaved mcp, a weak protease band, but no detectable portal band. G54Y showed uncleaved mcp and protease bands, along with a light portal band. F58L and D59A showed uncleaved mcp bands, weaker than WT portal bands but WT level protease bands. Q47A showed uncleaved mcp, a very light protease band, and no detectable portal band. A65E showed uncleaved mcp and protease bands, but no detectable portal band. S66F showed uncleaved mcp and protease bands, and a weaker than WT portal band. Compared to WT, these mutants had a portal incorporation defect while Q38P, L43R, and Q47A showed a double defect with both portal and protease incorporation. The asterisk (*) denotes a unique 12 kDa band in the S66F, which is a trypsin digestion product, sometimes seen in Prohead preps.

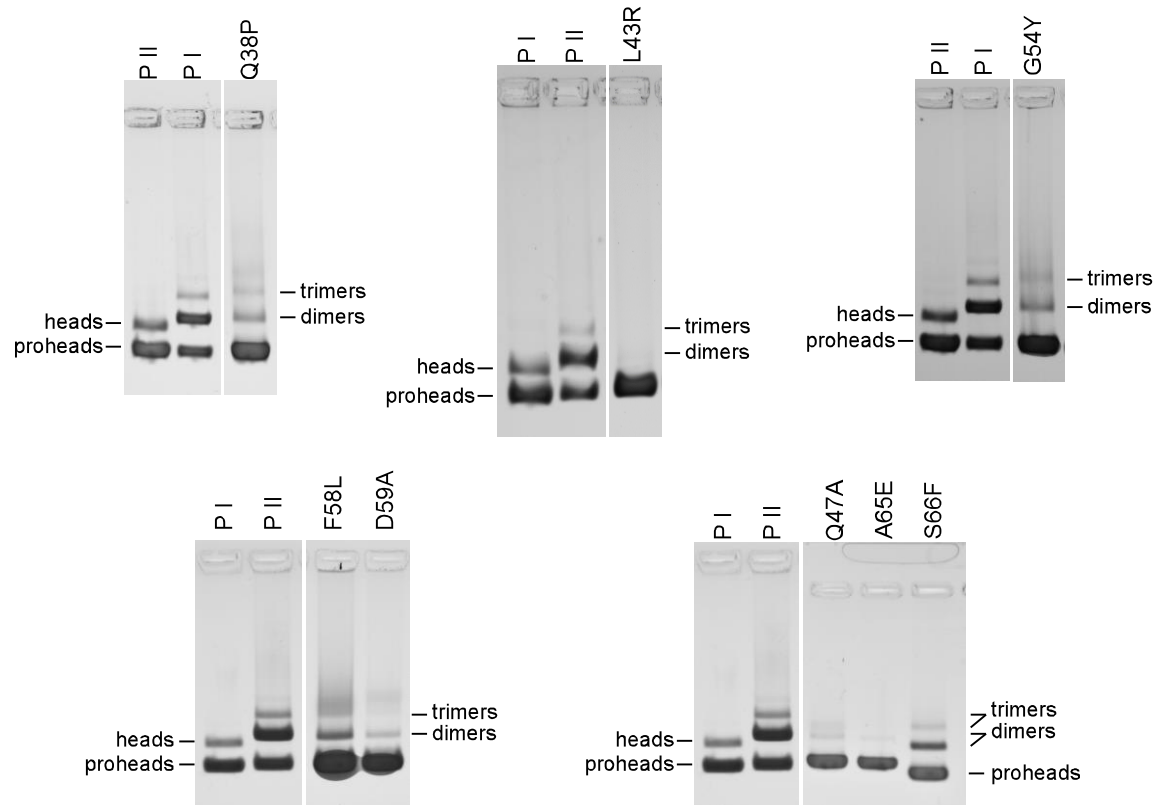


Figure 42. Prohead Prep agarose gels of mutants expressed in portal and inactivated protease plasmid

Purified prohead samples were run on 0.9% native agarose gels. Prohead II and Prohead I with portal samples were used as controls. Prohead II produced proheads and heads. Prohead I produced proheads, and prohead dimers and trimers. Q38P produced a stronger prohead band and weak dimer and trimer bands. L43R produced only prohead bands. G54Y produced a strong prohead band and weak dimer and trimer bands. F58L and D59A produced strong prohead bands and weaker dimer and trimer bands. Q47A and A65E showed prohead bands and barely detectable dimer bands. S66F produced prohead bands, along with dimer and trimer bands. The dimer and trimers are slightly weaker than WT. S66F had a shifted mobility and runs slightly faster than WT. Dimer and trimer bands weaker than WT suggest a defect in portal incorporation.

which bind together to create the weak dimer and trimer bands. Q38P also caused defects in portal and protease incorporation. However, introducing a proline can cause a kink in an α -helix and drastically disrupt secondary structure. Q38P could be causing assembly defects solely based on this steric disruption. Therefore, I mutated this residue to an alanine and tested its assembly affects in a miniprohead prep. Q38A possessed WT like phenotypes and produced functional capsid protein (Figure 36 and 37, Table 1), suggesting that it does not play a critical role in delta domain function.

Portal incorporation mutants lie on the same side of the predicted 2nd α -helix

Our analysis of point mutations in the 2nd predicted helix have identified five mutants that solely affect portal incorporation during capsid assembly, F58L, D59A, Q62A, A65E, and S66F. In contrast, three mutants, L43R, G54Y, and E61A, had interesting double defects for both portal and protease incorporation. In order to visualize how these residues may be related to each other in space, the amino acid sequence of the 2nd predicted helix was threaded onto a helical model using Pymol. Residues in red indicate mutations made at those locations involved with portal incorporation. Blue residues indicate mutations at those sites involved with both portal and protease incorporation. From the model, all of the portal incorporation mutants lie on the same side of this predicted helix (Figure 43), suggesting that this particular region of the delta domain plays an important role in making interactions with the portal proteins.

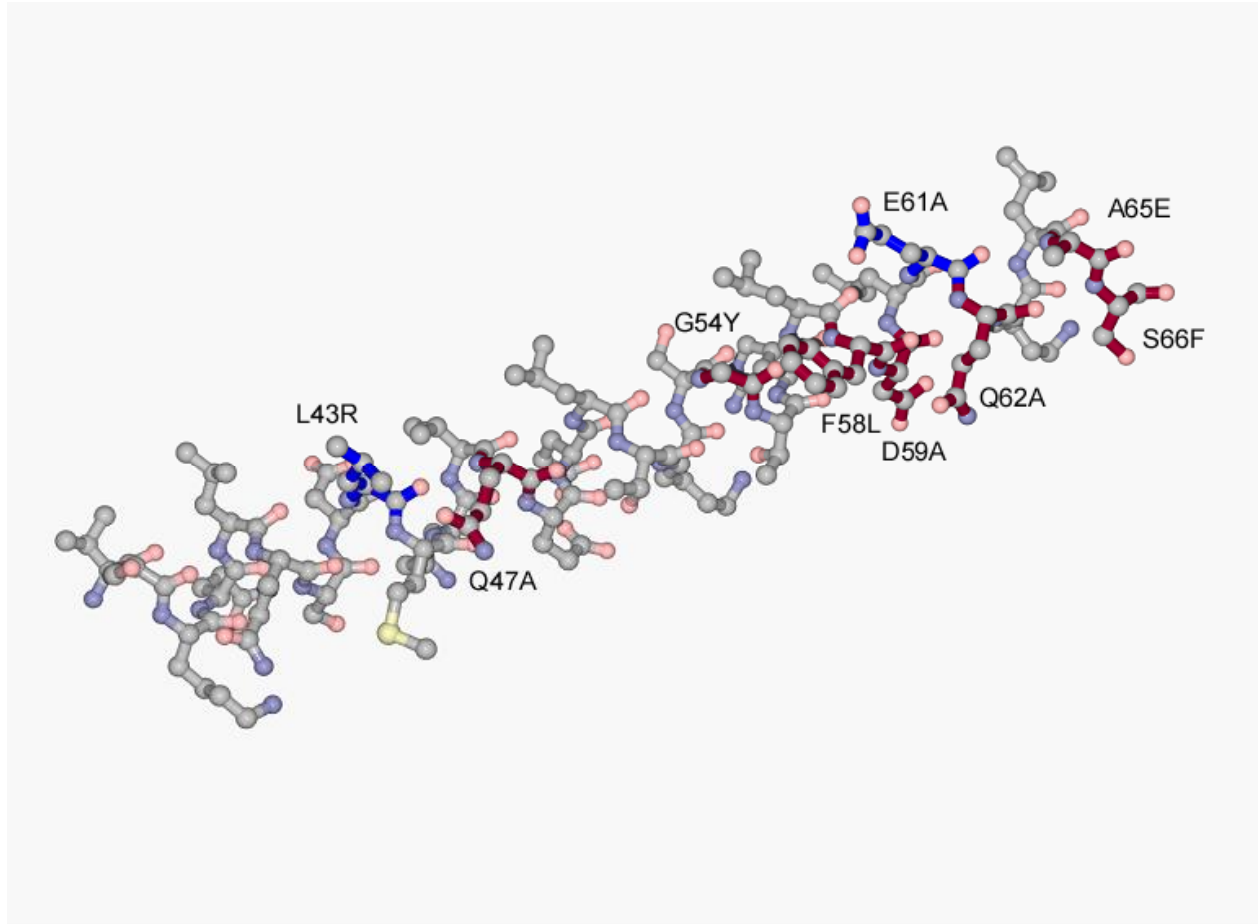


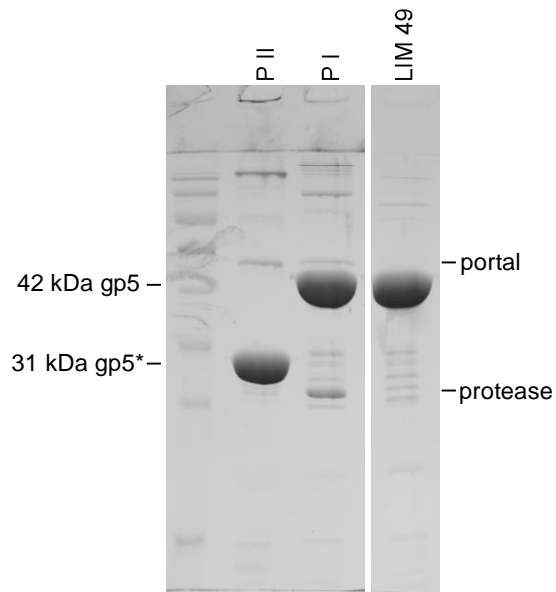
Figure 43. Helical model of 2nd predicted α -helix of the delta domain showing portal and protease incorporation mutants.

Residues K37 to S66 of the 2nd predicted helical region of the delta domain were threaded onto a helical model using Pymol. The side chains of the model are the original WT residues. The mutants made at critical residues are labeled. The red residues represent the mutations, which caused portal incorporation defects. The blue residues represent the mutations which caused a double defect in both portal and protease incorporation. From this view of the model, all of these critical residues lie on the same side of the helix.

LIM 49 (in the 2nd predicted helix) also has a portal and protease incorporation defect

Now that we have some evidence that the 2nd predicted helix plays a role in portal incorporation, we can test other mutations for similar defects in this region. LIM 49 was an insertion mutation described in the previous chapter which caused a cleavage defect and only produced Proheads. Perhaps this mutation has a cleavage defect because it is unable to incorporate the protease. LIM 49 was moved into a plasmid containing the portal and inactivated protease genes to test for portal or protease incorporation defects. Purified mutant and WT control Prohead I and Prohead II samples were run on SDS and agarose gels. LIM 49 only showed uncleaved mcp and a very light protease band. There was no detectable portal band (Figure 44A). LIM 49 was also run on a 0.9% native agarose gel to detect the presence of dimers and trimers. Prohead II showed proheads and heads. Prohead I showed prohead, prohead dimer, and trimer bands. LIM 49 only showed a prohead band (Figure 44B). The lack of portal band in the SDS gel, and the lack of dimers and trimers in the agarose gel indicate that this linker insertion mutation is unable to incorporate the portal during capsid assembly. Also, the very low level of protease in the SDS gel, compared to WT, suggests that this mutation is also defective in protease incorporation. LIM 49 has a double defect in portal and protease incorporation.

A.



B.

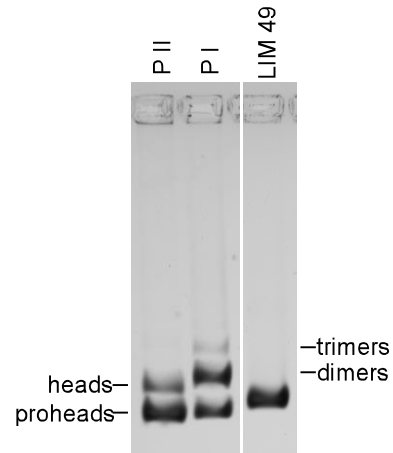


Figure 44. LIM 49 is defective in portal and protease incorporation

A) Purified samples were prepared and run on a SDS gel. Prohead II and Prohead I were used as controls. Prohead II produced portal and 31 kDa cleaved mcp bands. Prohead I produced portal, uncleaved 42 kDa mcp, and inactivated protease bands. LIM 49 did not have a portal band, and only had a very light protease band compared to WT. B) In a 0.9% agarose gel, Prohead II showed prohead and head bands. Prohead I produced proheads, prohead dimers, and a weak trimer band. LIM 49 only showed a prohead band. LIM 49 is defective in both portal and protease incorporation.

3.2.2 The portal can enhance capsid assembly

The ring shaped portal takes the place of a pentamer at one vertex of the capsid. The delta domain is responsible for making specific interactions with the portal to ensure that there is only one portal per capsid. Some believe that the portal acts as an initiator of assembly to make assembly more efficient and to prevent the formation of capsids with multiple portals. Does it provide the capsid proteins with a base to begin assembly, thus aiding in efficient, proper, and complete assembly? While HK97 plasmid expression studies show that the portal is not required for capsids to assemble, there are a few mutants (Del1, L6R will be discussed later in this chapter) that appear to assemble slowly and we have used them to show that the presence of the portal can accelerate capsid assembly.

E363A shows complete mcp cleavage in the presence of the portal

E363A was a mutation made and studied by C.L Peebles and R. Duda and studied by a previous undergraduate student, Lindsey Dierkes. This mutation removed a cross-linking catalytic site and is located in the P-domain of the capsid protein (Dierkes et al. 2009). E363A only produced proheads in the agarose gel and produced an approximately equal amount of cleaved and uncleaved mcp bands in the SDS gel. This partial cleavage defect could be due to a slowed or inefficient assembly. It was speculated that the capsid proteins take longer than normal to build the capsid, and the protease is degraded before capsid assembly is complete (Dierkes et al. 2009). Inadequate protease activity could cause partial mcp cleavage. To test if the portal can enhance capsid assembly, and possibly promote complete proteolysis, E363A was moved into a plasmid containing the portal gene (pVP0). A large scale Prohead Prep were performed and SDS gels and native agarose gels were run to test for mcp cleavage and portal incorporation.

Figure 45 shows the gel data from the Prohead Prep. Prohead I and Prohead II were used as controls. When E363A was expressed with the portal, the mcp was able to be cleaved nearly completely. There was only a very small amount of uncleaved mcp band present in the SDS gel. The agarose gel showed a prohead band and a very light head band (denoted by circle) (Figure 44), indicating the presence of cleaved and expanded particles.

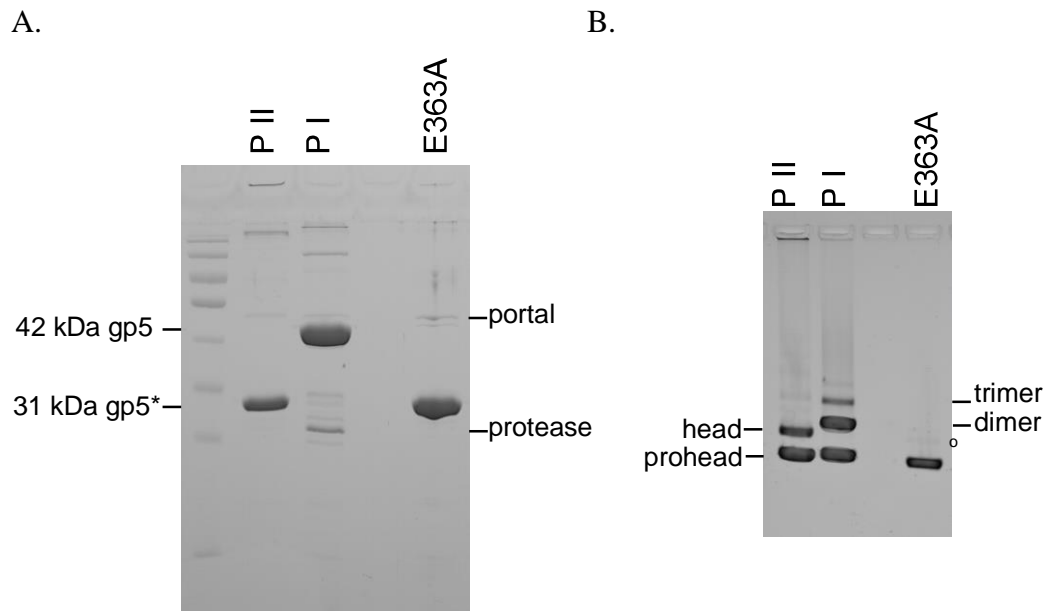


Figure 45. E363A produces cleaved mcp when the portal is present

Prohead preps were performed for E363A with portal and inactivated protease. A) E363A was run on a SDS gel with PII and PI controls. Prohead II produced a cleaved mcp band and portal band. Prohead I produced uncleaved mcp, along with a portal and protease band. E363A showed PII like results with cleaved mcp and the portal. There was a very small amount of uncleaved mcp. B) On agarose gel, Prohead II produced proheads and heads. Prohead I produced proheads, prohead dimers, and trimers. E363A produced proheads and a very light head band (denoted by circle).

K63A causes a cleavage defect

K63 lies in the predicted 2nd helix, in the conserved EQK region described earlier. This residue was mutated to an Alanine to remove the positive charge property. In initial miniprohead prep experiments, this mutation showed a cleavage defect and only produced uncleaved mcp and proheads (Figure 46). By EM, K63A PEG samples showed WT-like prohead particles (Figure 47). In complementation tests, K63A was three log downs in both capsid gene amber and protease gene amber phage complementation (Table 1). The K63A mcp is unable to function properly and build viable phage, possibly due to an inability to incorporate the protease, which could explain why this protein does not cleave like WT.

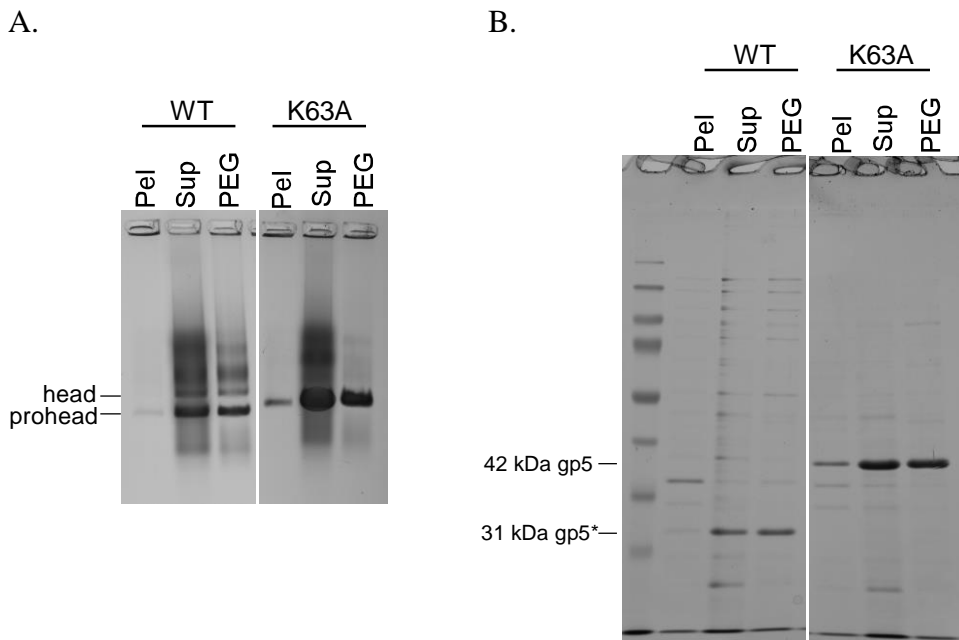


Figure 46. Miniprohead prep results of K63A shows a cleavage defect

A) Pellet, supernatant, and, PEG samples were loaded on a 0.9% agarose gel to detect the assembly products made. WT produced proheads and heads. K63A produced a strong prohead band only. B) Samples were run on a 12% low cross-linking SDS gel, and stained with coomassie. WT showed cleaved 31 kDa mcp. K63A showed only uncleaved 42 kDa mcp.

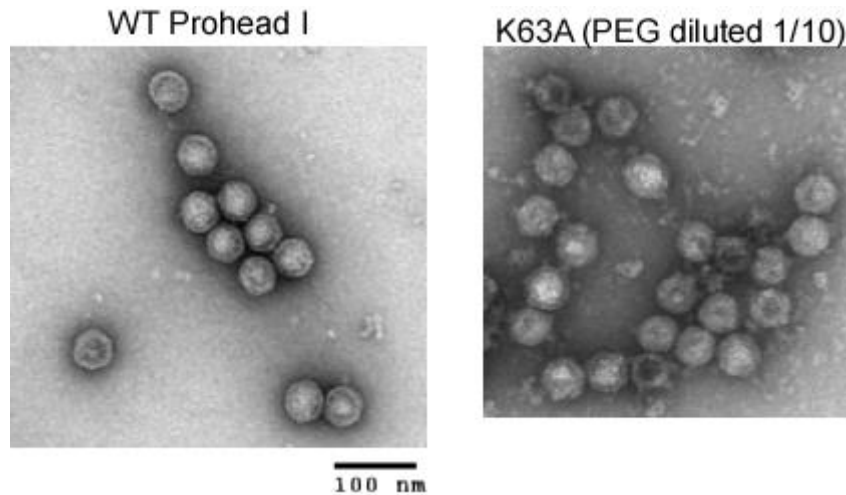


Figure 47. Representative EM images of WT PI and K63A

WT Prohead I is used as a comparison. The miniprohead prep PEG samples were diluted 1/10 in 1x calorimetry buffer and stained with 1% uranyl acetate. K63A produced WT like Prohead I particles. Scale bar: 100 nm.

K63A is able to incorporate the portal and inactivated protease like WT

K63A was moved into a portal and inactivated protease plasmid to test for portal and protease incorporation. WT Prohead I and II, and K63A purified samples were run on SDS and agarose gels. On the SDS gel, K63A showed portal, uncleaved mcp, and protease bands (Figure 48A). On the agarose gel, Prohead II produced proheads, and heads while Prohead I produced prohead, dimer, and trimer bands as expected. K63A showed a WT Prohead I like banding pattern of prohead, dimer, and trimer bands (Figure 48B). These results show that the K63A mutant was able to incorporate the portal and protease proteins at WT like levels. The protease protein is present inside the mutant proheads, but cleavage did not occur. Therefore, the lack of protease is not the cause of the cleavage defect we first detected.

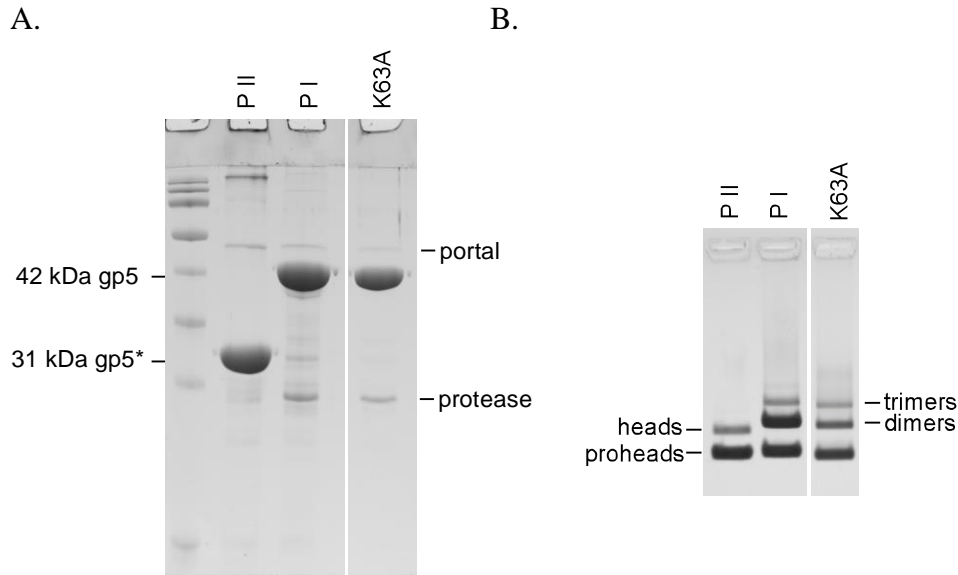


Figure 48. K63A shows WT-like portal and inactivated protease incorporation

A) Purified prohead samples prepared for SDS gels and stained with coomassie. P II and P I with portal act as controls. Prohead II showed the portal and the cleaved mcp. Prohead I showed the portal, uncleaved mcp, and the protease. K63A had a WT like phenotype with portal, uncleaved mcp, and protease bands. B) Purified prohead samples were loaded on a 0.9% agarose gel. Prohead II produced proheads and heads. Prohead I produced proheads, prohead dimers, and prohead trimers. K63A produced proheads, dimers, and trimers like the Prohead I control.

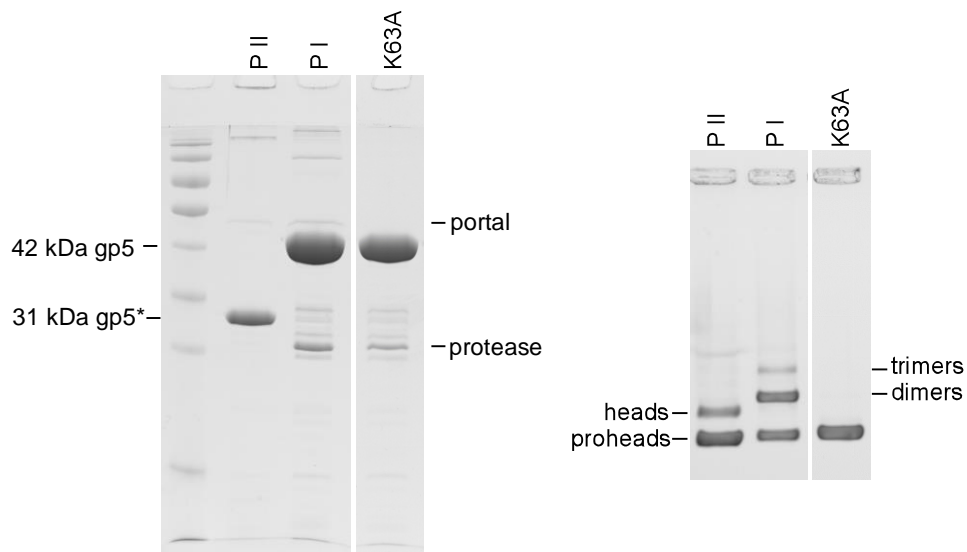
K63A produces cleaved major capsid protein when the portal is present

We moved K63A to a portal-less plasmid that contained an inactivated protease to test if the protease can still be incorporated when the portal is not present. Prohead II and Prohead I were again used as controls. In the SDS gel, K63A was able to incorporate the protease, although the protease band is a little weaker than WT (Figure 49A). In the agarose gel, K63A produced prohead band. The presence or absence of the portal does not affect protease incorporation.

K63A was yet again moved to another plasmid that contained the portal and active protease. The purified samples were run, along with WT Prohead II and Prohead I on SDS and agarose gels. On the SDS gel, surprisingly, K63A with portal and active protease produced

cleaved mcp like the Prohead II control. There was only a very little bit of uncleaved mcp detected (Figure 49B). On the agarose gel, a prohead band and a light head band is present (denoted by circle). K63A capsids were only able to cleave and mature properly when the portal was present. This suggests that the portal is able to enhance the capsid assembly process. Perhaps the presence of the portal has helped to overcome an energy barrier that the point mutation created, thus allowing proteolysis. Comparing the effect of the portal on capsid expansion was performed and time points were run on SDS gels. By comparing the ratio of heads to proheads, the rate of expansion was determined to be approximately 10 times faster when the portal was present (Josh Maurer, unpublished results). With HK97, the portal may act as a nucleator of assembly and aid in capsid maturation. The portal may allow the capsomers to assemble faster, compared to when the capsomers have to assemble around a pentamer, allowing for a faster rate of shell completion and maturation.

A.



B.

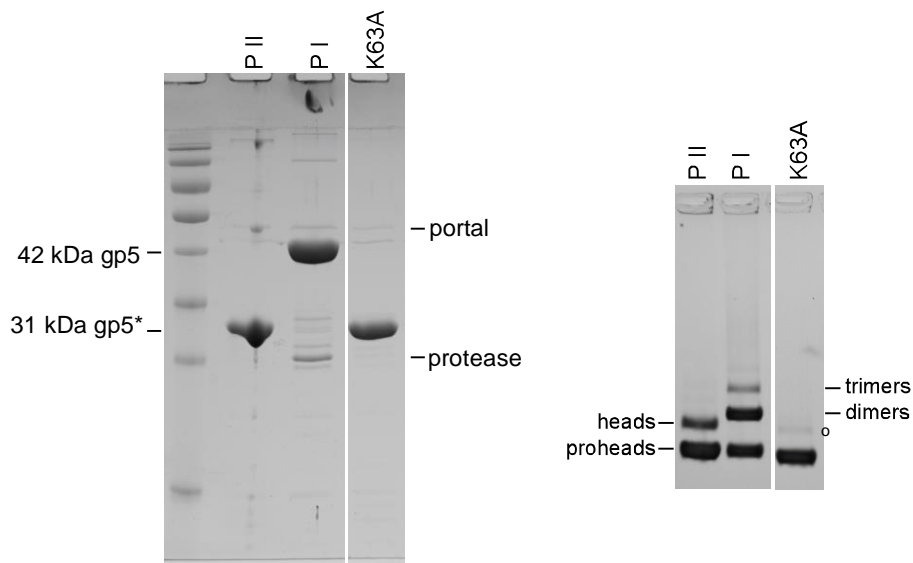


Figure 49. K63A only produces cleaved mcp when the portal is present

K63A was expressed in a plasmid with no portal and an inactivated protease, and also in a WT plasmid with portal. PI and P II with portal were used as controls. On SDS gels, Prohead II produced cleaved mcp while Prohead I produced uncleaved mcp. On agarose gels, Prohead II produced proheads and heads while Prohead I produced proheads, dimers, and trimers. A) On the SD gel, K63A was able to incorporate the protease, even when the portal was not present. It produced uncleaved mcp and only proheads on the agarose gel. B) On the SDS gel, K63A produced cleaved mcp, and very little uncleaved mcp in the present of portal and active protease. On the agarose gel, K63A produced a strong prohead band and a weaker head band (denoted by circle).

3.2.3 Identifying a 2nd site suppressor in the portal

The site directed mutagenesis approach to studying the delta domain has provided us with an array of mutations that cause different types of assembly defects. One of these mutations, A65E, produced prohead and head like particles but had a portal incorporation defect. A65E seemed like an interesting candidate for moving into a HK97 prophage to select a 2nd site suppressor mutation. I again used the technique, recombineering, for making my mutant constructs. After many trials of using tetR negative selection, I decided to go back to using galK recombineering. An A65E fragment with HK97 homology arms was transformed into galK competent cells. Instead of a 4.5 hour outgrowth and recovery period at 30°C, I did an overnight recovery. The next day, I pelleted and washed the cells before plating on 2-DOG selection plates. The plates were incubated at 42°C overnight and then moved to 28°C until colonies grew. Colonies were picked and re-streaked on 2-DOG plates to purify and incubated at 28°C until colonies grew. Colony PCR was conducted to identify HK97 DNA. Restriction digestions were done to identify the presence of the A65E mutation in the DNA. When A65E was made, a silent mutation was made nearby to add a unique restriction site, KasI to allow for identification.

There was one colony, out of 96, that digested as expected. A portion of the major capsid gene was sequenced and this colony was positive for the A65E mutation! This lysogen carrying a recombinant prophage was cultured and prepared for UV induction. The cells were exposed to 0, 5, and 10 seconds of UV light and shaken in LB medium to allow for phage growth. The lysate was collected and plaque assays were conducted. There are different possible types of phage that could be made: phage that have reverted to WT, phage that have replaced the glutamate with another functional residue, or phage that have created a suppressing mutation elsewhere in the

genome. The suppressing mutations are the ones that I am most interested in because these phage will show us interactions between the new suppressing residue and the initial lethal mutation made in the delta domain. I was successfully able to produce plaques from the A65E prophage. 11 plaques were sequenced and three contained the A65E mutation of interest. The portal, protease, and major capsid genes were sequenced directly from the three positive phage stocks and all three contained a 2nd site point mutation in the portal gene: D135G. This second site mutation shows that residue 135 in the portal may be in close contact with residue 65 in the delta domain. The initial lethal mutation changed a small residue to a charged residue (A to E) in the 2nd helix of the delta domain. The suppressing mutation in the portal changed a charged residue to a small residue (D to G) possibly to maintain this charge and small residue interaction or prevent repulsing forces. This genetic change supports my biochemical data that A65 is an important residue for binding and incorporating the portal during capsid assembly.

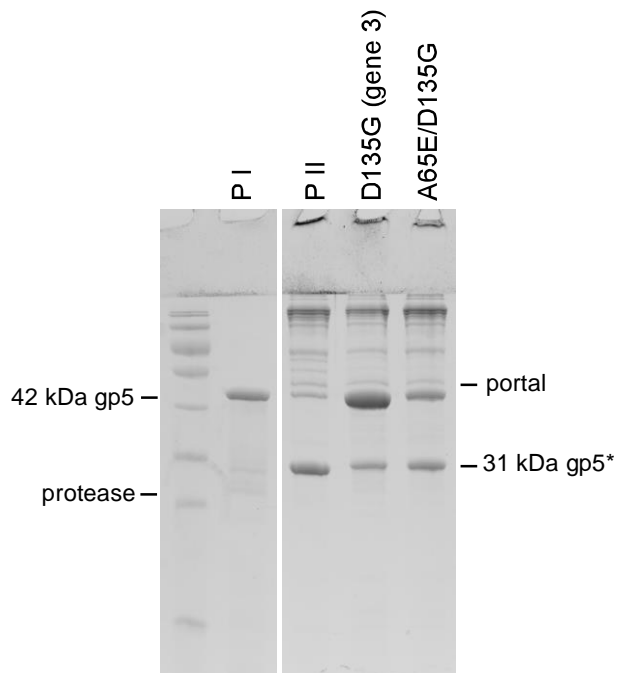
D135G in the portal rescues A65E function in vitro

Our genetic tests showed that D135G (portal) is in some sort of interaction with A65E (delta domain). A65E showed a defect in portal incorporation, and was 3 logs down in complementing phage with an amber mutation in the capsid gene. (Figures 41 and 42, Table 1). We wanted to see if the rescuing effect of this pair of mutations could be replicated using our plasmid expression system. Single mutant and double mutant plasmids, pVP0 D135G and pVP0 A65E (gp5)/D135G (gp3), were made and expressed in miniprohead preps. Along with WT controls, these mutants were run on SDS and agarose gels, and also tested for protein functionality in complementation spot assay. On the SDS gel, D135G produced a portal band, mostly uncleaved mcp and some cleaved mcp (Figure 50A). D135G on its own causes a partial cleavage defect. In the spot complementation tests, D135G was able to complement protease and capsid gene amber

phage like WT, showing complete functionality of protein, even though cleavage is incomplete. However, D135G causes a slight defect in portal protein functionality because it is one log down in complementation efficiency of phage with an amber mutation in the portal gene (Table 2).

On the SDS gel, the double mutant, A65E/D135G produced equal amounts of cleaved and uncleaved mcp (Figure 50A). On the agarose gel, D135G and the double mutant produced similar bands: prohead, head, and prohead dimers. Prohead I showed prohead and dimer bands. An A65E sample is shown to compare the before and after D135G mutation addition. With the addition of D135G, the double mutant showed portal incorporation and the presence of prohead dimer bands, showing that D135G was able to rescue the portal incorporation defect phenotype (Figure 50B). In the complementation tests, the double mutation is able to complement amber phage at WT levels, showing that it produces fully functional protein capable of forming viable phage particles (Table 2).

A.



B.



Figure 50. Prohead preps of pVP0 D135G(gp3) and double mutant pVP0 A65E(gp5)/D135G(gp3) show that the double mutant is able to rescue the portal incorporation defect of A65E.

A) SDS gel of PI and PII controls with mutants. The portal mutant, D135G produced a cleavage defect, having some cleaved 31 kDa mcp and mostly uncleaved mcp, and the portal band. The double mutant showed partial cleavage with relatively equal amounts of cleaved and uncleaved, along with the portal band. B) The agarose gel shows A65E, D135G, and the double mutant. As described before, A65E only produced proheads when expressed in the portal and inactivated protease plasmid. It could not form prohead dimers because it was defective in portal incorporation. D135G and the double mutant showed prohead and prohead dimer bands, and a light head band. The double mutant is now able to produce prohead dimers because it is able to incorporate the portal.

Making a homology model of the HK97 portal protein

There is no crystal structure of the HK97 portal available but there is one phage in the HK97 family, a *Corynebacterium diphtheria* phage, whose portal has been solved to a resolution of 2.9 Å by crystallography (Nocek et al. 2009). The *C. diphtheria* phage portal is 349 amino acids in length while the HK97 portal is 424 amino acids. An alignment using ClustalX showed approximately 20% sequence identity between these two proteins. In the alignment, D135 in HK97 aligns with D121 in the *C. diphtheria* phage portal (Figure 51). The residues are located in a small region in the portal structure that is conserved in the sequence alignment. Using the swissmodel program, a homology model of the HK97 portal was made based on the crystalized *C. diphtheria* phage portal structure (Figure 52). The left shows the *C. diphtheria* phage portal structure. The crystal structure included two disordered regions, which are shown by the dotted lines. The right image is the HK97 homology model. The corresponding aspartic acid residues are highlighted on each structure. The residue is located at the end of a β -sheet region located on the edge of the portal structure in the interior of the capsid. We can imagine that this edge of the portal, exposed to the interior of the capsid, could be making interactions with the surrounding delta domains.



Figure 51. Sequence alignment of the *C. diphtheria* phage portal and HK97 portal

Using the ClustalX alignment program, there is a 20% sequence identity between these two phage portals. The arrow points to D121 (*C. diphtheria* phage, top line) and D135 (HK97, bottom line), which is located in a conserved region

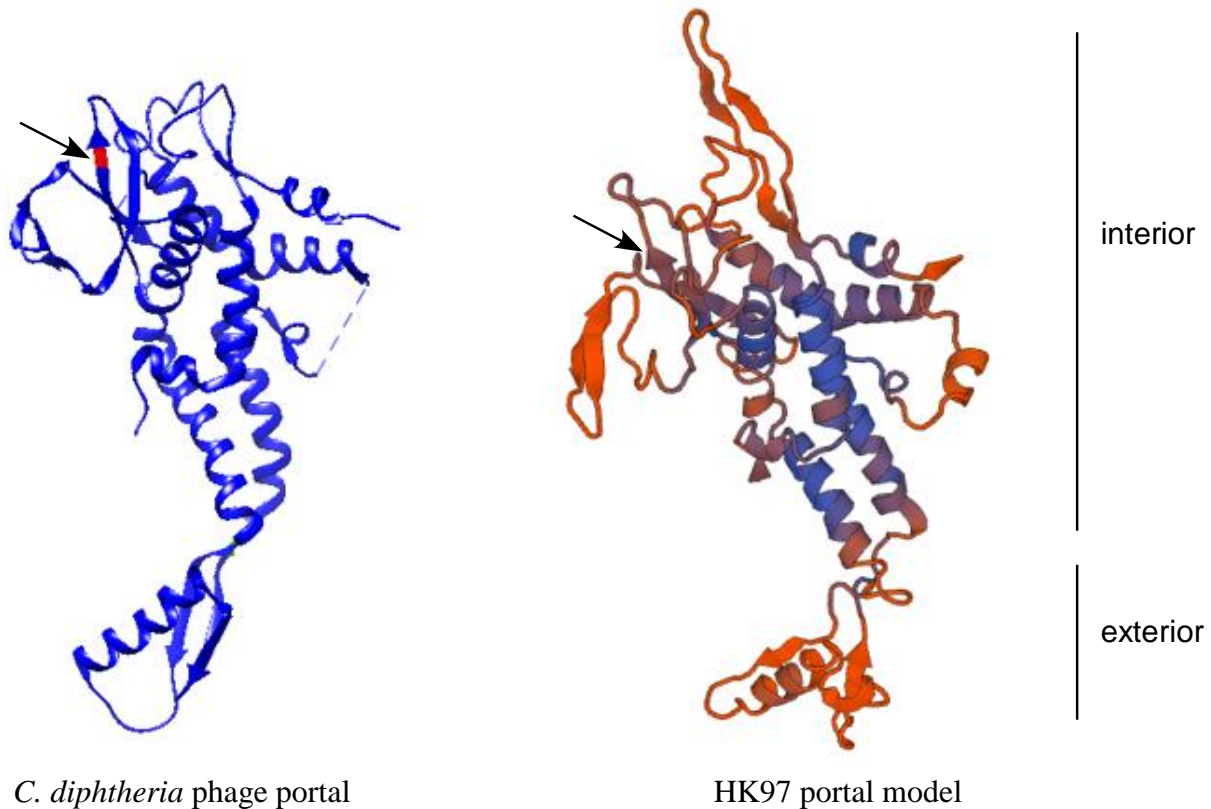


Figure 52. Homology model of HK97 portal based on the *C. diphtheria* phage portal crystal structure

The left shows the crystal structure of the *C. diphtheria* phage portal protein subunit. The red residue and the black arrow highlights residue D121. The right image shows the HK97 portal homology model. The black arrow highlights residue D135. These aspartic acid residues are located at the end of a β -sheet region. The highlighted areas differentiate the regions that would be in the interior or exterior of the capsid.

3.2.4 Discussion

Point mutations in the delta domain have shown us that it plays a role in portal incorporation during capsid assembly. I was able to identify a specific region of the delta domain, the 2nd predicted α -helix, as the main region responsible for making interactions with the portal proteins. Nine point mutations: L43R, Q47A, G54Y, F58L, D59A, E61A, Q62A, A65E, and S66F resulted in portal binding defects. Interestingly, when mapped onto a helical model, these important residues all lie along the same side of the helix, suggesting that one side of a delta domain helical region is interacting with the portal. Using coiled coil prediction algorithms, the first and second predicted helices have a high probability of making coiled coils (http://embnet.vital-it.ch/software/COILS_form.html). The 2nd helix mutations were all able to produce proheads; a few were able to expand and crosslink to create head particles. Therefore, these mutations do not affect the ability of the capsid protein to fold or interact with each other because proheads were made. In some cases, the proheads were able to be processed correctly by the protease and produce heads.

An interaction between the capsid protein and the portal is not required for HK97 capsid assembly *in vitro*. However, in order to form functional phage particles, one portal must be incorporated into a capsid. We believe this can be achieved if the portal complex acts as a nucleator of assembly. The delta domain is responsible for binding to the portal to begin capsid assembly. Without a portal, DNA packaging into the capsid is impossible, which would explain the lack of complementation by these particular mutants in the spot tests. L43R, G54Y, and E61A showed a protease incorporation defect in addition to the portal defect. LIM 49, a four amino acid insertion in the 2nd predicted helix also produced a double portal and protease defect.

This slight elongation of the delta domain could have disrupted the structure of this region of the delta domain, thus preventing proper interactions with the protease and portal. L43R, G54Y, and E61A may be affecting the delta domain to prevent an important protease binding site, or could be affecting the secondary structure so that the delta domain is not able to function correctly. Along with determining that the delta domain plays an important role in portal incorporation, we learned more about how the portal itself affects assembly. As the initiator, the portal aids in proper capsid assembly, and ensuring that all capsids contain one and only one portal. When the portal is present, it can act as a docking base for hexamers to assemble around, and once this interaction is made, additional capsomers can add more easily and quickly, while bringing in the protease to complete a functional Prohead I. We learned through point mutations, that the portal also enhances the rate of assembly and maturation. In certain mutants, like K63A, and E363A, the presence of the portal allowed for complete mcp cleavage. K63A can only cleave the mcp when the portal is present. E363A cleaves fully when the portal is present. One explanation is that the portal causes an increased rate of capsid assembly, allowing the incorporation of active proteases, which have not had time to degrade before assembly is complete. The delta domain plays many roles in capsid assembly including protein solubility, capsid geometry, and capsid size. Now, we have learned that this dynamic N-terminal extension of the capsid protein is also responsible for ensuring proper portal incorporation during capsid assembly.

K63A is an interesting mutation, as the mcp is only processed when the portal is present. We know that this mutation has the potential to cleave and mature, but this process is blocked, unless the portal is there. This mutation does not block the binding and interaction between the protease and the delta domain. Perhaps this point mutation affects the delta domain conformation so that the protease is unable to activate or cleave at necessary points. There are estimated to be

60-120 copies of the protease inside the capsid. There are 60 hexamers in a T=7 HK97 capsids; it is possible that one or two proteases are binding to each hexamer during shell assembly. When the portal is present, we believe that the capsomers assemble around it, so the portal would be surrounded by five hexamers. Perhaps these capsomers are bound to proteases and now the extra density of the portal has pushed the delta domains into a less sterically hindered conformation. Perhaps now, the proteases bound to these specific delta domains can activate or reach necessary cleavage sites and begin the cleaving process, starting a chain reaction of delta domain processing. It is very interesting that proper assembly depends on many different factors and precise protein interactions. Thus, in some cases, protease activity depends on the portal.

The structural integrity of the delta domain is very important for its function. Q38P introduced a proline, a small residue usually found in flexible and bent regions of a protein. Q38P is located near the beginning of the 2nd predicted helical region. When the secondary structure of the delta domain was disrupted by this proline, the protein was still able to produce proheads, but the mcp was unable to be cleaved. Further tests showed that this mutation was defective in both portal and protease incorporation. The changes that this mutation made in the structure of the delta domain prevented it from appropriately binding to the proteins that are crucial for capsid maturation and function. This shows that the structure of the delta domain plays an important role in its function. As shown in Chapter 2 with the 'hinge' deletion mutants, and this Q38P point mutation, disturbing the delta domain structure prevents proper protein-protein interactions.

Our biochemical analyses of the delta domain provides evidence that this domain is important for portal incorporation, and specifically that the 2nd predicted helix of this domain is mainly responsible for this interaction. The identification of a 2nd site suppressor in the portal

gene has provided us with genetic evidence to support our mutational assays. Using the portal incorporation defect mutant, A65E, in the delta domain, we were able to create viable phage that contained a 2nd site mutation in the portal gene, D135G. This result argues that there is an interaction between the corresponding regions of the portal and the delta domain that is important for portal incorporation during assembly. We can speculate on how this interaction occurs but will need more data to thoroughly understand how the portal and delta domain interact. For example: this suppressing mutation changed a charged residue to a small residue in the portal. The initial mutation created a negatively charged residue, which disrupted the current interaction between the portal and the delta domain, as two negatively charged residues would repel. Therefore, D135 mutated to a glycine, to keep this negative charge-small residue interaction between the delta domain and the portal. The 2nd site suppressor suggests that the 2nd predicted helical region of delta domain is in close proximity to the portal.

Genetically, we showed that there is some sort of interaction between A65E in the delta domain, and D135G in the portal. To test if this double mutation could rescue protein function *in vitro*, D135G and a double mutant, A65E/D135G were moved into plasmids containing the portal gene and tested in miniprohead preps. D135G (gp3) showed a partial cleavage defect, producing mostly uncleaved mcp. However, the cleaved mcp is functional and can assemble into viable phage particles because the complementation tests showed that D135G had WT complementation of protease and capsid gene amber phage. However, D135G did show a one log decrease in portal protein functionality. This charge change in the portal caused a slight decrease in the efficiency of the portal protein to complement phage with an amber mutant in the portal gene. This portal mutation could be slightly interfering with how the portal interacts with the capsid shell, which could interfere with assembly initiation, causing this slight decrease in

complementation efficiency. The double mutation allowed for WT levels of portal incorporation but also showed a cleavage defect with relatively equal amounts of cleaved and uncleaved protein produced. However, the double mutation showed WT complementation in phage with amber mutations in the portal, major capsid, and protease genes. Like D135G, the smaller amount of cleaved mcp were sufficient to form viable capsids. Compared to the single mutation, A65E, this double mutant rescued protein functionality. The presence of D135G rescued the defect, allowing the capsid protein to function properly and bind to incorporate the portal. This double mutant brought D135G complementation to WT levels and was therefore able to rescue both single point mutation defects. These results support our genetic data that residue A65 in the delta domain and residue D135 in the portal are in close contact inside the capsid.

The portal sequence alignment and homology model created based on the *C. diphtheria* phage portal provides more evidence that this region of the portal could be making contacts with the delta domain. To further study the delta domain and the portal, we can model its interaction using available capsid density maps and crystal structures. The *C. diphtheria* phage portal crystal structure can be fit into the HK97 crystal structure to hypothesize what a portal containing HK97 prohead might look like. Using this model, we can learn more about how the delta domains could be interacting with the portal. We can also make a hypothetical model based on the reconstructions of the Del 2nd Hinge T=7 and T=4 capsids. We can use this model to identify possible interacting points between the mcp and the portal. In Del 2nd Hinge, the mutant portal is elongated and structured as towers in these mutants, it would be interesting to see how a portal crystal structure would fit in and interact with mutant delta domains. We can compare how the delta domain interacts with a portal between mutant and WT capsids. By tracing in the sequence

in our models, we may learn more about how the delta domain functions as a regulator of capsid assembly.

3.2.5 The N-terminal region plays a role in protease incorporation

Del1, a deletion of 9 residues at the N-terminus of the delta domain was discussed in the previous Chapter. This deletion produced only a few Prohead I like particles and was unable to efficiently complement phage with an amber mutation in the capsid gene. This phenotype suggests a defect in protease incorporation, so this mutation was moved into a plasmid expressing the portal and the inactivated protease.

Del1, a deletion of 9 residues in the N-terminus has defective protease incorporation

Prohead I and/or Prohead II with portal capsids were used as controls. During purification, there were two bands present in the glycerol gradient, but only the top band samples were used for gel analyses. On the SDS gel, Del1 produced portal and uncleaved mcp bands. The mcp band was weak and there was no detectable protease band. Even when larger amounts of Del1 protein were loaded on the gel to match the Prohead I control, there was still no detectable protease protein (Figure 53A). On the agarose gel, Del1 produced only prohead dimer and prohead trimer bands; there were no prohead monomers (Figure 53B). A small deletion at the N-terminal region of the delta domain causes a protease incorporation defect. I wanted to identify specific residues that were involved with this interaction between the delta domain and the protease. Four point mutations were made within the Del1 region: L6R, Q8A, I11F, and E12A. Two other mutations were made near the end of the first predicted helix: Q20A, and I29F. These residues were

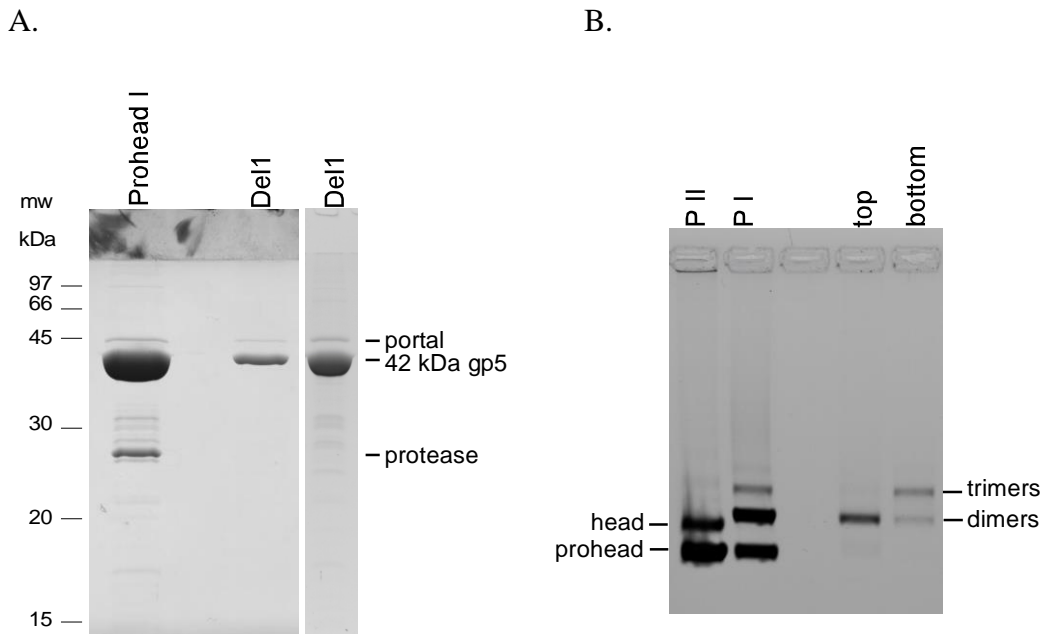


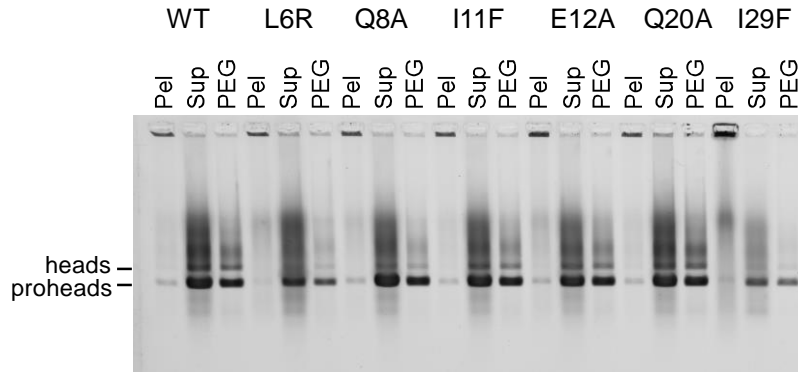
Figure 53. Del1 is defective in protease incorporation

Prohead prep samples were banded through a glycerol gradient and then pelleted in the ultracentrifuge in a Ti45 for 2 hours at 4 °C. Del1 produced two distinct bands in the gradient: a top band, and a bottom band. A) On the SDS gel, Prohead I produced a portal, uncleaved mcp, and protease band. Del1 (top band sample shown only) produced a portal band and a much lighter uncleaved mcp. Even when a larger amount of protein was loaded to match the Prohead I control, no protease band was detected. B) Pelleted purified samples were run on a 0.9% agarose gel along with Prohead II and Prohead I controls. Prohead II produced proheads and heads. Prohead I produced proheads, prohead dimers, and trimers. The top band sample produced a strong prohead dimer with barely detectable prohead or prohead trimer bands. The bottom band sample showed a prohead dimer band and a stronger prohead trimer band.

targeted based on sequence alignments of the HK97 delta domain and other related delta domains. Conserved hydrophobic residues were mutated to a completely different residue which was not found elsewhere in the alignment at that site (Figure 31 and R. Duda <http://gigapan.com/gigapans/b806a9da80b4a66bcb1dd1b273d5b7a4/>). The goal was to produce the biggest change possible to affect capsid assembly.

These N-terminal mutants were in a plasmid, pVP1, which is similar to the pV0 plasmid and expresses the protease and capsid genes. The pellet, supernatant, and PEG precipitated fractions were electrophoresed on native agarose gels and SDS gels, and studied by TEM. The functionality of each mutant protein was also tested using spot complementation assays. On the agarose gel, WT produced prohead and heads bands, which are mostly in the supernatant and PEG fractions, as expected. L6R produced proheads and heads, but at less than WT levels. Q8A, I11F, E12A, and Q20A produced proheads and heads. I29F produced less than WT levels of proheads and heads (Figure 54A). On the SDS gels, WT supernatant and PEG fractions showed mostly cleaved mcp. L6R, Q8A, I11F, E12A, and Q20A also produce mostly cleaved mcp in supernatant and PEG fractions like WT. I29F produced a large uncleaved mcp band in the pellet fraction, along with small amounts of cleaved and uncleaved mcp in the supernatant and PEG fractions (Figure 54B). In the spot complementation assays, L6R, I11F, E12A, and Q20A were able to complement phage with amber mutations in their capsid gene and protease gene, like WT. Q8A and I29F, however, were 1 log down in capsid gene amber phage complementation (Table 1). Electron micrographs showed that these mutations were able to produce WT like proheads and heads. Some capsids are damaged or broken, which is common from the crude purification methods of miniprohead preps (Figure 55).

A.



B.

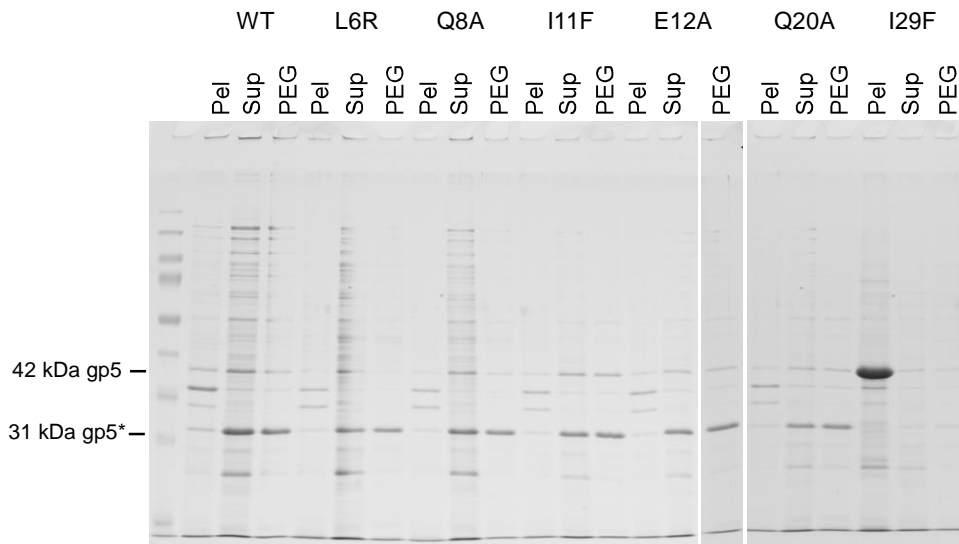


Figure 54. Miniprohead prep results of point mutations in the N-terminus of the delta domain.

A) Pellet, supernatant, and PEG fractions were collected and run on a 0.9% agarose gel. WT control produced proheads and heads. L6R produced lower than WT levels of proheads and heads. Q8A, I11F, E12A, and Q20A produced W like results. I29F produced less than WT levels of proheads and heads. B) Sample fractions were prepared and run on SDS gel, and stained with coomassie. WT control produced mostly cleaved mcp, which mostly ended up in the supernatant and PEG fractions as expected. L6R, Q8A, I11F, E12A, and Q20A produced similar results to WT. I29F produced mostly uncleaved mcp in the pellet fraction. I29F produced very light uncleaved and cleaved mcp in the supernatant and PEG sample lanes.

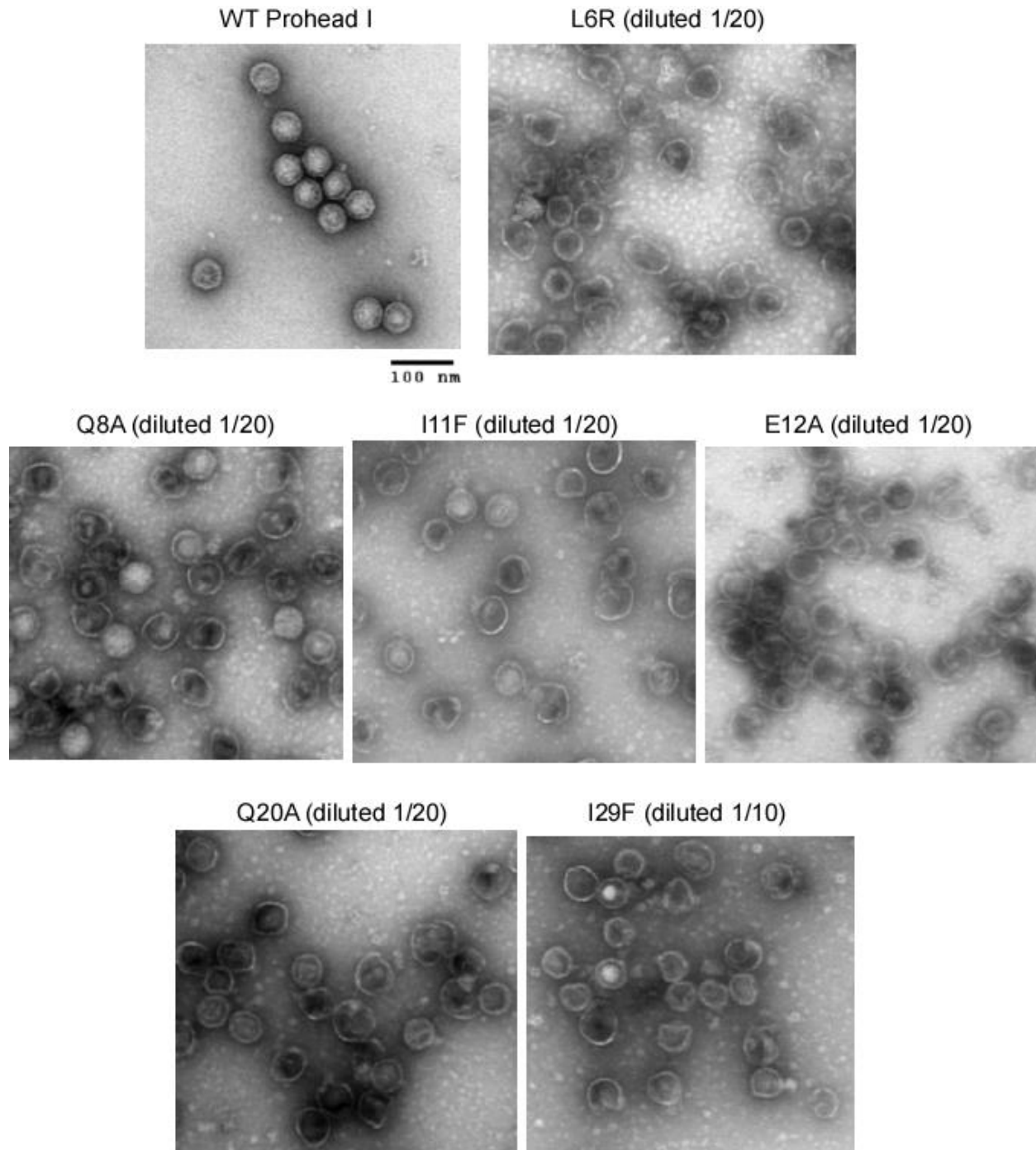


Figure 55. Representative EM images of mutant samples from miniprohead preps.

WT Prohead I is used as a comparison control. PEG samples were diluted in 1x calorimetry PBS, stained with 1% uranyl acetate, and imaged. All mutants produced prohead and head like particles. These crude purification samples usually contain some broken capsids and background material from cell debris. All images taken with 56,000x magnification. Scale bar: 100 nm.

I29F shows a protease incorporation defect

To further characterize these mutants, they were moved into a plasmid that expressed the portal and inactivated protease genes to test for portal or protease incorporation. The PEG samples from the miniprohead preps were further purified by pelleting in the ultracentrifuge. Prohead II and Prohead I were used as controls. On the SDS gel, L6R, Q8A, I11F, E12A, and Q20A produced portal, uncleaved mcp, and protease bands. I29F produced portal and uncleaved mcp bands only. There was no protease band detectable, indicating a protease incorporation defect. I29F also produced less protein than the other mutants (Figure 56A). On an agarose gel, L6R produced a very light prohead band, a strong dimer band, and a weak trimer band. Q8A, I11F, E12A, and Q20A produced strong prohead and prohead dimer bands, along with weak trimer bands. I29F barely produced any protein represented by a weak prohead and prohead dimer bands (Figure 56B). These assays showed that these N-terminal mutants are able to incorporate the portal during assembly and have mostly WT like phenotypes. However, I29F has a protease incorporation defect.

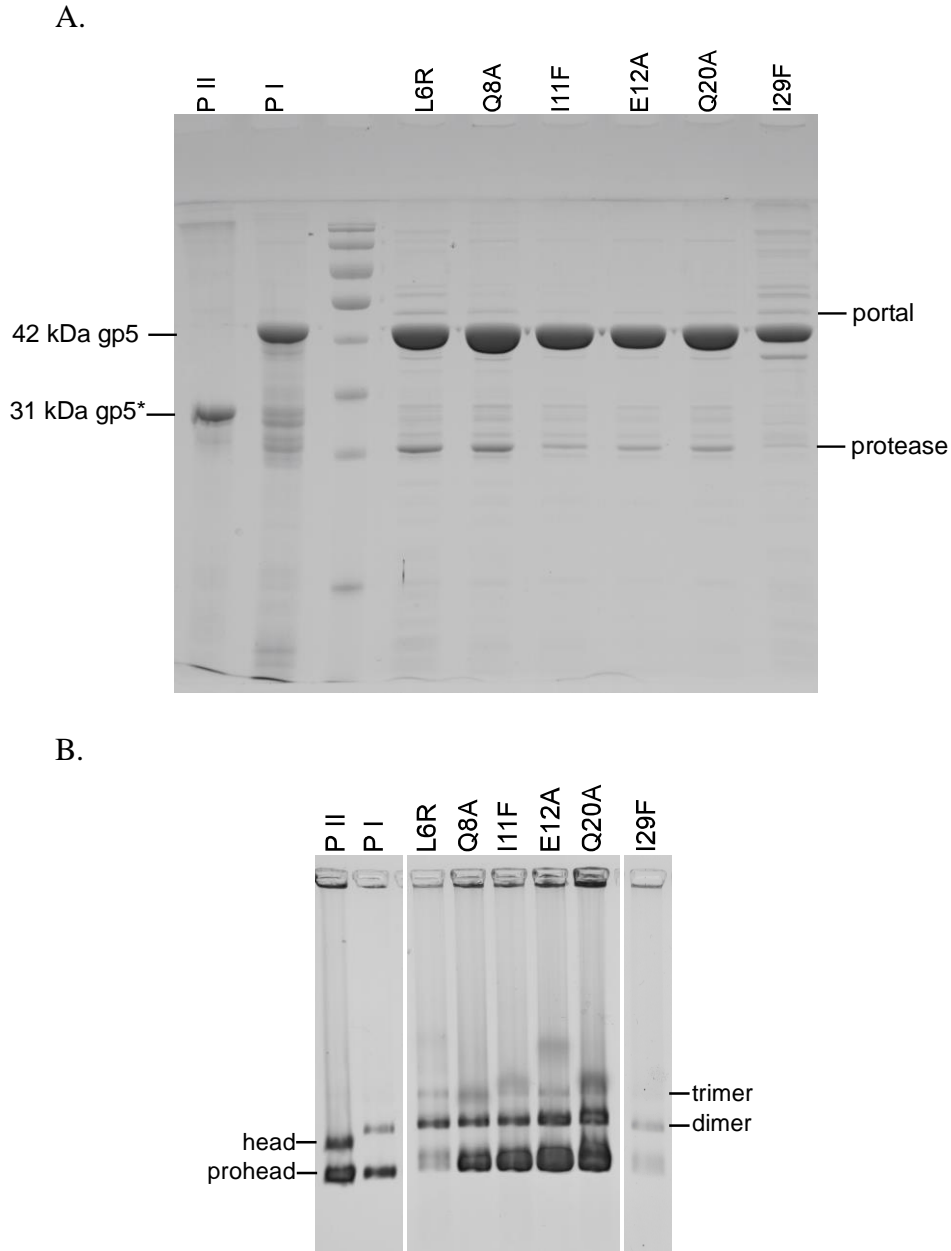


Figure 56. N-terminal point mutants expressed with the portal and inactivated protease.

After the miniprohead prep, the PEG fractions were further purified by pelleting in the ultracentrifuge in the Ti80 for 42 minutes at 41,000 rpm in the cold. Prohead II and Prohead I containing portals were used as controls. These control samples were older samples, which explains the weaker bands and the larger number of mcp degradation products in the P I lane (the smear and multiple light bands underneath the mcp) A) Samples were prepared for SDS gels. Prohead II showed a portal band and the cleaved mcp band. Prohead I showed a portal, an uncleaved mcp, and a protease band. L6R, Q8A, I11F, E12A, and Q20A produced portal, uncleaved mcp, and protease bands. I29F produced a portal band, an uncleaved mcp band (which is at lower levels than the others) and no protease band. B) Pelleted PEG samples were run on a 0.9% agarose gel. Prohead II produced proheads and heads. Prohead I produced proheads and prohead dimer bands. L6R produced a small amount of proheads and mostly prohead dimers and trimers. Q8A, I11F, E12A, and Q20A produced strong prohead, prohead dimers, and trimer bands. I29F produced very low levels of proheads and prohead dimers, indicated by the weak bands in the gel.

LIM 20 shows a protease incorporation defect

LIM 20 is a mutation located in the N-terminal region of the delta domain that was shown in Chapter 2 to have a cleavage defect and only made Proheads. This mutation was moved into the portal and inactivated protease plasmid and tested for incorporation defects. LIM20 produced three bands in the glycerol gradient, which were all used for gel analysis. Prohead I and Prohead II with portal were used as controls. On the agarose gel, the LIM 20 top band produced mostly proheads, and a light dimer band. LIM 20's middle band produced a strong dimer band and weaker prohead and prohead trimer bands. LIM 20's bottom band produced a strong trimer band, and weaker monomer and dimer bands (Figure 57A). On an SDS gel, all of the LIM 20 bands produced portal protein and uncleaved mcp. The top band had a weaker portal band than the other two band samples. There was no protease protein detected, indicating that LIM 20 has a protease incorporation defect (Figure 57B).

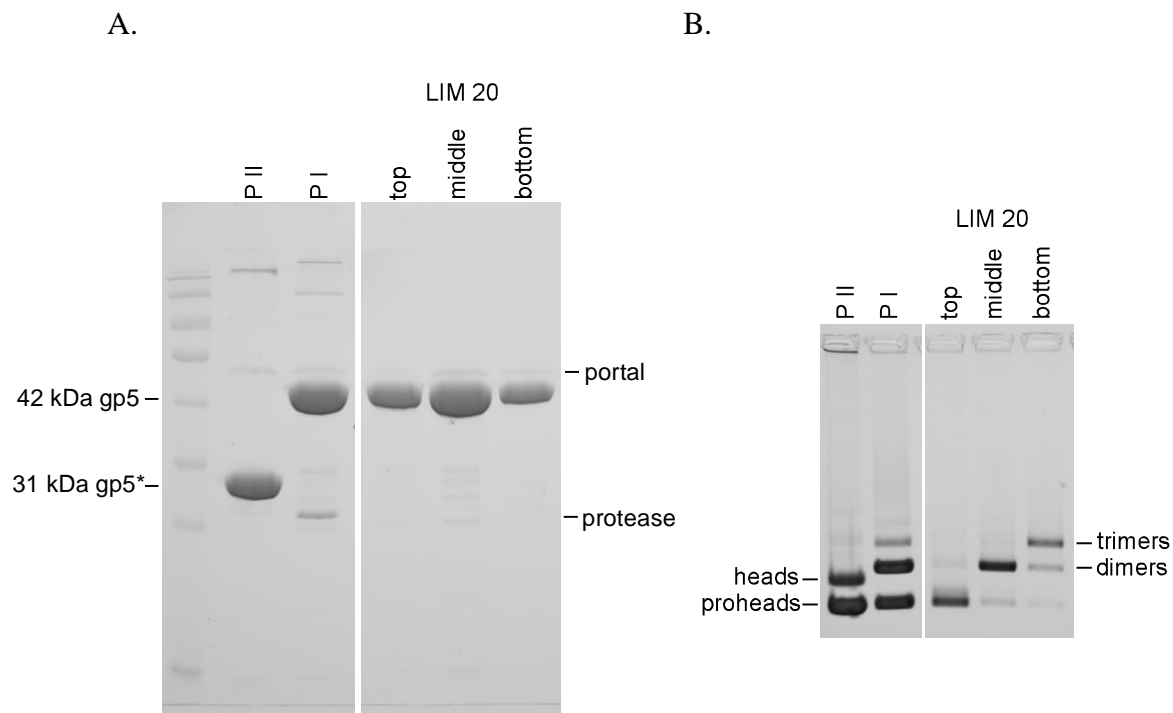


Figure 57. Prohead Prep expressing LIM20 with the portal and inactivated protease.

In the glycerol gradient, LIM20 separated into three protein bands: top, middle, and bottom bands. Prohead I and Prohead II containing portals were used as controls. A) Samples were prepared and run on SDS gels. Prohead II produced portal and 31 kDa cleaved mcp. Prohead I produced portal, full length uncleaved mcp, and inactivated protease bands. The top, middle, and bottom bands of LIM20 contained portal and uncleaved mcp bands. The portal band is weaker in the top band than the other fractions. LIM20 samples did not produce any detectable protease bands. B) Purified samples were loaded on a 0.9% agarose gel. Prohead II produced proheads and heads. Prohead I produced proheads, prohead dimers, and trimers. The top band produced mostly proheads, and some prohead dimers. The middle band produced mostly prohead dimers, with weak prohead and prohead trimer bands. The top band produced proheads, dimers, and trimers, with the trimer band being the strongest.

3.2.6 Discussion

Mutational analyses of the N-terminal region of the delta domain showed that it plays a critical role in interacting with the protease to ensure proper incorporation during assembly. I have identified three mutations in the N-terminal predicted helix which cause a defect in protease incorporation. Del1, a deletion of amino acid residues 4-13, LIM20, a four amino acid insertion, and the point mutation I29F, were only able to produce proheads due an inability to incorporate the protease proteins. LIM20 could have disrupted the secondary structure of the delta domain and changed how the delta domain can interact with the protease. I29F could have blocked a critical binding site that the protease needs to bind with the delta domain, or the assembly process could have been slowed, so that by the time the proheads were completed, the protease has degraded. These mutations showed that disruptions to the N-terminal helical region affect the delta domain's ability to interact with the protease during assembly.

The native agarose gel data of Del1 expressed with the portal and inactivated protease showed the absence of prohead monomers. This meant that practically all of the proheads assembled with the portal. As mentioned earlier, our HK97 expression system is very efficient in producing proheads, and the portal is not required for capsid assembly and maturation. The fact that almost all of the Del1 capsids contained a portal showed that assembly for this mutant is not as efficient as WT, that the portal was needed to initiate capsid assembly. In the earlier biochemical tests, this mutant was able to produce a small amount of proheads without the portal. However, when the portal was present, there were more proheads made because assembly was nucleated more efficiently. All of the proheads incorporated the portal because they needed it as an initiator. This supports the idea that the portal can enhance capsid assembly. There is no

structure available for the HK97 protease, but secondary structure prediction programs predict that the C-terminal region of the protease is α -helical. Perhaps the N-terminal region of some of the delta domains are making coiled coil interactions with the C-terminal region of the protease. This interaction is crucial for protease-delta domain binding, which allows for ~120 copies of the protease to be brought into the growing capsid shell.

To further delve into Del1, I made specific point mutations within the deleted region to identify specific points of contact between the delta domain and the protease. The point mutations L6R, Q8A, I11F, E12A, and Q20A produced WT like Proheads, which could cleave and mature into Head particles. They also produced functional capsid protein, which could assemble into infectious phage particles. Only Q20A showed a one log decrease in capsid gene complementation. I was unsuccessful in pinpointing any particular residues in the Del1 region that were responsible for protease incorporation. However, L6R showed a slight defect in capsid assembly efficiency. In a majority of the biochemistry assays, L6R showed WT like phenotypes. However, when this mutant was expressed in the portal and inactivated protease plasmid was run on a native agarose gel, there was a strong prohead dimer band, but a very light prohead monomer band. As with the Del1 mutation, this phenotype indicated that a majority of the proheads contain portal protein. When WT prohead with portal and inactivated protease is expressed, efficiency is good enough that the portal is not required to initiate capsid assembly. We estimate that about 50% of the capsids produced under these conditions are portal-less in the WT background. By producing more prohead dimers than prohead monomers, L6R seems to be most efficient when the portal is present. L6R can assemble like WT without the portal, but with the portal to initiate, assembly occurs more efficiently. This mutation is another example of our hypothesis that the portal, as an initiator of assembly, enhances the assembly process.

3.3 DIFFERENT REGIONS OF THE DELTA DOMAIN PLAY DIFFERENT ROLES IN CAPSID ASSEMBLY

The biochemical and genetic tests of delta domain mutations have shown that this region of the HK97 capsid protein plays multiple functional roles during capsid assembly. The full length delta domain is required for capsid protein solubility, suggesting that this domain is acting as a sort of chaperone to ensure proper capsid protein folding. Even small length deletions and four amino acid insertions caused defects in protein solubility and functionality. A deletion of 7 residues, Del 2nd Hinge, was a very interesting mutation, in that it was able to produce mutant capsids of different sizes with triangulation numbers of T=7 and T=4. This deletion was made in a predicted ‘hinge’ region in between two predicted α -helices. When these capsids were reconstructed, we were able to see more stable and elongated delta domains compared to the WT Prohead I density map. With further modeling and fitting with these mutant capsids, we can learn more about how the delta domain is structured inside the capsid.

The delta domain is able to affect the size and shape of the capsid. Point mutations in the C-terminal region of the delta domain caused abnormal and tube like structures to form. In other phage scaffolding proteins, the C-terminal regions interact with the capsid shell. In HK97, the C-terminal end of the delta domain is attached to the rest of the capsid shell subunit. Therefore, changes made in this region can have a direct effect on how the rest of the capsid protein is structured. Aside from capsid protein expression, capsid size and geometry, the delta domain is also involved with interacting with other proteins that are required for proper capsid assembly. The phage-encoded protease is required to be present inside the capsid, and once assembly is complete, cleaves the delta domain and itself into smaller peptides, which escape through pores

in the capsid. Without the protease, the capsid would not be able to mature. Previous capsid assembly experiments showed that when the C-terminal end of the HK97 protease was fused to GFP, assembled proheads fluoresced due to the incorporated GFP (Duda et al, unpublished). This suggests that the C-terminal region of the protease interacts with the major capsid protein during assembly. We have shown that the protease interacts with the N-terminal region of the capsid protein, the delta domain, to incorporate into the capsid. We have showed that it is mostly the N-terminal region of the delta domain that is responsible for this role. The portal is another important protein required for capsid assembly. Without the portal, no DNA packaging and tail attachment can occur. Mutational analyses have also shown that the delta domain is important for portal incorporation. Specifically, it is the 2nd predicted helical region, or the middle of the delta domain, that plays this portal incorporation role.

It is fascinating that these roles correlate to different regions of the delta domain. Figure 58 shows a predicted model of the delta domain with a summary of assembly defects and how they map to different regions of the domain. The N-terminal region of the delta domain likely interacts with the C-terminal region of the protease. The 2nd predicted helical region of the delta domain likely interacts with the portal. The C-terminal region of the delta domain likely interacts with the rest of the mcp, ensuring proper capsid size and geometry. This multifunctional 102 amino acid extension of the capsid protein is able to fulfill all of these scaffolding-like roles during assembly. While some specific residues play important parts in the delta domain's function, it is the structure of the delta domain- its helical nature, its ability to form coiled coils, its flexibility - which allows it to function and coordinate the interaction of different types of proteins during the initial stages of capsid assembly.

Possible Future Directions

The delta domain has been a fascinating object of study. It is exciting to learn that this small peptide plays so many roles in assembly. Del 2nd Hinge was a very interesting mutation provided some support that the delta domain plays some role in capsid size determination. I think it would be very interesting to try and make a similar deletion in other phage capsids that contain the HK97-like fold. For example, D3 or Phi1026b are T=9 capsids that have the HK97-like fold. If we deleted a homologous region in their delta domains, would it also produce different sized capsids? While I have made some different sized deletions with this domain, I have not made extensions. I think it would be interesting to see if we can increase the capsid size or change its shape by extending regions of the delta domain, particularly the predicted helical regions. Other possible directions are discussed briefly in the appendices. The spokes that we see in the WT and mutant capsids have always interested me. It was fascinating that the different types of capsids showed different patterns of spoke densities and weakness. It seems that the stability of the spokes depends on where it is located inside the capsid. Pentamer spokes always seemed to be more stable than hexamer spokes. While they are made of the same subunit, they are in slightly different conformations and must be able to make different interactions that we see in the skewed and symmetrical hexamers and pentamers. It would be useful to be able to pinpoint the amino acids that make up these densities. Delta domains and scaffolding proteins are responsible for interacting with a number of proteins to build a macromolecular complex. Their ability to be stable and structured in certain cases, and flexible in other cases show us just how versatile a small protein, or portion of a protein can be.

4.0 MATERIALS AND METHODS

Expression plasmids

The expression strains are *E. coli* BL21(DE3)plysS (Studier et al. 1990). HK97 plasmids contain a T7 promoter that can be induced with lactose or IPTG. These strains are used for (mini)prohead preps and complementation tests. Plasmids are based on the expression vector pT7-5 (GenBank: AY230150). The WT HK97 plasmid, pV0 (pT7-Hd2.9) contains full length genes 4 and 5, and a portion of gene 3. pV0SacI contains the same genes as pV0 but contains a SacI restriction site in the beginning of gene 5. Plasmid pVP1 is similar to pV0 in expression. pVB has the protease gene knocked-out. Mutations of interest are made and sub-cloned into either pV0 or pVP1 expression vectors. Sequences are verified using Genewiz. These plasmids were generally used for testing and screening new mutants for assembly defects. pVP0 contains genes 3, 4, and 5. pVP0 g4 (H65A) contains genes 3, 4, and 5, but has an inactivated protease due to the point mutation H65A. This plasmid is typically used to test for portal and protease incorporation (Robert L. Duda, Oh, and Hendrix 2013; Oh et al. 2014)

Site directed mutagenesis

Mutations were made using PCR and fragment ligation (Adereth et al. 2005) or with the Q5 site directed mutagenesis kit (New England BioLabs). N-terminal and C-terminal fragments were made using 2 sets of primers. One of the fragments would carry the base change(s) to make the mutation. Also, optionally, a silent mutation was also included near the point mutation to allow

for later identification when necessary. The two inner primers were phosphorylated on their 5' ends with T4 Kinase. Phusion polymerase was used in the PCR reactions of the upstream and downstream fragments before they were extruded from a 0.8-1% agarose gel. The fragments were ligated using NEB Ligase for 1 hr at RT or 20-30 minutes at 16-18 °C in an ultrasonic waterbath. A 2nd round of PCR was done utilizing the two outer primers. This full length fragment was then digested using SacI and DraIII enzymes and then ligated with the HK97 expression vector fragment.

The mutant plasmid was transformed into DH10b competent cells and allowed to recover in 1 mL SOC media at 37°C degrees for at least 30 minutes. Cells were plated on LB amp50 plates, and incubated overnight at 37°C. Plasmids were collected using the Qiagen miniprep kit and sent to Genewiz for sequencing to ensure the correct mutation was present. 0.3 uL of plasmid and 0.3 uL of plysS plasmid were transformed into BL21(DE3) competent cells and allowed to recover in 1 mL SOC media at 37 °C degrees for at least 30 minutes before plating on LB amp50 cam25 plates.

Miniprohead preps

An overnight culture of expression cells are grown in MDG (non-inducing media) (Studier 2005). The culture is diluted into 1.5 mL TYM5052 (autoinduction media) with 50 ug/mL ampicillin and 25 ug/mL chloromphenicol and shaken at 300 rpm at 37°C for 24 hours. The cell pellets are suspended in Lysis buffer (50 mM Tris-HCl pH 8.0, 0.008 M EDTA pH 8.0) and 1% X100-Triton, frozen in dry ice, and thawed at room temperature. 1 M MgSO₄ and 1mM DNase was added. The cells were spun in a table top centrifuge at 14 K rpm for 10 minutes in 4 C. The supernatant was divided into two tubes: one supernatant and one for PEG precipitation (150 uL

each). 150 uL of 20% PEG was added to the PEG tube and incubated on ice for at least 20 minutes. The PEG samples are spun in a table top centrifuge at 14 K rpm for 10 minutes in 4 C. The supernatant is removed and the PEG pellet is gently resuspended in 150 uL Buffer G. The sample was separated into three fractions: a pellet, supernatant, and PEG precipitate. The remaining pellet is suspended in 300 uL of Buffer DL.

In some miniprohead preps, the entire supernatant was PEG precipitated. This sample would then be concentrated in the ultracentrifuge by spinning in the Ti80 for 42 min at 41K rpm in the cold

Prohead preps

Overnight cultures are diluted 1:500- 1:2000 in LB amp50cam25 and grown at 37°C at 300 rpm until the OD550~0.4. 0.4 mM IPTG was added and the cells were induced overnight at 28°C. Cells were pelleted and resuspended in lysis buffer (50 mM Tris HCl PH 8.0, 5 mM EDTA (pH 8.0). Triton X-100 was added to 0.4% to cells were cycled between cold and warm (22-24°C) to aid in lysis. MgSO₄ is added to 7.5 mM and DNase I is added to 20 ug/mL and the cells are incubated at warm temp to reduce the viscosity. Cell debris is pelleted by low speed centrifugation at 10K, 10-15 minutes. The supernatant is PEG precipitated by adding NaCl to 0.5 M and PEG 8000 (6000) to 6% (w/v) and held in ice for at least 20 minutes. The PEG precipitate is pelleted and gently resuspended in TKG₅₀ (20 mM Tris HCL pH 7.5, 50 mM Potassium Gluterate). Another spin is done to further purify the PEG sample. Proheads are diluted and pelleted by ultracentrifugation in the Ti45 at 35K rpm for 2 hours in the cold. The pellets were resuspended in TKG₅₀ buffer. The insoluble material is removed by spinning at 8K rpm for 10 minutes. The remaining supernatant is run through a 10-30% (v/v) glycerol gradients for 1.75-2.5 hours in the cold. The prohead band(s) were pulled from the gradient and dialyzed against 5 mM

Tris pH 7.5 at room temperature for an hour. Ion exchange chromatography was performed using an HQ20 anion exchange. Peak fractions were collected and concentrated by ultracentrifugation at 35K rpm for 2 hours in the cold. The pellets are covered in a small volume of Buffer and allowed to resuspend overnight at 4°C.

In some prophead preps, the dialysis and chromatography steps were replaced by pelleting in the Ti45 at 35K rpm for 2 hours in the cold. The pellets were resuspended in a small volume of TKG₅₀ buffer overnight at 4°C and syringed filtered.

SDS Gel Electrophoresis

For miniprohead preps, 10 uL of samples were diluted in 215 uL 5 mM Tris pH 7.5 buffer. Protein was precipitated with 25 uL of 10% TCA, 2 mg/mL sodium deoxycholate (DOC) or 10% TCA and incubate on ice for 10-20 minutes. The samples are spun at 14K rpm in the cold for 10 minutes. Samples were washed with acetone, pelleted, vacuum dried, suspended in 1x SDS sample buffer (Laemmli 1970), and boiled for 2.5 minutes. Samples were electrophoresed in 12% low-crosslinking SDS polyacrylamide gels (33.5% (w/v) acrylamide/0.3% (w/v) methylene bisacrylamide). Gels with samples containing portal and/or inactivated protease were run on 12% SDS gels with double the amount of bis-acrylamide (30% (w/v) acrylamide/1.6% (w/v) methylene bisacrylamde) (Laemmli 1970) and stained with Coomassie Brilliant Blue R250.

Native Agarose Gel Electrophoresis

Protein samples are diluted with TAMg buffer dye-glycerol mix (40 mM Tris base, 20 mM acetic acid pH 8.1, 1 mM magnesium sulfate) and run on 0.8-0.9% agarose gel. Gels are electrophoresed and stained with Coomassie Brilliant Blue R250 stain (Duda, Hempel, et al. 1995).

Transmission Electron Microscopy

Samples were applied on carbon/formvar grids (400 mesh, Ted Pella, Redding, CA) (Grids were glow-discharged before use) and rinsed with water before staining with 1% uranyl acetate. Micrographs were taken using a Morgagni 268(D) Electron Microscope (FEI, Eindhoven, Netherlands) at 56000x magnification (one sample at 86000x).

Reconstruction of Del 2nd Hinge Capsids

Sample grids were frozen using a Vitrobot. Images were taken in the Polara FEI cryo-electron microscope using a Falcon II direct electron detection camera. About 1,000 images were taken from 10 grid squares. Capsids were manually selected as T=4 or T=7 sized using the x3d program. Ultimately, 58304 small particles and 1616 T=7 sized particles were collected. An average icosahedral map of each sample was calculated using AUTO3DEM (Yan, Sinkovitis, and Baker 2007).

Complementation Spot Tests

Bacterial lawns were made from a mixture of overnight cultures of the BL21(DE2)plysS expression mutant strains (BL21, ~1% lactose (to induce gene expression) and soft agar on an LB (amp₅₀ cam₂₅) plate. Dilutions (10⁹ pfu/mL to 10⁴ pfu/mL) of WT phage, *am1* (gene 5 amber mutation), *amU4* (gene 4 amber mutation), *amC2* (negative control amber mutation), and sometimes *am3* (gene 3 amber mutation) were spotted as 4 uL spots. Plates were incubated at 37°C overnight. WT pV0 was used as a positive control. Relative complementation efficiency is calculated. A score of 10 was assigned for a clear spot and a score of 3 was assigned for a partly clear spot and the values are multiplied together. For example, WT usually produces 5 clear

spots and one partly clear spot so it's score would be $10 \times 10 \times 10 \times 10 \times 10 \times 3 = 3 \times 10^5$. The mutant complementation efficiency score is divided by the WT control to get the relative value.

Making and selecting for HK97 mutant prophage

DT005 cells (Tso 2010) are grown up in 30°C overnight shaking at 300 rpm. The overnight culture was then diluted 1:100 in 30 mL SOB (LB + 2.5 mM KCl, 10 mM MgCl₂, 10 mM MgSO₄) and 100 ug/ul ampicillin and shaken at 300 rpm in a 30°C waterbath until O.D₅₅₀ ~ 0.4. There are two samples prepared-induced and uninduced samples. The induced samples contained 10 mM L-arabinose. The cultures were cooled in an ice water slurry for about 10 minutes and pelleted at 4500 g for 7 minutes at 4°C. The pellet was initially gently suspended in 1-2 mL ice cold dH₂O. Then 28 mL of ice cold water was added and the cells are pelleted again. Each time, the pellet was gently suspended in a small volume, before bringing up the volume. The sequential wash volumes were 10, 5, and 1 mL. The 1 mL of cells were then pelleted in a cold microcentrifuge at max speed for 30 seconds and resuspended in 200 uL ice cold 10% glycerol.

For transformation, 30-40 uL of cells are used. There are three test samples: Induced with DNA, Induced without DNA, and uninduced with DNA. The controls are used to show the background of cells. The cells are electroporated in 0.1 mm cuvettes and transformed with at least 200 ng of fragment DNA. The time constant should be greater than 5 ms. After transformation, the cells were diluted into 10 mL SOB amp₁₀₀ and recovered by shaking in a 30°C waterbath for at least 4.5 hours or overnight. The recovered cells were then pelleted at 4500 g for 3-5 minutes in the cold. The cells were gently washed in 1x minimal salts (M9 or M63) and 1 mM MgSO₄ and resuspended as previously described in 10, 5, and eventually 1 mL volumes. The final pelleting in 1 mL is repeated.

Cells are diluted 10^3 , 10^4 , and 10^5 and 100 uL is spread on selection plates. Plates are incubated at 30°C overnight and then moved to 42°C until pickable colonies appear, about 3-4 days. Colonies are picked, resuspended in 15 uL T1/10E buffer, and restreaked 6 per plate on DOG plates. This restreaking is to reduce the amount of DNA contamination that could be present from dead cells. These new plates are incubated at 42°C for 3-4 days until colonies appear.

2-DOG plates for galK recombineering

2 grams of 2-deoxygalactose is dissolved in 200 mL 5x M63 or M9 salts. 100 uL of 0.1 g/mL thiamine and 5 mL 40% glycerol is added before sterile filtering. This mixture is kept warm in a 55°C waterbath and added into 1 L LB agar (sterilized). 4 mL of 0.5% Uracil and 10 mL of 0.1 M $MgSO_4$ are added last.

Bochner-Maloy plates for tetR recombineering

Flask A: 12 g agar, 4 g tryptone, 4 g yeast, 40 mg chlorotetracycline, 400 mL water

Flask B: 8 g NaCl, 8 g NaH_2PO_4 , 400 mL water

Flasks A and B are separately sterilized and allowed to cool. Fusaric Acid dissolved in DMF (9.6 mg in 500 mL DMF) and 4 mL of 20 mM $ZnCl_2$ is added to Flask B. Both mixtures are combined and poured. Best to use within 36 hours. (Bochner et al. 1980; Maloy and Nunn 1981)

Colony PCR

Using sterile toothpicks, individual colonies are picked and resuspended in 10-15 uL of T1/10E buffer in 96 well plates. As each colony is suspended in the 96 well plate, they are subsequently

spotted onto LB plates (grown overnight at 37°C). The plates are UV sterilized for about 10 minutes before use. PCR using ExpandHF or Phusion enzymes was performed in 10 uL (or 20 uL) reactions. 4 uL (or 8 uL) of the colony were used. The primers were at concentration of 6 uM. With tetR recombineering, a set of three different primers were used. Two different forward primers (one that was complemented to the HK97 sequence and one that complemented to tetR sequence) were used to differentiate between a recombined and tetR fragment. The same reverse primer was used that bound to the HK97 sequence downstream of the recombination region. With galK recombineering, only one forward and one reverse primer were used. Samples underwent 30 cycles. 5 uL of sample were run in 0.9% agarose gels. The gels were stained with 0.5 ug/mL Ethidium Bromide and imaged with a UV camera. Samples containing the expected fragment size for our HK97 sequence (which had lost the marker sequence) were further tested using restriction digestion.

Lysogen Streak Test

50 uL of WT HK97 phage were pipetted in a line across an LB plate. A sample of the resuspended colonies were streaked across the line of phage and the plates were incubated overnight at 37°C. A lack or lower level of colony growth after passing over the phage line indicated the presence of a lysogen, which prevented superinfection from the WT phage.

Digestions to check for recombinants

The mutations used to test for 2nd site suppressors/revertants were made with unique restriction sites to allow for identification. The colony PCR samples were digested in 10 uL reactions with their unique restriction enzyme for 2 hours at 37 °C. Digestions were run on 0.9% agarose gels

and stained with 0.5 ug/mL Ethidium Bromide. Colonies that showed a similar digestion pattern as the positive control were grown up from their overnight colony (from the LB plate) and frozen for glycerol stocks.

Sequencing

Fragments from the possible recombinant was made using PCR and sent to Genewiz for sequencing. The presence or absence of our mutation of interested was identified using the program Sequencher.

Phage induction

An overnight culture was grown from the frozen glycerol stock of our HK97 delta domain mutant lysogen. The overnight was diluted 1:60 into a 30 mL of LB and grown at 37°C at 300 rpm until the OD₅₅₀~0.2. Cells were were spun down at room temperature at 6700 rpm for 7 minutes and resuspended in 30 mL phage induction buffer (10 mM Tris-HCl pH 7.5, 5 mM MgSO₄). 5 mL of sample were aliquoted into plates and exposed to UV light for 0, 5, or 10 seconds. 5 mL of prewarmed 2x LB was added to each plated and moved to flasks. They were shaken (in the dark) at 37 C for 2 hours. A few drops of chloroform was added after 1.5 hours to aid lysis. The cell debris is spun down at 7000 rpm for 10 minutes (I used the 15 mL centrifuge tubes from Corning®). The supernatants were used in plaque assays on LE392 cells.

Mutant	WT complementation	Protease amber complementation	MCP amber complementation
WT	1	1	1
S2C	1	1	1
L6R	1	1	0.5
Q8A	1	1	0.1
I11F	1	1	1
E12A	1	1	1
E28A	1	1	1
I29F	1	1	0.1
K37A	1	1	1
Q38P	1	1	0.0001
Q38A	1	1	1
Q40A	1	1	1
S41F	1	1	1
L43R	1	0.01	0.001
M44K	1	1	1
Q47A	1	0.05	0.0001
E48A	1	1	1
T51A	1	1	1
G54Y	1	0.1	0.001
T55I	1	1	1
T55F	1	1	1
F58L	1	1	0.001
D59A	1	0.1	0.001
E61A	1	0.1	0.001
Q62A	1	0.1	0.001
K63A	1	0.001	0.001
A65E	1	1	0.0001
S66F	1	1	0.01
F77S	1	0.1	0.001
E83A	1	1	1
L85R	0.1	0.0001	0.001
L85V	1	1	1
S88C	1	1	1
W89A	0.1	0.0001	0.001
W89Y	1	1	1
D90A	0.1	0.001	0.001
D90G	1	0.01	0.0001
D90E	1	0.5	0.01
K92A	1	0.5	0.01
K92N	1	0.5	0.001
F96L	1	0.01	0.001
F96Y	1	1	1

Table 1. Complementation Spot Test Results

Mutant	WT complementation	Protease amber complementation	MCP amber complementation
pNoDelta2	1	n/a	0.0001
Del1 (4-13)	1	1	0.01
Del2 (4-29)	1	1	0.005
Del3 (4-50)	1	1	0.001
Del4 (4-62)	1	1	0.001
Del 1 st Hinge	1	1	0.001
Del 2 nd Hinge	0.1	0.01	0.001
LIM 20	1	1	0.01
LIM 33	1	1	0.01
LIM 49	1	0.01	0.0001
LIM 82	1	0.0001	0.001

Table 1. Complementation Spot Tests Results, continued

Mutant	WT phage complementation	Portal amber Complementation	Protease amber complementation	MCP amber complementation
WT	1	1	1	1
A65E (gp5)	1	n/a	1	.0001
D135G (gp3)	1	0.1	1	1
D135G (gp3)/ A65E (gp5)	1	1	1	1

Table 2. Complementation Spot Tests of A65E and D135G

Mutant	Spontan- eous XL/tubes	MCP Cleavage	Agarose gel results	Spot test –Does it complement?		Electron Micrograph Results	Portal Incorporation	Inactive protease binding
				mcp amber	protease amber			
S2C	No	Yes	Prohead, Head	Yes	Yes	Proheads, Heads		
L6R	No	No	Prohead, Head	½ log↓	Yes	Proheads	Yes	Yes
Q8A	No	No	Prohead, Head	1 log↓	Yes	Proheads	Yes	Yes
I11F	No	No	Prohead, Head	Yes	Yes	Proheads	Yes	Yes
E12A	No	No	Prohead, Head	Yes	Yes	Proheads	Yes	Yes
Q20A	No	No	Prohead, Head	Yes	Yes	Proheads	Yes	Yes
E28A	Yes	partial	Prohead, Head	Yes	Yes	Proheads, Heads		
I29F	No	No	Light Prohead band	1 log↓	Yes	Proheads	Yes	No
K37A	No	Mostly	Prohead, Head	Yes	Yes	Proheads, Heads		
Q38P	No	No	Prohead	4 log↓	Yes	Proheads	Little	Little
Q38A	A little	Yes	Prohead, Head	Yes	Yes	Proheads, Heads		
Q40A	A little	Yes	Prohead, Head	Yes	Yes	Proheads, Heads		
S41F	No	Partial	Prohead, Head	Yes	Yes	Proheads, Heads		
L43R	No	No	Prohead	3 log↓	2 log↓	Proheads, few tubes	No	No
M44K	No	Mostly	Prohead, Head	Yes	Yes	Proheads, Heads		
Q47A	No	No	Prohead, caps	4 log↓	1½ log↓	Proheads	Little	No
E48A	No	Partial	Prohead, Head	Yes	Yes	Proheads, Heads		
T51A	No	Mostly	Prohead, Head	Yes	Yes	Proheads, Heads		
G54Y	No	Partial	Prohead, Head	3 log↓	1 log↓	Proheads, Heads	Partial	Yes
T55I	No	Mostly	Prohead, Head	Yes	Yes	Proheads, Heads		
T55F	No	No	Prohead, Head	Yes	Yes	Proheads, Heads	Yes	Yes
F58L	No	Mostly	Prohead, head	3 log↓	Yes	Proheads, Heads	Partial	Yes

D59A	No	Mostly	Prohead, head	3 log↓	1 log↓	Proheads, Heads	Little	Yes
E61A	No	No	Prohead	3 log↓	1 log↓	Proheads	Little	No
Q62A	No	Yes	Prohead, Head	3 log↓	1 log↓	Proheads, Heads	No	Yes
K63A	No	No	Prohead	3 log↓	3 log↓	Proheads	Yes	Yes
A65E	No	Mostly	Prohead, Head	4 log↓	Yes	Proheads, Heads	No	Yes
S66F	No	Yes	Prohead, Head	2 log↓	Yes	Proheads, Heads	Partial	Yes
F77S	Yes	No	Light Prohead band	3 log↓	1 log↓	Abnormal round structures		
E83A	No	Mostly	Prohead, head	Yes	Yes	Proheads, Heads		
L85R	Yes	No	None	3 log↓	4 log↓	Abnormal round structures, some smaller than normal sized capsids		
L85V	Yes	Partial	Little Prohead, Head	Yes	Yes	Proheads, tubes, abnormal		
S88C	No	Partial	Prohead, Head, capsomer	Yes	Yes	Proheads, Heads		
W89A	Yes	No	None	3 log↓	4 log↓	Round, abnormal open and closed structures, tubes - some kinked		
W89Y	Yes	Partial	Little Prohead, Head	Yes	Yes	Proheads, Heads, tubes, abnormal	Yes	Yes
D90A	Yes	No	None	3 log↓	3 log↓	Round, abnormal structures, mostly closed, tubes - some kinked		
D90G	Yes	No	None	4 log↓	2 log↓	Round, abnormal mostly closed structures; some capsids; some tubes		

D90E	Yes	No	Light Prohead	2 log↓	½ log↓	Tubes, abnormal		
K92A	No	Partial	Prohead, Head, capsomers	2 log↓	½ log↓	Mostly Proheads and Heads, some partially assembled capsids, few tubes	Yes	Yes
K92N	No	Partial	Prohead, Head, capsomer	3 log↓	½ log↓	Mostly Proheads and Heads, some partially assembled capsids, few tubes		
F96L	Yes	No	None	3 log↓	2 log↓	Some round, abnormal closed structures, mostly closed tubes (longer than other mutants)		
F96Y	No	Yes	Prohead, Head	Yes	Yes	Proheads, Head		
LIM 20	No	No	Prohead	2 log↓	Yes	Prohead	Yes	No
LIM 33	No	No	None	2 log↓	Yes	Some small round structures, very few capsid like particle		
LIM 49	Yes(light)	No	Prohead (shifted slower)	4 log↓	2 log↓	Proheads	No	No
LIM 82	Yes	No	None	3 log↓	4 log↓	Round, abnormal structures, clumps together		
pNoDelta1	No	n/a	None	3 log↓	n/a	Inclusion bodies		
pNoDelta2	No	n/a	None	4 log↓	n/a	Inclusion bodies		
Del1(4-13)	No	No	Prohead	2 log↓	Yes	Proheads	Yes	No
Del2 (4-29)	No	No	None	2½ log↓	Yes	Inclusion bodies		
Del3 (4-50)	No	No	None	3 log↓	Yes	Inclusion bodies		
Del4 (4-62)	No	No	None	3 log↓	Yes	Inclusion bodies		

Del1 st hinge (S31-S36)	No	No	None	3 log↓	Yes	Inclusion bodies		
Del2 nd hinge (G67-E73)	Yes (light)	No	Prohead (runs faster) light normal Prohead band, caps in sup	3 log↓	2 log↓	Few Proheads, mostly smaller than normal capsids (T=4), many abnormal structures	No	Partial

Table 3. Mutant Summary Table

Extra Notes:

Del1: requires portal for efficient assembly- almost every particle produced contains portal

L6R produced more dimers than portal-less proheads when expressed with portal and inactivated protease on agarose gel

LIM 20 + portal: 2 bands in gradient- top band is proheads, bottom band is a little bit of proheads and trypsin like cleavage products (24 and 18 kDa) S66F also showed digestion products (and ran slightly faster than others in agarose gel when expressed with portal and inactivated protease)

K63A: only cleaves in the presence of the portal even though it can bind protease no matter if portal is present or not

Does portal enhance processing/assembly? E363H and E363A are cleavage defect mutants, H makes tubes along with proheads. With the addition of the portal, E363A makes mostly cleaved proheads, but E363H still only has partial cleavage. Both are able to bind the portal.

Del2ndhinge makes smaller than normal capsids (T=4) and some T=7 and mostly monsters

K92A has partial cleavage defect. Incorporates portal and protease at higher than WT levels. In the presence of portal and inactivated protease, K92A is no longer able to produce proheads or heads and instead produces partially assembled shells (no closed capsids) and possibly a large number of portals (small round things visible in EM). Overexpression of portal causing assembly defect?

APPENDIX A

A.1 INTERESTING AND DIFFICULT TO EXPLAIN DELTA DOMAIN MUTATION K92A

A few mutations studied in the delta domain gave very interesting phenotypes that are difficult to explain. K92A was a useful control because it caused a cleavage defect. However, studies of K92A with the portal showed unexpected and difficult to explain results to show how important the delta domain is in capsid assembly and protein incorporation. K99E, K103L, and the double mutant K99E/K103L produced results that seem contradictory with regards to complementation test data but may show us that there is a particular order to the delta domain cleavage process.

K92A has a cleavage defect

Residue K92 resides in the C-terminal end of the delta domain, near the end of the 3rd predicted helical region. This mutation was made because we hypothesized that it resided in the spoke densities which lie against the internal surface of the capsid. We thought this charged residue could be involved in the 3 point spoke interactions at the 3 fold and quasi 3 fold symmetry axes. K92 was mutated to an Alanine and tested in our miniprohead preps. On the agarose gel, K92A produced proheads, heads, and capsomers (Figure A-1a). The presence of capsomers in the agarose gel shows that either assembly is less efficient than WT, or that the proheads are less

stable than WT and fall apart easily, or both. On the SDS gel, K92A showed partial cleavage as there are uncleaved and cleaved mcp bands present (Figure A-1b). K92A was about one log down in both capsid gene and protease gene amber phage complementation, suggesting a slight defect in protein functionality (Table 1). Electron micrographs of the K92A PEG sample show heads and proheads, as expected from the gel data. There were also very rarely, abnormal tube structures (Figure A-1c). The fact that this mutant produces both cleaved and uncleaved mcp makes this a useful control for SDS gel assays. K92 was also mutated to the uncharged polar group, Asparagine. From the biochemical and spot tests, K92N is phenotypically equivalent to K92A (data not shown). Perhaps this mutation has a cleavage defect because it is defective in protease incorporation, or assembly has less efficient so that the protease has degraded before capsid assembly is complete. It is possible that this mutation has blocked an important cleavage site from being fully accessible to the protease.

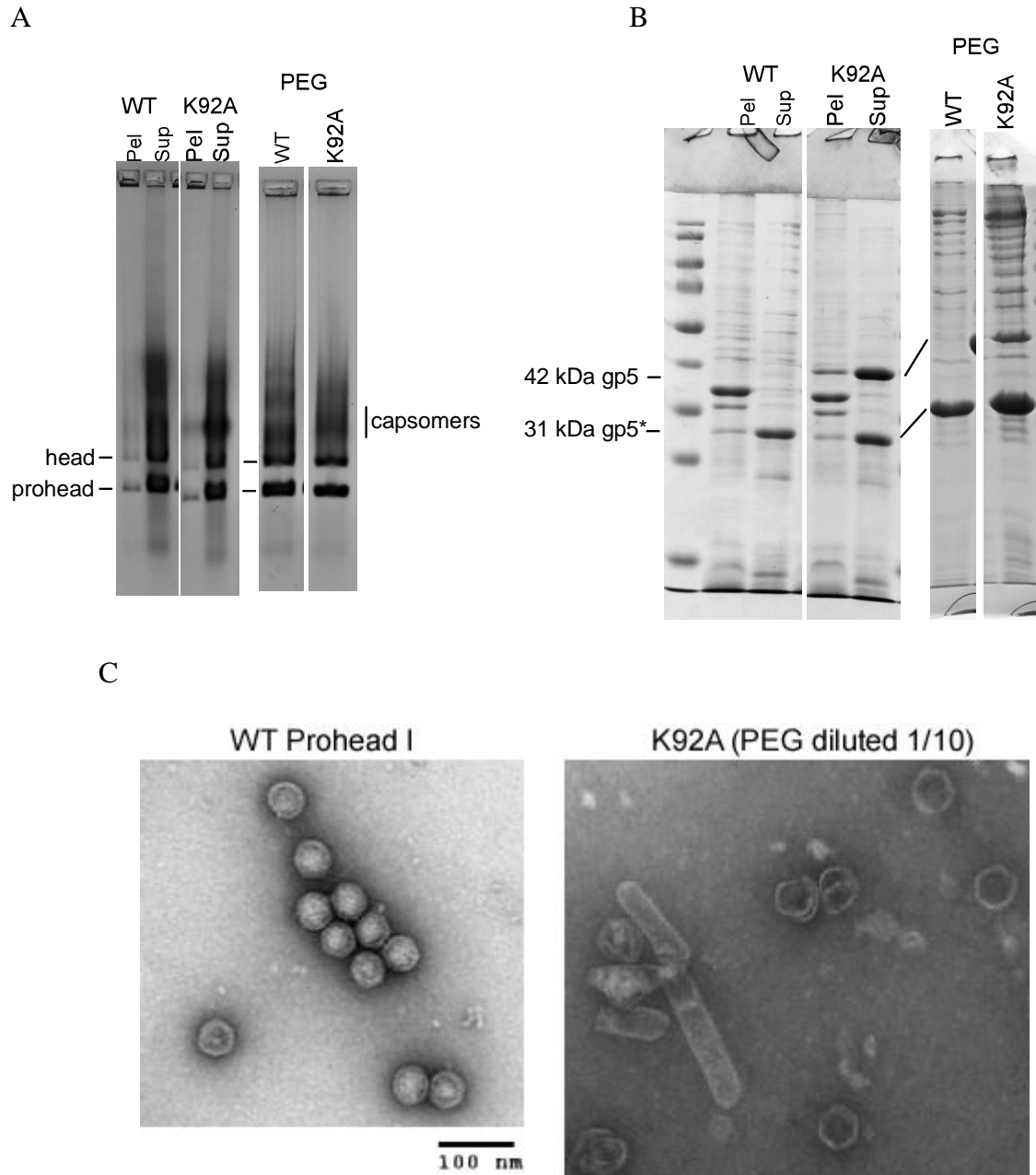


Figure A-1. K92A has a cleavage defect, and produces proheads, heads, and capsomers

A) Pellet, supernatant, and PEG samples were run on agarose gels along with WT controls. WT produced prohead and head bands. K92A produced proheads, heads, and capsomers. B) Samples were precipitated with 10% TCA, run on a 12% acrylamide gel, and stained with commassie. WT produced cleaved mcp while K92A produced both cleaved and uncleaved mcp bands. C) The K92A PEG sample was diluted with 1/10 1x calorimetry buffer and stained with 1% uranyl acetate for transmission electron microscopy. K92A produced proheads, heads, and few abnormal particles. WT Prohead I is shown as a control. Scale bar: 100 nm.

A.2 K92A INCORPORATES HIGHER LEVELS OF PORTAL AND PROTEASE

To further delve into the interesting properties of K92A, this mutation was sub-cloned into the portal and inactivated protease plasmid (pVP0 g4 H65A) and a miniprohead prep and ultracentrifuge purification was conducted to test for portal and protease incorporation. Figure A-2a shows the agarose gel results of the pellet, supernatant, and PEG fractions of WT and K92A. WT produced proheads and heads while K92A did not produce any prohead bands. Instead, there was a fuzzy band that is strongly present in the supernatant and PEG fractions. Usually, when we see this type of fuzzy band in the supernatant fraction, this denotes the presence of capsomers. However, this is unique in that a fuzzy band is in the PEG fraction. Perhaps this is a combination of capsomers aggregated with abnormally assembled structures or abnormal assembly products. In the SDS gel, WT produced cleaved mcp while K92A produced uncleaved mcp as expected from the inactivated protease (Figure A-2b).

The PEG samples were further purified by pelleting in the ultracentrifuge and run on native and denaturing gels. On the agarose gels, K92A showed a weak band that ran slightly slower than where prohead dimers run. There was also a slight smear above that band in the gel (Figure A-2c). In the SDS gel, the Prohead I and portal control produced portal, uncleaved mcp, and protease bands. K92A produced strong portal and protease bands. This mutant did not produce much capsid protein, so for the amount of capsid protein present, there is a high proportion of portal protein present (Figure A-2d). It is possible that the mutant assemblies are incorporating more than one portal, indicating the interaction between the capsid protein and portal have been altered.

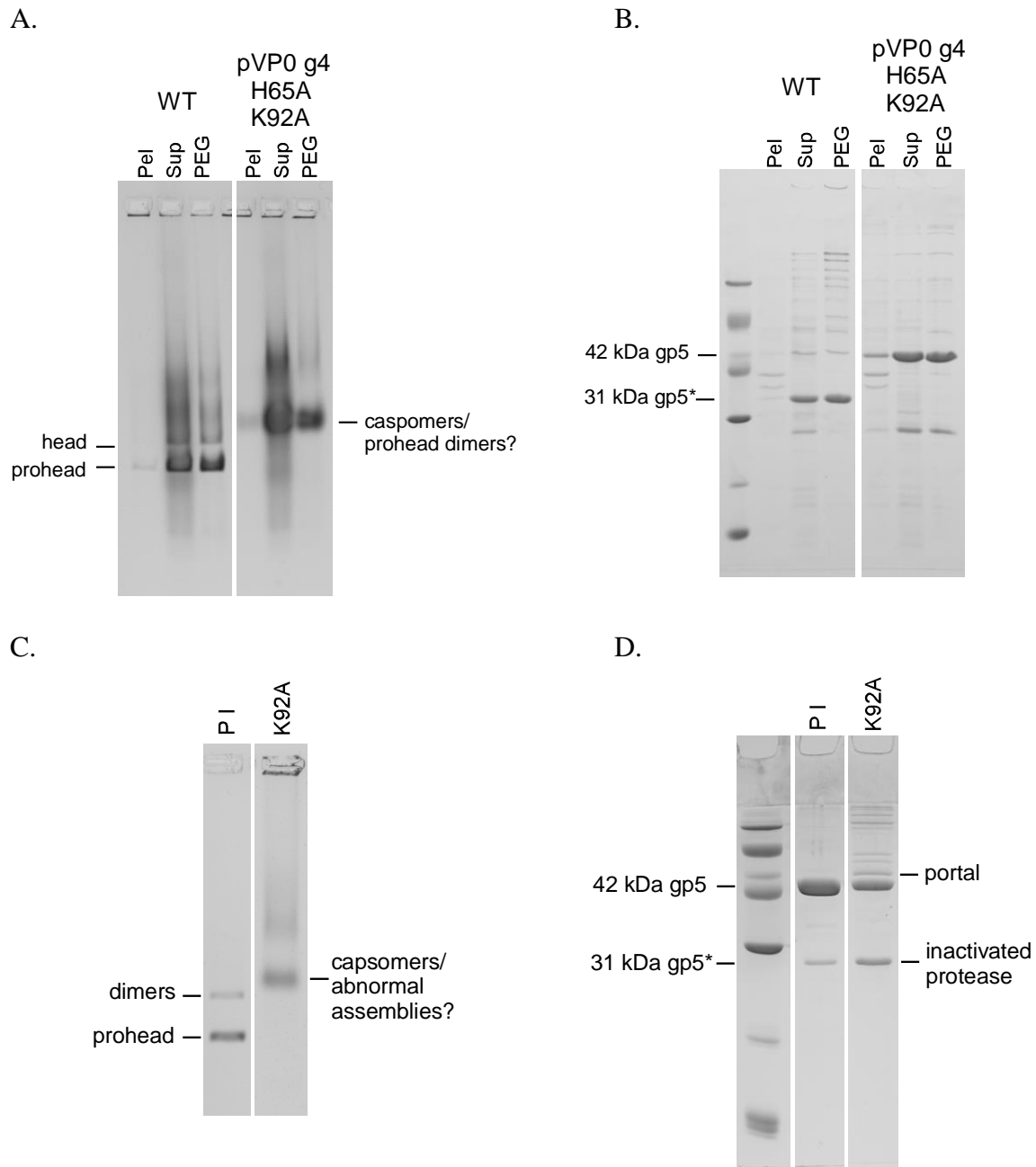


Figure A-2. K92A is able to incorporate the portal and protease

A). Pellet, supernatant, and PEG samples were loaded on a 0.9% native agarose gel. WT produced proheads and heads. K92A produced capsomers in the supernatant fraction and a fuzzy capsomer-like band in the PEG fraction. B) Pellet, supernatant, and PEG samples were run on a SDS gel. WT fractions show cleaved mcp. K92A fractions show uncleaved mcp, which was expected as the protease is inactivated. C) The PEG sample from the K92A miniprohead prep was ultracentrifuged for further purification. PI containing portal was used as a control. On a 0.9% agarose gel, PI produced proheads and prohead dimers. K92A produced a slightly fuzzy band that runs slightly slower than WT prohead dimers. D) Samples from Figure B-7C were run on a SDS gel. P I with portal produced portal, uncleaved mcp, and protease bands. K92A shows similar bands. However, for the amount of mcp present, it is expressing a much stronger portal band than the control.

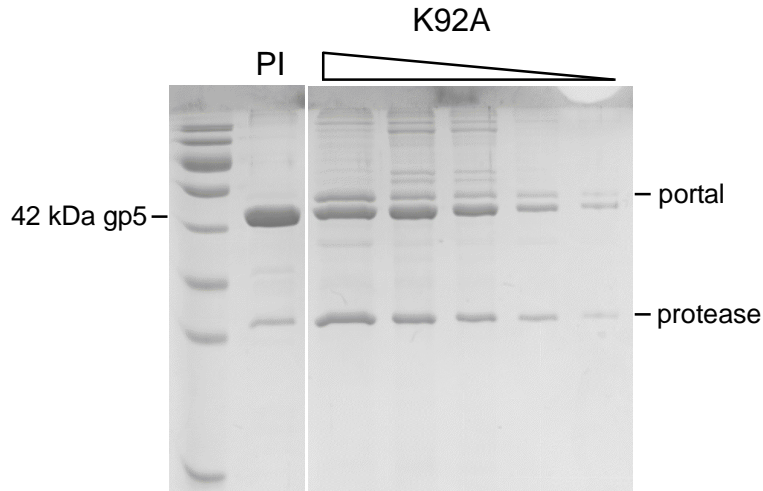


Figure A-3. Dilutions of K92A expressed with portal and inactivated protease

In order to quantify the amount of portal and protease present with the K92A assemblies, different amounts were loaded along with a WT Prohead I sample on a SDS gel. K92A does not produce as much capsid protein as WT, but these lower levels of gp5 are accompanied by higher than WT levels of portal and protease incorporation.

To study this interesting result further, I used gel band intensity analysis to compare the relative ratio of portal:mcp and protease:mcp between this mutant and WT. While this type of quantification is not always reliable, this will give us some information of the relative amount of portal proteins being incorporated into the capsid. A dilution series of this purified pVP0 g4 (H65A) K92A sample was run on a SDS gel for band quantification. A sample of pVP0 g4 (H65A) was loaded as a control (Figure A-3). The relative intensities of the portal, major capsid protein, and protease bands were quantified and are shown in Table 3. For the WT control, I halved the value for the mcp because not all of the WT capsids incorporate the portal from our expression preps (The quantified value is shown in parentheses). From our agarose gel assays, we estimate that about 50% of the capsids are portal-less (Duda, Maurer, Hendrix, unpublished).

In previous agarose gels I have shown that PI with portal and inactivated protease produces a prohead band, a prohead dimer, and sometimes a prohead trimer band. We estimate that about half of the proheads produced make up the dimer and trimer bands. If all the proheads incorporated the portal, we would expect to see only dimer and trimer bands. To estimate the amount of portal protein per capsid and protease protein per capsid, I took a ratio of their relative intensities. The ratios and the average ratio of the K92A mutant are shown in Table 4. From these relative intensities, K92A contains about 5-10x more portal than WT and about 5x more protease than WT.

We can assume that for WT the relative band intensities represent the relative copies of proteins in a capsid. For example, the WT value for the portal band (0.0242) represents 12 copies of the portal and the value of the mcp band (0.4304) represents 415 copies of the capsid protein. I used the 20 uL K92A lane to compare with WT because this sample had the closest value of relative mcp intensity as WT (0.4405 vs 0.4304) (shaded in Table 3). With K92A, we can assume that 0.4405 represents 415 copies of the mcp. Therefore, we can assume that the portal band intensity of 0.2203 represents 118 copies ($0.2203/0.0242 = 9.1$, $\sim 9 \times 12$ portal proteins = 118) of the portal. From the 20 uL sample, it seems that K92A contains 9 times the normal amount of portal protein. While these are simply crude estimations of the relative band intensities, we can see that K92A protein samples do indeed contain more portal and protease protein than WT.

Bands	WT (6 uL)	K92A (20 uL)	K92A (10 uL)	K92A (6 uL)	K92A (4 uL)	K92A (2 uL)
Portal	0.0242	0.2230	0.1599	0.1352	0.1917	0.1874
MCP	0.4304 (0.8608)	0.4405	0.5308	0.5481	0.4809	0.5097
Protease	0.1150	0.3364	0.3093	0.3167	0.3275	0.3029

Table 4. Relative Intensities of WT and K92A protein bands on SDS gel

	WT (6 uL)	K92A (20 uL)	K92A (10 uL)	K92A (6 uL)	K92A (4 uL)	K92A (2 uL)	K92A average
Portal: mcp	0.056	0.506	0.301	0.247	0.399	0.368	0.291
Protease: mcp	0.134	0.764	0.583	0.578	0.681	0.594	0.640

Table 5. Ratios of portal:mcp and protease:mcp for WT and K92A protein bands on SDS gel

The gel and band quantification data show that pVP0 g4 (H65A) K92A produces a larger amount of portal and protease proteins than WT. Does that mean that there each capsid has incorporated multiple portals? Can there be capsids with a portal at each vertex? What would we see under the TEM? Undiluted ultracentrifuge purified PEG samples were visualized using the electron microscope and the results were very interesting. Figure A-4 shows a comparison of K92A expressed without the portal (left image) and K92A with the portal and inactivated protease (right image). The presence of the portal and inactivated protease with this mutation has caused a drastic assembly defect. K92A with the portal and inactivated protease show very few proheads, but many capsomers, abnormal, partially assembled products (Figure A-4). Under higher magnification (86,000x), we can see very small round products, which we predict to be

portals (black arrows in Figure A-5). With this higher magnification we can also more clearly see 4 dotted cube like products that are commonly seen in our protein preps (black triangles in Figure A-5). These cubes are the E2 components of *E coli*. 2-oxoglutarate dehydrogenase or pyruvate dehydrogenase (Knapp et al. 1998; Hendle et al. 1995).

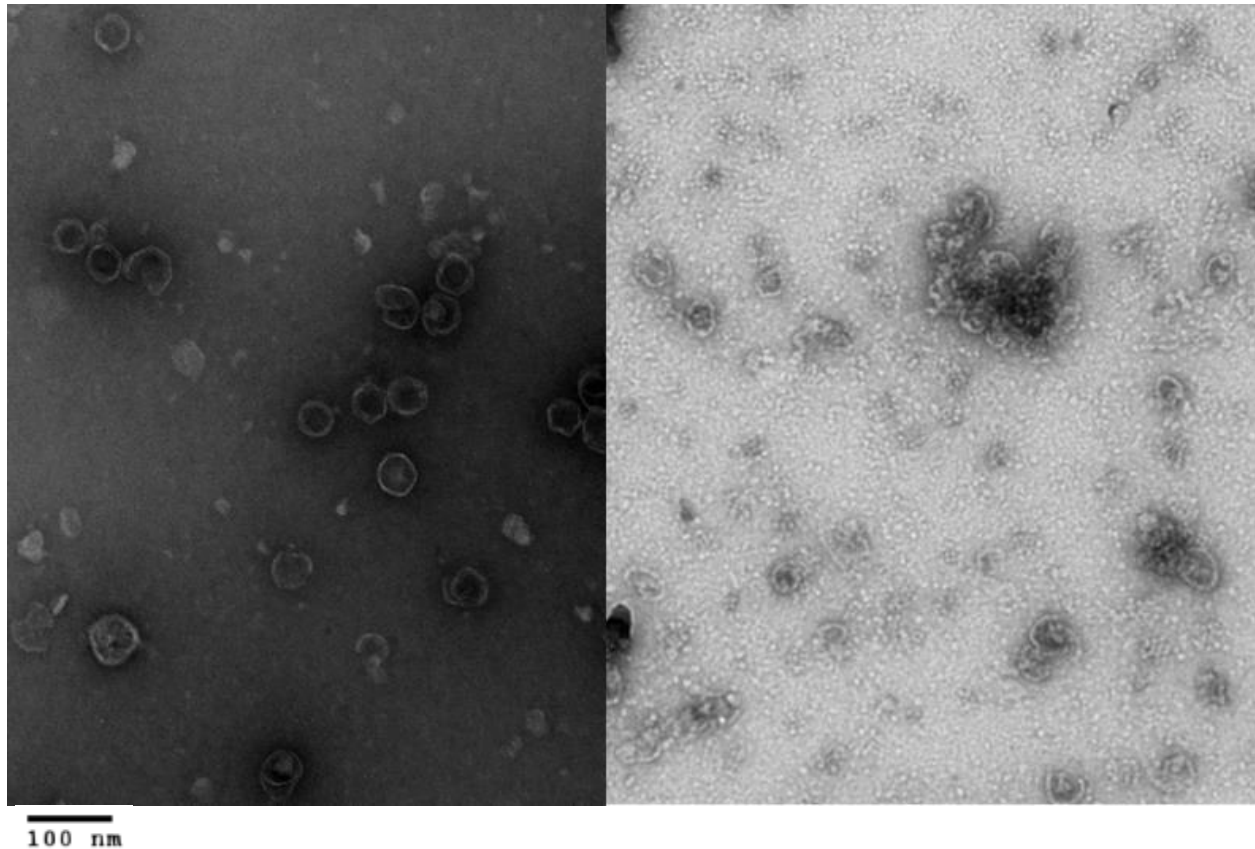


Figure A-4. EM images of pV0 K92A (left) and pVP0 g4 (H65A) K92A (right)

K92A expressed without the portal produces proheads and heads (left). When expressed with the portal and inactivated protease, there are no regular proheads formed. Instead, there were some irregular assemblies and broken shells. Samples were diluted 1/10 in 1x calorimetry buffer and stained with 1% uranyl acetate. Images were taken at 56,000x magnification.

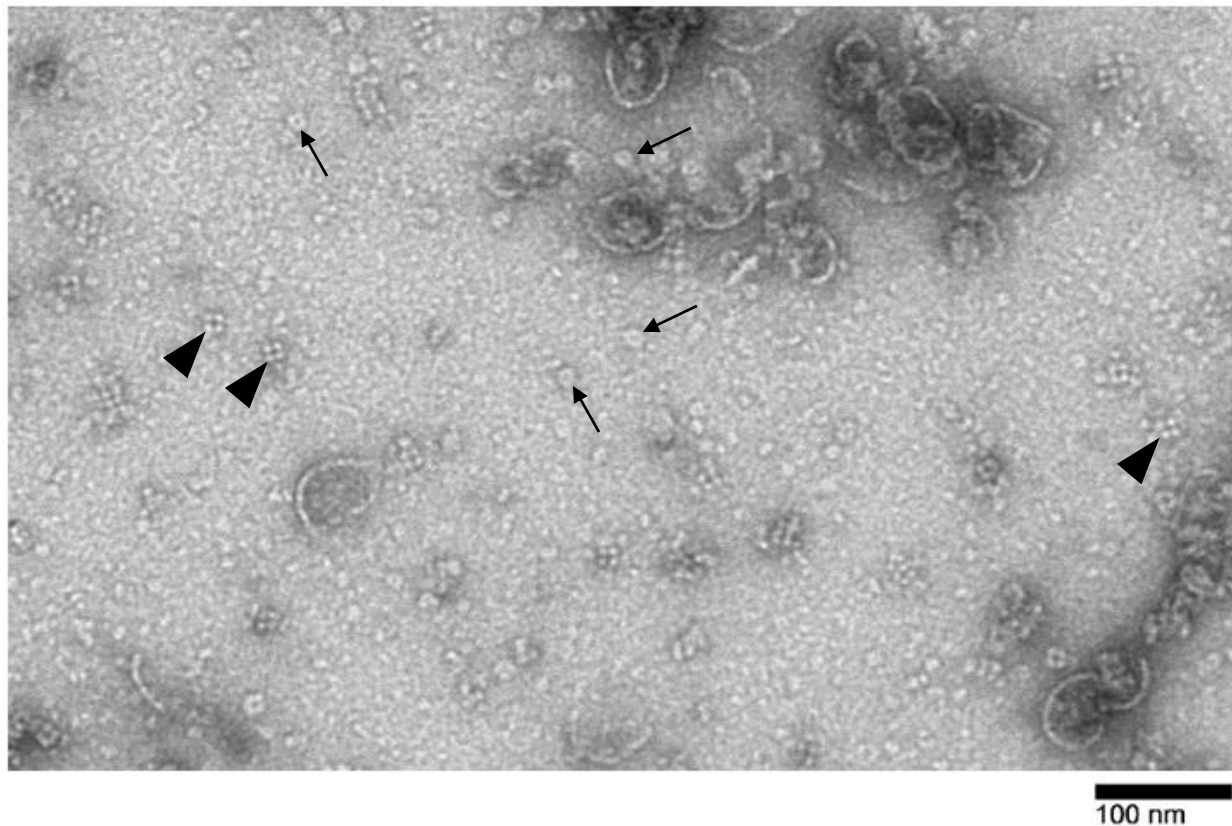


Figure A-5. Representative EM image of pVP0 g4 (H65A) K92A

With the addition of the portal and inactivated protease, K92A produces irregular assemblies and broken shells. This higher magnification image shows more of the smaller objects. The arrows point to small round proteins which we believe to be HK97 portals. The black triangles are pointing to the E2 components of *E. coli* 2-oxoglutarate dehydrogenase or pyruvate dehydrogenase. The sample was diluted 1/10 in 1x calorimetry buffer and stained with 1% uranyl acetate. Image taken at 86,000x magnification.

In HK97, overexpression of the portal can cause a loss in assembly efficiency (unpublished data, Duda and Maurer). K92A could be causing an overexpression of the portal, which is interfering with the nucleation event of capsid assembly. Perhaps capsids are beginning assembly around multiple portals, disrupting proper assembly, and causing the abnormal and partially assembled products visible in the EM. If this is the case, this shows that the balance of expressed capsid proteins is important for ensuring proper assembly. Is this mutation actually

causing more portal to be expressed from the plasmid? Or, are there really capsids with multiple portals which fall apart easily into what we visualize in the electron microscope? The images were taken about 3 days after the prep was made. It would be interesting to see what a fresh sample of pVP0 (g4 H65A) K92A looks like in the EM. Other delta domain mutations described earlier like E363A, K63A, and Del1 show that the portal can enhance capsid assembly and maturation.

To test if the presence of the portal could enhance K92A cleavage and assembly, this mutation was moved into a plasmid containing the portal and active protease. A miniprohead prep was conducted and pellet, supernatant, and PEG fractions were run on agarose and SDS gels. WT with portal was used as a control. On the agarose gel, K92A showed similar results as when it was expressed without the portal- it produced proheads, heads, and a fuzzy capsomer spot in the supernatant fraction (Figure A-6A). On the SDS gel, K92A produced cleaved and uncleaved mcp (Figure A-6B). For this cleavage defect mutant, the portal does not aid in capsid maturation. Complementation tests also show that there was no effect with the presence of the portal, this mutant is still slightly defective in protein functionality.

These assays show that the inactivated protease has an interesting effect on assembly. One future test would be to express K92A with the inactivated protease and no portal to see if the protease is incorporated when no portal is present. This would show if there is a dependence of protease incorporation on the presence of the portal. Also, if there is no portal expressed with K92A, would the abnormal and partial assemblies still be made? Somehow, the combination of the portal, this delta domain mutation, and an inactivated protease causes this abnormal incorporation of portal and assembly defects.

Hopefully, further tests with this interesting mutation can explain why it has a cleavage defect, and also shed more light on how the delta domain affects and regulates assembly and the incorporation of proteins into the growing capsid.

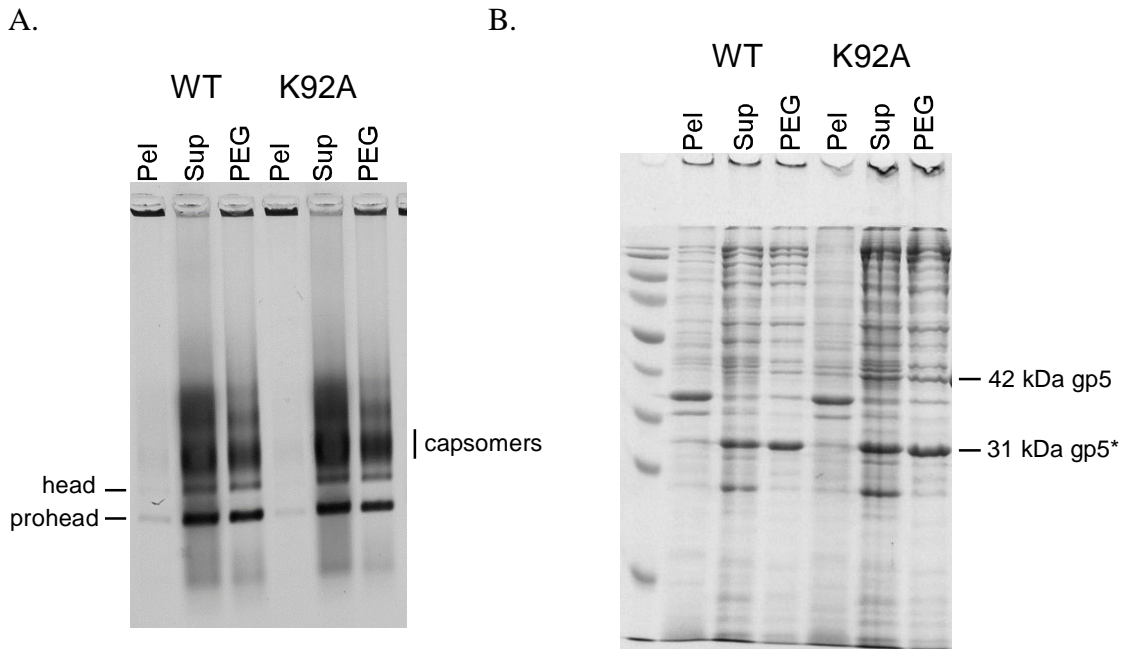


Figure A-6. Miniprohead prep results of K92A expressed with portal (pVP0 K92A)

WT with portal (pVP0) was used as a control. A) Pellet, supernatant, and PEG samples were run on a 0.9% agarose gel. WT produced proheads and heads. K92A produced proheads, heads, and a capsomer fuzzy spot in the supernatant fraction. B) On the SDS gel, WT produced cleaved 31 kDa mcp whereas K92A produced cleaved and uncleaved mcp. These results were similar to K92A expressed without the portal. The presence of the portal does not enhance capsid processing and maturation for this mutation.

APPENDIX B

B.1 STABILIZING THE DELTA DOMAIN

The delta domain is less ordered than the rest of the capsid protein, which has made visualization difficult. If we can stabilize the delta domain using disulfide bonds, we may be able to visualize more of the delta domain and the possible conformations it can make. There are 10 Serines in the delta domain: S2, S14, S31, S36, S41, S53, S66, S76, and S88. These residues can be mutated to cysteines and the presence of thiol (-SH) groups in these mutants allows the formation of disulfide bonds that would crosslink the delta domain. This would theoretically stabilize the domain and possibly allow us to visualize more of protein. From this, we could learn more about how delta domains interact with neighboring delta domains. These disulfide bonds would mostly likely occur between residues that would normally be able to make contact in the WT capsid.

Brandi Baros, a previous graduate student made 8 of 10 serine to cysteine mutants and knocked out the protease gene for mutants S41C, S66C, S76C, and S78C. Her experiments suggested that disulfide bonds were forming in some of these mutant Prohead I samples (Baros 2002). Other members of the lab created more protease knockouts of these S to C mutants and found that S41C Prohead I particles did not dissociate unless in the presence of a reducing agent (Duda, unpublished). Ying Sheng, a rotation student, conducted more in depth experiments with these 8 mutants, testing capsid stability. As mentioned earlier, Prohead I is not very stable and

can dissociate into capsomers. Mutant proheads were tested for their ability to dissociate or stabilize the capsid. Previous HK97 studies have shown that glucose can dissociate Proheads into capsomers. Dithiothreitol (DTT), a reducing agent, can counteract disulfide bonds, and in combination with glucose, dissociates Proheads into capsomers. By comparing the presence of proheads or capsomers in these mutants, we can determine if any particular disulfide bond is between delta domains and/or within one delta domain. Ying's studies confirmed that S41C stabilized the capsid because it could only be dissociated in the presence of 1 M DTT. She found similar results with S76C and S78C. Ying had also made S2C, and I tested this mutant and found that it did not increase capsid stabilization. To continue her project, I made S88C and studied its effect on capsid stability. Figure B-1A and B show the results of miniprohead prep results of S88C. S88C shows WT like phenotypes (is able to cleave mcp and produce proheads and heads). S88C was also able to complement phage with an amber mutation in the capsid gene like WT. The presence of the cysteine did not affect the phenotype.

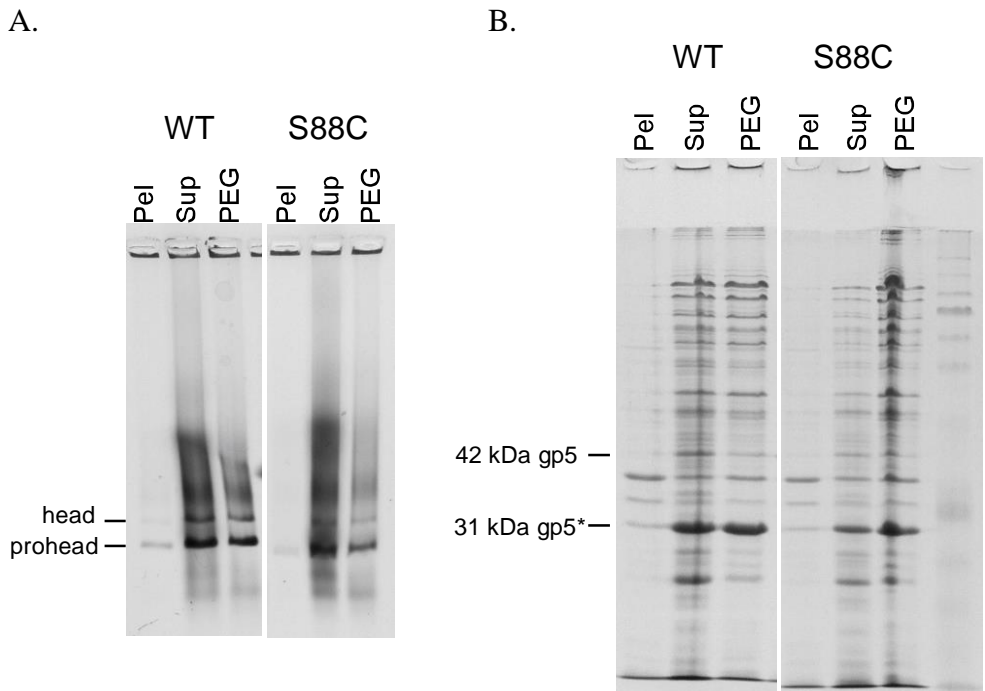


Figure B-1. Miniprohead prep of S88C shows WT like phenotypes

Pellet, supernatant, and PEG samples were run on a 0.9% agarose gel, and 12% low cross-linking SDS gel. A) On the agarose gel, S88C showed WT like phenotypes and produced proheads and heads. B) On the SDS gel, S88C produced cleaved mcp like WT.

Native agarose gels are able to show if there are disulfide bonds between capsomers. If there are proheads present, then we can assume that a disulfide bond is present between capsomers, preventing their dissociation into capsomers. Figure B-2 shows WT, S41C, and S88C in the presence of glucose with or without DTT. Untreated PI is as a control. The left gel shows samples after 3.5 hours; the right gel shows samples after 24 hours. WT Prohead I dissociates into capsomers when mixed with glucose (lanes 1, 2). S41C and S88C are stable in glucose, even after 24 hours (lanes 2, 3, 10, 11). With the addition of DTT, S41C shows some dissociation after

3.5 hours (lane 6) while S88C is mostly dissociated after 3.5 hours (lane 7). After 24 hours, both S41C and S88C have dissociated into capsomers (lanes 13, 14). Though S88C is not as stable as S41C, this mutation is a promising candidate in stabilizing the delta domain for visualization. This showed that S88C makes disulfide bonds between neighboring capsomers.

Similarly, native acrylamide gels that visualize HK97 pentamers and hexamers and can show if there are disulfide bonds between capsomers. If there is a disulfide bond between capsomers, then the capsid would be more resistant to dissociation and you would not detect hexamer and pentamer bands. Figure B-3 shows native samples in glucose with and without the addition of DTT. A 6% native polyacrylamide gel was used. WT PII is used as a control. PII is stable and resistant to dissociation, so no hexamers or pentamers is present with this sample. Without DTT, S41C and S88C proheads were intact. With DTT, S41C and S88C dissociated into hexamers and pentamers. This native gel provided more support that S88C forms disulfide bonds between capsomers.

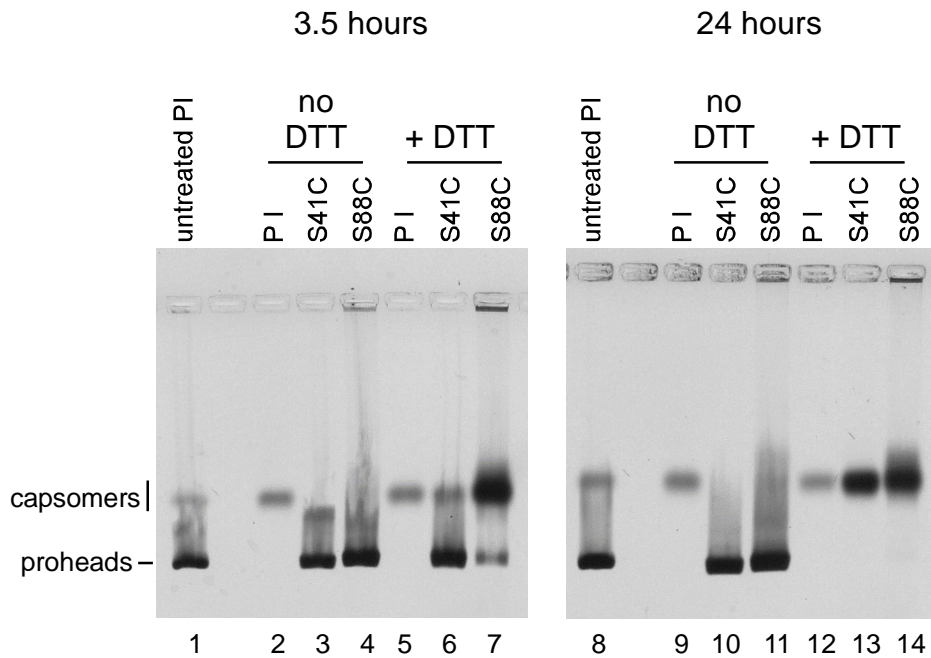


Figure B-2. S88C forms disulfide bonds in delta domains between capsomers, which only allows capsid dissociation in the presence of DTT.

Prohead samples were incubated for 3.5 (left gel) or 24 (right gel) hours at room temperature in 20% glucose \pm 1 M DTT. Untreated PI is shown as a control. Prohead I particles dissociate into capsomers in the presence of glucose (lanes 2, 9). S41C has been shown to stabilize the capsid and was used as a positive control. With glucose, S41C and S88C produced proheads (lanes 3, 4, 10, 11). With the addition of DTT, some of the S41C proheads began to dissociate into capsomers (lane 6) after 3.5 hours and they were completely dissociated after 24 hours (lane 13). S88C was mostly dissociated after 3.5 hours with DTT (lane 7) and was completely dissociated after 24 hours (lane 14). S88C is more stable than S41C, which is more stable than WT Prohead I.

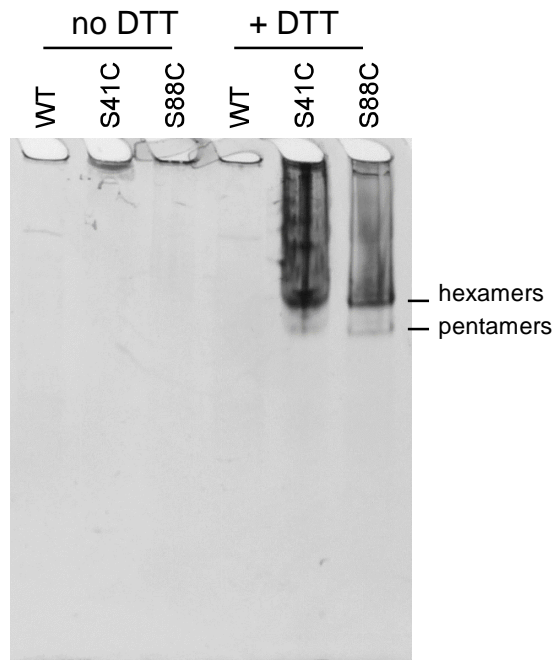


Figure B-3. Testing for prohead dissociation with or without DTT

Samples incubated with or without 1 M DTT were run on a 6% native polyacrylamide gel (with no top stack). WT PII is used as a negative control. Incubation with glucose and no DTT did not dissociate the proheads. Only when DTT was added did the capsids dissociate into hexamers and pentamers. This showed that there is some stability with these mutations due to disulfide bonds forming in delta domains between capsomers.

Non-reducing acrylamide gels show HK97 mcp and linked mcp in dimers or higher order associations and can be used to determine if there are delta domain disulfide bonds between and within capsomers. The presence of mcp dimers or higher order associations would indicate a disulfide bond between capsomers. S41C and S88C produced mcp dimers (Figure B-4). S41C produced a stronger dimer band, while S88c produced a weaker dimer band that ran slightly slower. S88C is able to form capsid protein dimers, indicating that this mutation has caused the formation of disulfide bond between neighboring capsomers that have stabilized the capsid.

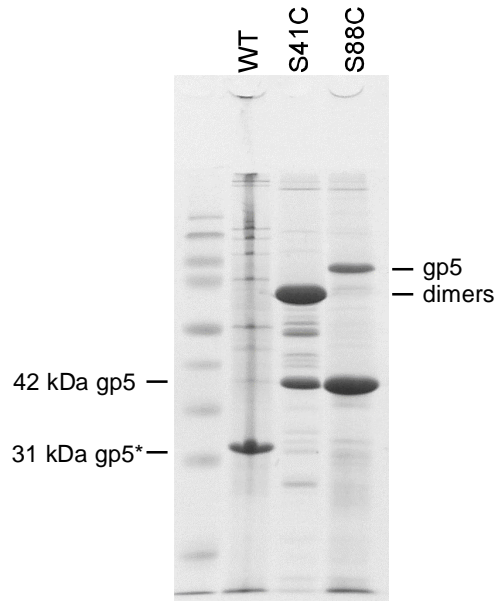


Figure B-4. S88C can form major capsid protein dimers due to disulfide bonds between delta domains

WT cleaved mcp was used as a control. Samples were prepared in non-reducing buffer and run on a 12% non-reducing acrylamide gel. WT produced cleaved mcp. S41C and S88C both produced uncleaved mcp and mcp dimers in the gel. The S41C dimer band is stronger than S88C dimer band. The S88C dimer ran at a higher molecular weight than S41C. The presence of dimers again show that capsid subunits are linked together by disulfide bonds between delta domains.

The Del 2nd Hinge mutant was able to stabilize the delta domain to create the strong towers and bridge densities inside the capsid. However, this mutant produced capsomers, indicating a stability issue. It is possible to combine this deletion mutation with a S to C mutation, which would prevent the dissociation of proheads. This may help resolve a better density map of the capsid and the delta domains. The S41C Prohead I has been reconstructed and surprisingly the delta domains have adopted a different conformation than WT. From the map, it seems that the delta domains between hexamers and pentamers are interacting to create start-like patterns inside the capsid (Sheng, Alasdair, Conway, Duda, Hendrix, unpublished). It would be very interesting to reconstruct the S88C Prohead I and visualize the new conformation that the delta domains have made.

BIBLIOGRAPHY

- A.Thuman-Commike, Pamela, Justine A. Malinski, Jonathan King, Wah Chiu, and Barrie Greene. 1998. "Role of the Scaffolding Protein in P22 Procapsid Size Determination Suggested by T=4 and T=7 Procapsid Structures." *Biophysical Journal* 74: 559–68.
- Ackermann, H W. 2006. "Classification of Bacteriophages." In *The Bacteriophages (2nd Ed.)*, edited by Richard Calendar, 8–16. New York: Oxford University Press.
- Adereth, Yair, Kristen J. Champion, Tien Hsu, and Vincent Dammai. 2005. "Site-Directed Mutagenesis Using Pfu DNA Polymerase and T4 DNA Ligase." *Biotechniques* 38 (6): 864–68.
- Akita, Fusamichi, Khoon Tee Chong, Hideaki Tanaka, Eiki Yamashita, Naoyuki Miyazaki, Yuichiro Nakaishi, Mamoru Suzuki, et al. 2007. "The Crystal Structure of a Virus-like Particle from the Hyperthermophilic Archaeon *Pyrococcus Furiosus* Provides Insight into the Evolution of Viruses." *Journal of Molecular Biology* 368 (5): 1469–83. doi:10.1016/j.jmb.2007.02.075.
- Baros, Brandi. 2002. "Thesis." University of Pittsburgh.
- Bazinet, C, and J King. 1988. "Initiation of P22 Procapsid Assembly in Vivo." *Journal of Molecular Biology* 202 (1): 77–86. doi:10.1016/0022-2836(88)90520-7.
- Bazinet, Christopher, and Jonathan King. 1985. "The DNA Translocating Vertex of dsDNA Bacteriophage." *Ann. Rev. Microbiol.* 39: 109–29.
- Benevides, James M., Priya Bondre, Robert L. Duda, Roger W. Hendrix, and George J. Thomas. 2004. "Domain Structures and Roles in Bacteriophage HK97 Capsid Assembly and Maturation." *Biochemistry* 43 (18): 5428–36. doi:10.1021/bi0302494.
- Bochner, B. R., H. C. Huang, G. L. Schieven, and B. N. Ames. 1980. "Positive Selection for Loss of Tetracycline Resistance." *Journal of Bacteriology* 143 (2): 926–33.
- Casjens, Sherwood. 1997. "Principles of Virus Structure, Function, and Assembly." In *Structural Biology of Viruses*, edited by W. Chiu, R. M. Burnett, and R L Garcea, 3–37. Oxford University Press.

- Casjens, Sherwood, and Roger Hendrix. 1988. "Control Mechanisms in dsDNA Bacteriophage Assembly." In *The Bacteriophages SE - 2*, edited by Richard Calendar, 15–91. The Viruses. Springer US. doi:10.1007/978-1-4684-5424-6_2.
- Caspar, D, and A Klug. 1962. "Physical Principles in the Construction of Regular Viruses." *Cold Spring Harb. Symp. Quant. Biol.* 27: 1–24.
- Cerritelli, M E, and F W Studier. 1996. "Assembly of T7 Capsids from Independently Expressed and Purified Head Protein and Scaffolding Protein." *Journal of Molecular Biology* 258 (2): 286–98. doi:10.1006/jmbi.1996.0250.
- Cerritelli, Mario E, James F Conway, Naiqian Cheng, Benes L Trus, and Alasdair C Steven. 2003. *Virus Structure. Advances in Protein Chemistry*. Vol. 64. Advances in Protein Chemistry. Elsevier. doi:10.1016/S0065-3233(03)01008-8.
- Choi, Kyung H., Marc C. Morais, Dwight L. Anderson, and Michael G. Rossmann. 2006. "Determinants of Bacteriophage ϕ 29 Head Morphology." *Structure* 14 (11): 1723–27. doi:10.1016/j.str.2006.09.007.
- Conway, J F, W R Wikoff, N Cheng, R L Duda, R W Hendrix, J E Johnson, and a C Steven. 2001. "Virus Maturation Involving Large Subunit Rotations and Local Refolding." *Science (New York, N.Y.)* 292 (5517): 744–48. doi:10.1126/science.1058069.
- Conway, J.F., N Cheng, R.W. Hendrix, A.C. Steven, and R.L. Duda. 1995. "Proteolytic and Conformational Control of Virus Capsid Maturation: The Bacteriophage HK97 System." *Journal of Molecular Biology* 253: 86–99.
- Conway, James F., Naiqian Cheng, Philip D. Ross, Roger W. Hendrix, Robert L. Duda, and Alasdair C. Steven. 2007. "A Thermally Induced Phase Transition in a Viral Capsid Transforms the Hexamers, Leaving the Pentamers Unchanged." *Journal of Structural Biology* 158 (2): 224–32. doi:10.1016/j.jsb.2006.11.006.
- Court, Donald L., J A Sawitzke, and L C Thomason. 2002. "Genetic Engineering Using Homologous Recombination." *Annu. Rev. Genet.* 36: 361–88.
- Datsenko, Kirill A., and Barry L. Wanner. 2000. "One-Step Inactivation of Chromosomal Genes in Escherichia Coli K-12 Using PCR Products." *PNAS* 97 (12): 6640–45.
- Dhillon, E. K., T. S. Dhillon, a. N. Lai, and S. Linn. 1980. "Host Range, Immunity and Antigenic Properties of Lambdoid Coliphage HK97." *Journal of General Virology* 50 (1): 217–20. doi:10.1099/0022-1317-50-1-217.
- Dierkes, Lindsay E, Craig L Peebles, Brian a Firek, Roger W Hendrix, and Robert L Duda. 2009. "Mutational Analysis of a Conserved Glutamic Acid Required for Self-Catalyzed Cross-Linking of Bacteriophage HK97 Capsids." *Journal of Virology* 83 (5): 2088–98. doi:10.1128/JVI.02000-08.

- Ding, Yuan-hua, Roger W. Hendrix, John M. Rosenberg, and Robert L Duda. 1995. "Complexes between Chaperonin GroEL and the Capsid Protein of Bacteriophage HK97." *Biochemistry* 34: 14918–31.
- Dokland, T. 1999. "Scaffolding Proteins and Their Role in Viral Assembly." *Cellular and Molecular Life Sciences* 56: 580–603.
- Dokland, T, R A Bernal, A Burch, S Pletnev, B A Fane, and M G Rossmann. 1999. "The Role of Scaffolding Proteins in the Assembly of the Small, Single-Stranded DNA Virus phiX174." *J Mol Biol* 288 (4): 595–608. doi:S0022-2836(99)92699-2 [pii] 10.1006/jmbi.1999.2699.
- Dokland, T., and H. Murialdo. 1993. "Structural Transitions during Maturation of Lambda Capsid--Dokland and Murialdo, 1993.pdf." *Journal of Molecular Biology*. doi:10.1006/jmbi.1993.1545.
- Duda, R L, J Hempel, H Michel, J Shabanowitz, D Hunt, and R W Hendrix. 1995. "Structural Transitions during Bacteriophage HK97 Head Assembly." *Journal of Molecular Biology* 247 (4): 618–35. doi:10.1016/S0022-2836(05)80143-3.
- Duda, R L, K Martincic, Z Xie, and R W Hendrix. 1995. "Bacteriophage HK97 Head Assembly." *FEMS Microbiol Rev* 17 (1-2): 41–46. doi:0168-6445(94)00059-X [pii].
- Duda, R.L., K. Martincic, and R. W. Hendrix. 1995. "Genetic Basis of Bacteriophage HK97 Prohead Assembly." *Journal of Molecular Biology* 247 (4): 636–47. doi:10.1016/S0022-2836(05)80144-5.
- Duda, Robert L. 1998. "Protein Chainmail: Catenated Protein in Viral Capsids." *Cell* 94 (1): 55–60. doi:10.1016/S0092-8674(00)81221-0.
- Duda, Robert L., Bonnie Oh, and Roger W. Hendrix. 2013. "Functional Domains of the HK97 Capsid Maturation Protease and the Mechanisms of Protein Encapsidation." *Journal of Molecular Biology* 425 (15): 2765–81.
- Duda, Robert L., Philip D. Ross, Naiqian Cheng, Brian a. Firek, Roger W. Hendrix, James F. Conway, and Alasdair C. Steven. 2009. "Structure and Energetics of Encapsidated DNA in Bacteriophage HK97 Studied by Scanning Calorimetry and Cryo-Electron Microscopy." *Journal of Molecular Biology* 391 (2). Elsevier B.V.: 471–83. doi:10.1016/j.jmb.2009.06.035.
- Earnshaw, William, and S R Casjens. 1980. "DNA Packaging by the Double-Stranded DNA Bacteriophages." *Cell* 21 (2): 319–31. doi:10.1016/0092-8674(80)90468-7.
- Earnshaw, William, and Jonathan King. 1978. "Structure of Phage P22 Coat Protein Aggregates Formed in the Absence of the Scaffolding Protein." *J. Mol. Biol.* 126: 721–47.

- Effantin, G., P. Boulanger, E. Neumann, L. Letellier, and J. F. Conway. 2006. "Bacteriophage T5 Structure Reveals Similarities with HK97 and T4 Suggesting Evolutionary Relationships." *Journal of Molecular Biology* 361 (5): 993–1002. doi:10.1016/j.jmb.2006.06.081.
- Gan, Lu, James F. Conway, Brian a. Firek, Naiqian Cheng, Roger W. Hendrix, Alasdair C. Steven, John E. Johnson, and Robert L. Duda. 2004. "Control of Crosslinking by Quaternary Structure Changes during Bacteriophage HK97 Maturation." *Molecular Cell* 14 (5): 559–69. doi:10.1016/j.molcel.2004.05.015.
- Gertsman, Ilya, Kelly Lee, Jeffrey A. Speir, Robert L. Duda, Roger W. Hendrix, Elizabeth A. Komives, John E. Johnson, and Miklos Guttman. 2009. "An Unexpected Twist in Viral Capsid Maturation." *Nature* 458: 646–50.
- Greene, Barrie, and Jonathan King. 1996. "Scaffolding Mutants Identifying Domains Required for P22 Procapsid Assembly and Maturation." *Journal of Virology* 225: 82–96.
- Hagen, E W, B E Reilly, M E Tosi, and D L Anderson. 1976. "Analysis of Gene Function of Bacteriophage Phi 29 of Bacillus Subtilis: Identification of Cistrons Essential for Viral Assembly." *J. Virol.* 19 (2): 501–17. <http://jvi.asm.org/cgi/content/long/19/2/501>.
- Helgstrand, Charlotte, William R. Wikoff, Robert L. Duda, Roger W. Hendrix, John E. Johnson, and Larsy Liljas. 2003. "The Refined Structure of a Protein Catenane: The HK97 Bacteriophage Capsid at 3.44 Å Resolution." *Journal of Molecular Biology* 334 (5): 885–99. doi:10.1016/j.jmb.2003.09.035.
- Hendle, J., A. Mattevi, A.H. Westphal, J. Spee, A. de Kok, A. Teplyakov, and W.G. Hol. 1995. "Crystallographic and Enzymatic Investigations on the Role of Ser558, His610, and Asn614 in the Catalytic Mechanism of Azotobacter Vinelandii Dihydrolipoamide Acetyltransferase (E2p)." *Biochemistry* 34 (13): 4287–98.
- Hendrix, R W, and R L Garcea. 1994. "Capsid Assembly of dsDNA Viruses." *Virology* 5: 15–26. doi:10.1006/smvy.1994.1003.
- Hendrix, Roger W., and Sherwood Casjens. 2006. "Bacteriophage Λ and Its Genetic Neighborhood." In *The Bacteriophages (2nd Ed.)*, edited by Richard Calendar, 409–47. New York: Oxford University Press.
- Hohn, Barbara. 1983. "Sequences Necessary for Packaging of Bacteriophage Lambda DNA." *Proc. Natl. Acad. Sci.* 80: 7456–60.
- Homa, Fred L., and Jay C. Brown. 1997. "Capsid Assembly and DNA Packaging in Herpes Simplex Virus." *Reviews in Medical Virology* 7 (2): 107–22. doi:10.1002/(SICI)1099-1654(199707)7:2<107::AID-RMV191>3.0.CO;2-M.

- Howatson, A.F., and C.L. Kemp. 1975. "The Structure of Tubular Head Forms of Bacteriophage Lambda; Relation to the Capsid Structure of Petit Lambda and Normal Lambda Heads." *Virology* 67 (1): 80–84.
- Huang, Rick K., Reza Khayat, Kelly K. Lee, Ilya Gertsman, Robert L. Duda, Roger W. Hendrix, and John E. Johnson. 2011. "The Prohead-I Structure of Bacteriophage HK97: Implications for Scaffold-Mediated Control of Particle Assembly and Maturation." *Journal of Molecular Biology* 408 (3). Elsevier Ltd: 541–54. doi:10.1016/j.jmb.2011.01.016.
- Kellenberger, E. 1980. "Control Mechanisms in the Morphogeneses of Bacteriophage Heads." *Biosystems* 12 (3-4): 201–23.
- King, J, E V Lenk, and D Botstein. 1973. "Mechanism of Head Assembly and DNA Encapsulation in Salmonella Phage P22. II. Morphogenetic Pathway." *Journal of Molecular Biology* 80 (4): 697–731. doi:10.1016/0022-2836(73)90205-2.
- King, Jonathan, and Sherwood Casjens. 1974. "Catalytic Head Assembling Protein in Virus Morphogenesis." *Nature* 251 (5471): 112–19. <http://dx.doi.org/10.1038/251112a0>.
- Knapp, James E., David T. Mitchell, Mohammad A. Yazdi, Stephen R. Ernst, Lester J. Reed, and Marvin L. Hackert. 1998. "Crystal Structure of the Truncated Cubic Core Component of the Escherichia Coli 2-Oxoglutarate Dehydrogenase Multienzyme Complex." *J. Mol. Biol.* 280: 655–68.
- Laemmli, U K. 1970. "Cleavage of Structural Proteins during the Assembly of the Head of Bacteriophage T7." *Nature* 227: 680–85.
- Lata, R, J F Conway, N Cheng, R L Duda, R W Hendrix, W R Wikoff, J E Johnson, H Tsuruta, and a C Steven. 2000. "Maturation Dynamics of a Viral Capsid: Visualization of Transitional Intermediate States." *Cell* 100 (2): 253–63. doi:Doi 10.1016/S0092-8674(00)81563-9.
- Lee, Choong-sik, and Peixuan Guo. 1995. "Sequential Interactions of Structural Proteins in Phage phi29 Procapsid Assembly" 69 (8): 5024–32.
- Little, John W. 2006. "Gene Regulatory Circuitry of Phage λ ." In *The Bacteriophages (2nd Ed.)*, edited by Richard Calendar, 74–82. New York: Oxford University Press.
- Maloy, Stanley R, and William D Nunn. 1981. "Selection for Loss of Tetracycline Resistance by Escherichia Coli." *Journal of Bacteriology* 146 (2): 831.
- Marinelli, Laura J., Graham F. Hatfull, and Mariana Piuri. 2012. "Recombineering: A Powerful Tool for Modification of Bacteriophage Genomes." *Bacteriophage* 2 (1): 5–14. doi:10.4161/bact.18778.

- Moore, Sean D, and Peter E Prevelige. 2002. "Bacteriophage p22 Portal Vertex Formation in Vivo." *Journal of Molecular Biology* 315 (5): 975–94. doi:10.1006/jmbi.2001.5275.
- Morais, Marc C, Shuji Kanamaru, Mohammed O Badasso, Jaya S Koti, Barbara a L Owen, Cynthia T McMurray, Dwight L Anderson, and Michael G Rossmann. 2003. "Bacteriophage phi29 Scaffolding Protein gp7 before and after Prohead Assembly." *Nature Structural Biology* 10 (7): 572–76. doi:10.1038/nsb939.
- Mosig, Gisela, and Fred Eiserling. 2006. "T4 and Related Phages: Structure and Development." In *The Bacteriophages (2nd Ed.)*, edited by Richard Calendar, 225–67. New York: Oxford University Press.
- Murialdo, H, and a Becker. 1978. "Head Morphogenesis of Complex Double-Stranded Deoxyribonucleic Acid Bacteriophages." *Microbiological Reviews* 42 (3): 529–76.
- Newcomb, William W, and Jay C. Brown. 1991. "Structure of the Herpes Simplex Virus Capsid: Effects of Extraction with Guanidine-HCl and Partial Reconstruction of Extracted Capsids." *J. Virol.* 65: 613–20.
- Newcomb, William W, Fred L Homa, and Jay C Brown. 2005. "Involvement of the Portal at an Early Step in Herpes Simplex Virus Capsid Assembly Involvement of the Portal at an Early Step in Herpes Simplex Virus Capsid Assembly" 79 (16): 10540–46. doi:10.1128/JVI.79.16.10540.
- O'Callaghan, D. J., M. C. Kemp, and C. C. Randall. 1977. "Properties of Nucleocapsid Species Isolated from in Vivo Herpesvirus Infection." *J. Gen. Virol.* 37: 585–94.
- Oh, Bonnie, Crystal L. Moyer, Roger W. Hendrix, and Robert L. Duda. 2014. "The Delta Domain of the HK97 Major Capsid Protein Is Essential for Assembly." *Virology* 456-457 (1). Academic Press Inc.: 171–78.
- Olins, P. O., C. S. Devine, S. H. Rangwala, and K. S. Kavka. 1988. "The T7 Phage Gene 10 Leader RNA, a Ribosome-Binding Site That Dramatically Enhances the Expression of Foreign Genes in Escherichia Coli." *Gene* 73 (1): 227–35. doi:10.1016/0378-1119(88)90329-0.
- Olins, Peter, and Shaikat H Rangwala. 1989. "Derived from Bacteriophage T7 mRNA Acts ELS an Enhancer of Translation of the lac2 Gene in," 16973–76.
- Oppenheim, Amos B., Alison J. Rattray, Mikhail Bubunenko, Lynn C. Thomason, and Donald L. Court. 2004. "In Vivo Recombineering of Bacteriophage Lambda by PCR Fragments and Single-Strand Oligonucleotides." *Virology* 319 (2): 185–89. doi:10.1016/j.virol.2003.11.007.

- Parker, M H, W F Stafford, and P E Prevelige. 1997. "Bacteriophage P22 Scaffolding Protein Forms Oligomers in Solution." *Journal of Molecular Biology* 268 (3): 655–65. doi:10.1006/jmbi.1997.0995.
- Paulson, J R, S Lazaroff, and U K Laemmli. 1976. "Head Length Determination in Bacteriophage T4: The Role of the Core Protein P22." *Journal of Molecular Biology* 103 (1): 155–74. doi:10.1016/0022-2836(76)90057-7.
- Popa, M P, T a McKelvey, J Hempel, and R W Hendrix. 1991. "Bacteriophage HK97 Structure: Wholesale Covalent Cross-Linking between the Major Head Shell Subunits." *Journal of Virology* 65 (6): 3227–37.
- Prevelige, P E, D Thomas, and J King. 1988. "Scaffolding Protein Regulates the Polymerization of P22 Coat Subunits into Icosahedral Shells in Vitro." *Journal of Molecular Biology* 202 (4): 743–57. doi:10.1016/0022-2836(88)90555-4.
- Prevelige, P. E., D. Thomas, and J. King. 1993. "Nucleation and Growth Phases in the Polymerization of Coat and Scaffolding Subunits into Icosahedral Procapsid Shells." *Biophysical Journal* 64 (3): 824–35. doi:10.1016/S0006-3495(93)81443-7.
- Prevelige, Peter E., and B A Fane. 2012. "Building the Machines: Scaffolding Protein Functions During Bacteriophage Morphogenesis." In *Viral Molecular Machines*, edited by Michael G. Rossmann and V.B. Rao, 325–50. Springer Science+Business Media, LLC. doi:10.1007/978-1-4614-0980-9.
- Rixon, F J. 1993. "Structure and Assembly of Herpesviruses." *Semin. Virol.* 4: 135–44.
- Roeder, G. Shirleen, and Paul D. Sadowski. 1977. "Bacteriophage T7 Morphogenesis: Phage-Related Particles in Cells Infected with Wild-Type and Mutant T7 Phage." *Virology* 76 (1): 263–85.
- Roger W. Hendrix, Robert L Duda. 1998. "Bacteriophage HK97 Head Assembly: A Protein Ballet." *Advances in Virus Research* 50: 235–88.
- Ross, P D, L W Black, M E Bisher, and a C Steven. 1985. "Assembly-Dependent Conformational Changes in a Viral Capsid Protein. Calorimetric Comparison of Successive Conformational States of the gp23 Surface Lattice of Bacteriophage T4." *Journal of Molecular Biology* 183 (3): 353–64.
- Ross, Philip D, Naiqian Cheng, James F Conway, Brian a Firek, Roger W Hendrix, Robert L Duda, and Alasdair C Steven. 2005. "Crosslinking Renders Bacteriophage HK97 Capsid Maturation Irreversible and Effects an Essential Stabilization." *The EMBO Journal* 24 (7): 1352–63. doi:10.1038/sj.emboj.7600613.
- Sawitzke, J A, L C Thomason, N Costantino, M Bubunencko, S Datta, and D L Court. 2007. "Recombineering: In Vivo Genetic Engineering in E. Coli, S. Enterica, and beyond."

Methods Enzymol 421: 171–99. doi:S0076-6879(06)21015-2 [pii] 10.1016/S0076-6879(06)21015-2.

- Simon, L D. 1969. “The Infection of Escherichia Coli by T2 and T4 Bacteriophages as Seen in the Electron Microscope. III. Membrane-Associated Intracellular Bacteriophages.” *Virology* 38 (2): 285–96.
- Simon, L D. 1972. “Infection of Escherichia Coli by T2 and T4 Bacteriophages as Seen in the Electron Microscope: T4 Head Morphogenesis.” *Proceedings of the National Academy of Sciences of the United States of America* 69 (4): 907–11. doi:10.1073/pnas.69.4.907.
- Steven, A C, H L Greenstone, F P Booy, L W Black, and P D Ross. 1992. “Conformational Changes of a Viral Capsid Protein. Thermodynamic Rationale for Proteolytic Regulation of Bacteriophage T4 Capsid Expansion, Co-Operativity, and Super-Stabilization by Soc Binding.” *Journal of Molecular Biology* 228 (3): 870–84.
- Steven, A.C., E. Couture, U. Aebi, and M.K. Showe. 1976. “Structure of T4 Polyheads. II. A Pathway of Polyhead Transformation as a Model for T4 Capsid Maturation.” *J Mol Biol* 106 (1): 187–221.
- Steven, Alasdair C., J. Bernard Heymann, Naiqian Cheng, Benes L. Trus, and James F. Conway. 2005. “Virus Maturation: Dynamics and Mechanism of a Stabilizing Structural Transition That Leads to Infectivity.” *Current Opinion in Structural Biology* 15 (2): 227–36. doi:10.1016/j.sbi.2005.03.008.
- Studier, F. W. 2005. “Protein Production by Auto-Induction in High Density Shaking Cultures.” *Protein Expr. Purif.* 41 (1): 207–34.
- Studier, F. W., A. H. Rosenberg, J. J. Dunn, and J. W. Dubendorff. 1990. “Use of T7 RNA Polymerase to Direct Expression of Cloned Genes.” *Methods Enzymol* 185: 60–89.
- Suhanovsky, Margaret M., and Carolyn M. Teschke. 2015. “Nature's Favorite Building Block: Deciphering Folding and Capsid Assembly of Proteins with the HK97-Fold.” *Virology* 479-480. Elsevier: 487–97. doi:10.1016/j.virol.2015.02.055.
- Sun, Y, M H Parker, P Weigele, S Casjens, P E Prevelige, and N R Krishna. 2000. “Structure of the Coat Protein-Binding Domain of the Scaffolding Protein from a Double-Stranded DNA Virus.” *Journal of Molecular Biology* 297 (5): 1195–1202. doi:10.1006/jmbi.2000.3620.
- Sutter, Markus, Daniel Boehringer, Sascha Gutmann, Susanne Günther, David Prangishvili, Martin J Loessner, Karl O Stetter, Eilika Weber-Ban, and Nenad Ban. 2008. “Structural Basis of Enzyme Encapsulation into a Bacterial Nanocompartment.” *Nature Structural & Molecular Biology* 15 (9): 939–47. doi:10.1038/nsmb.1473.
- Suttle, Curtis a. 2007. “Marine Viruses--Major Players in the Global Ecosystem.” *Nature Reviews. Microbiology* 5 (10): 801–12. doi:10.1038/nrmicro1750.

- Teschke, Carolyn M, Amy McGough, and Pamela a Thuman-Commike. 2003. "Penton Release from P22 Heat-Expanded Capsids Suggests Importance of Stabilizing Penton-Hexon Interactions during Capsid Maturation." *Biophysical Journal* 84 (4). Elsevier: 2585–92. doi:10.1016/S0006-3495(03)75063-2.
- Thomason, L C, N Costantino, D V Shaw, and D L Court. 2007. "Multicopy Plasmid Modification with Phage Lambda Red Recombineering." *Plasmid* 58 (2): 148–58. doi:S0147-619X(07)00027-3 [pii] 10.1016/j.plasmid.2007.03.001.
- Thomason, Lynn C., Donald L. Court, M Bubunenko, Nina Costantino, Helen Wilson, Simanti Datta, and Amos B. Oppenheim. 2007. "Recombineering: Genetic Engineering in Bacteria Using Homologous Recombination." *Current Protocols in Molecular Biology*, 1.16.1–1.16.24.
- Thuman-Commike, Pamela A., Barrie Greene, Joanita Jakana, B.V. Venkataram Prasad, Jonathan King, Peter E. Prevelige, and Wah Chiu. 1996. "Three-Dimensional Structure of Scaffolding-Containing Phage P22 Procapsids by Electron Cryo-Microscopy." *Journal of Molecular Biology* 260: 85–98.
- Tso, Danju. 2010. "Genetic Analysis of Bacteriophage HK97 Prohead Assmebly and Head Protein Crosslinking."
- Tsugita, A., L. W. Black, and M. K. Showe. 1975. "Protein Cleavage during Virus Assembly: Characterization of Cleavage in T4 Phage." *J Mol Biol* 98 (1): 217–5.
- Tuma, R, M H Parker, P Weigele, L Sampson, Y Sun, N R Krishna, S Casjens, G J Thomas Jr., and P E Prevelige Jr. 1998. "A Helical Coat Protein Recognition Domain of the Bacteriophage P22 Scaffolding Protein." *J Mol Biol* 281 (1): 81–94. doi:S0022-2836(98)91916-7 [pii] 10.1006/jmbi.1998.1916.
- Tuma, Roman, Peter E. Prevelige, and George J. Thomas. 1996. "Structural Transitions in the Scaffolding and Coat Proteins of P22 Virus during Assembly and Disassembly." *Biochemistry* 35 (14): 4619–27. doi:10.1021/bi952793l.
- Van Driel, R., F. Traub, and M. K. Showe. 1980. "Probable Localization of the Bacteriophage T4 Prehead Proteinase Zymogen in the Center of the Prehead Core." *Journal of Virology* 36 (1): 220–23.
- Warming, Søren, Nina Costantino, Donald L. Court, Nancy a. Jenkins, and Neal G. Copeland. 2005. "Simple and Highly Efficient BAC Recombineering Using galK Selection." *Nucleic Acids Research* 33 (4): 1–12. doi:10.1093/nar/gni035.
- Weigele, P. R., L. Sampson, D. Winn-Stapley, and S. R. Casjens. 2005. "Molecular Genetics of Bacteriophage P22 Scaffolding Protein's Functional Domains." *J Mol Biol* 384: 831–44.

- Wikoff, W R, L Liljas, R L Duda, H Tsuruta, R W Hendrix, and J E Johnson. 2000. "Topologically Linked Protein Rings in the Bacteriophage HK97 Capsid." *Science (New York, N.Y.)* 289 (5487): 2129–33. doi:10.1126/science.289.5487.2129.
- Wikoff, William R., Robert L. Duda, Roger W. Hendrix, and John E. Johnson. 1999. "Crystallographic Analysis of the dsDNA Bacteriophage HK97 Mature Empty Capsid." *Acta Crystallographica Section D: Biological Crystallography* 55 (4). International Union of Crystallography: 763–71. doi:10.1107/S0907444998017661.
- Wommack, K E, and R R Colwell. 2000. "Virioplankton: Viruses in Aquatic Ecosystems." *Microbiology and Molecular Biology Reviews : MMBR* 64 (1): 69–114. doi:10.1128/MMBR.64.1.69-114.2000.
- Xie, Z, and R W Hendrix. 1995. "Assembly in Vitro of Bacteriophage HK97 Proheads." *Journal of Molecular Biology* 253 (1): 74–85. doi:10.1006/jmbi.1995.0537.
- Yan, X., R.S. Sinkovitis, and T.S. Baker. 2007. "AUTO3DEM-an Automade and High Throughput Program for Image Reconstruction of Icosahedral Particles." *J Struct Biol* 157: 73–82.
- Zhou, Z H, S J Macnab, J Jakana, L R Scott, W Chiu, and F J Rixon. 1998. "Identification of the Sites of Interaction between the Scaffold and Outer Shell in Herpes Simplex Virus-1 Capsids by Difference Electron Imaging." *Proceedings of the National Academy of Sciences of the United States of America* 95 (6): 2778–83. doi:10.1073/pnas.95.6.2778.